CARBON DIOXIDE SEQUESTRATION THROUGH MICROBIALLY-INDUCED CALCIUM CARBONATE PRECIPITATION USING UREOLYTIC ENVIRONMENTAL MICROORGANISMS

A Dissertation

Presented To

the Faculty of the Department of Civil and Environmental Engineering

University of Houston

In Partial Fulfillment

of the Requirements for the Degree

Doctor of Philosophy

in Environmental Engineering

by

Tugba Onal Okyay

May 2015

CARBON DIOXIDE SEQUESTRATION THROUGH MICROBIALLY-INDUCED CALCIUM CARBONATE PRECIPITATION USING UREOLYTIC ENVIRONMENTAL MICROORGANISMS

_____
Tugba Onal Okyay

Approved:

_____
Chair of Committee
Debora F. Rodrigues, Assistant Professor,
Civil and Environmental Engineering

Committee Members:

_____
Yandi Hu, Assistant Professor,
Civil and Environmental Engineering

_____
William G. Rixey, Associate Professor
Civil and Environmental Engineering

_____
Timothy Cooper, Associate Professor
Biology and Biochemistry Department

_____
Richard Willson, Professor
Chemical Engineering

_____
Suresh K. Khator, Associate Dean
Cullen College of Engineering

_____
Hanadi S. Rifai, Director,
Environmental Engineering
Graduate Program

Acknowledgements

First of all, I would like to thank my family for showing constant support, love and encouragement and for believing in me.

I would like to thank specially my Advisor, Dr. Debora F. Rodrigues, who taught me many academic and personal life skills throughout my journey in the doctoral program. I appreciate all her time and research guidance to make my doctoral life productive and stimulating. Her dedication and perseverance are some of her remarkable talents, which I will take on for my future life. In addition, I also would like to thank her for trusting me through all the research steps with her unconditional support and encouragement. I am also thankful for having the opportunity to meet such a successful woman professor, teacher, mother and advisor. She is an outstanding role model to female students like me.

My acknowledgements are also extended to all the UH faculty for enriching my knowledge in the field of Environmental Engineering and many other related research areas. I am also grateful to the thesis committee for giving me valuable suggestions on this research project to enhance its quality and impact.

I also would like to thank Dr. Yavuz Bayam (Gediz University) for enriching my doctoral experience through a side collaborative project from my dissertation work. In this side project, I was able to learn about materials sciences and nanomaterials while working with him. I truly admire his kindness, humbleness, and technical expertise.

I would like to extend my gratitude to my laboratory peers: Dr. Catherine M. Santos, Dr. Charisma Latteo, Dr. Farid Ahmed, Dr. Isis Mejias Carpio, Dr. Felipe Ferrera, Jingjing Fan, Sean Smith, and others at UH who helped me academically and personally. Our research group has been a source of friendship as well as an excellent environment for interaction and

collaboration. Special thanks to Hang Nguyen, she was always helpful, supportive, and a joy in the laboratory and office. She was a true friend to me. I admire your sincerity, respect, handiness, and smartness.

My time at Houston was enjoyable in large part due to the many friends that became part of my life. I am grateful for the time spent with the Haberdar family (Hakan, Rubabe, and Zehra), the Yeniaras family (Erol, Ozge, and Akin), and my other Turkish friends.

Finally, I would like to acknowledge the people who helped me in collecting water samples in “Cave Without A Name” in Texas-USA and “Pamukkale travertines” in Denizli-Turkey. I also would like to acknowledge my sponsor, the Turkish Government, which made my doctoral work in USA possible. I am deeply thankful for their funding support, which allowed me to have a life changing experience in the US and obtain my doctoral degree.

My husband, M. Serhat Okyay, deserves the greatest acknowledgement of all for being a constant source of love and joy in my life. His unwavering love and trust, remarkable support and patience, and endless encouragement provided me strength and energy to go through many happy and rough times in my life. I love you very much, and I am everyday thankful for having you as my husband.

Tugba Onal Okyay

University of Houston

May 2015

CARBON DIOXIDE SEQUESTRATION THROUGH MICROBIALLY-INDUCED CALCIUM CARBONATE PRECIPITATION USING UREOLYTIC ENVIRONMENTAL MICROORGANISMS

An Abstract

Presented To

the Faculty of the Department of Civil and Environmental Engineering

University of Houston

In Partial Fulfillment

of the Requirements for the Degree

Doctor of Philosophy

in Environmental Engineering

by

Tugba Onal Okyay

May 2015

Abstract

The development of affordable and eco-friendly strategies for carbon dioxide sequestration has become a matter of paramount importance to reduce or mitigate the effects of global climate changes. Today, the most used solution to sequester CO_2 is its immobilization in geological reservoirs, commonly referred to as carbon capture and storage; however this technique is not completely reliable because of leakage risks, when storing vast quantities of CO_2 in geological strata. Alternatively, precipitation of CO_2 as solid carbonates may constitute an alternative strategy for carbon immobilization. The reaction to form calcium carbonates is generally not chemically favorable in the environment, unless at pH values higher than 9. On the other hand, microorganisms, through metabolic activities, have been shown to induce calcium carbonate precipitation, provided that certain environmental conditions are met. In this dissertation, I investigate the diversity and physiology of diverse ureolytic consortia and isolates able to induce calcium carbonate precipitation to better understand their roles in carbon sequestration. These microorganisms were obtained from karstic environments that are rich in calcium and present natural input of urea, which are considered to be key factors in calcium carbonate precipitation. These urease-positive microorganisms were classified phylogenetically and their physiology was investigated. The relationship amongst urease activity, microbially-induced calcium carbonate precipitation (MICP), and carbon sequestration by the different consortia and isolates were shown to be dependent on the species and directly influenced by their growth conditions.

Table of Contents

List of Figures

List of Tables

CHAPTER 1 RESEARCH HYPOTHESIS AND LITERATURE REVIEW

1.1 RATIONALE AND HYPOTHESIS DEVELOPMENT

Calcite or calcium carbonate ($CaCO_3$) is one of the most widespread minerals on Earth, and is naturally found in sedimentary rocks, as limestone, marble and calcareous sandstones in marine, freshwater and terrestrial environments [1, 2]. This mineral is commonly used in many industries [3]. In natural systems, calcium carbonate precipitation can occur as a chemical reaction when supersaturated solutions of calcium and carbonate are present. Moreover, calcite precipitates by evaporation or temperature and pressure changes [4]. Recently, researchers demonstrated that microorganisms can facilitate calcium carbonate precipitation under non-supersaturated solutions of calcium [4]. In this case, the process is called "microbially-induced calcium carbonate precipitation" (MICP). This biomineralization process is designated as "induced", since the precipitation occurs as a result of the microbial metabolic activity.

Amongst various metabolic pathways, photosynthesis, sulfate reduction, iron reduction, and urea hydrolysis have been associated with the MICP, however, urea hydrolysis is the most well studied pathway [5, 6]. Researchers suggest that the calcium carbonate precipitation induced by ureolytic bacteria occurs as a result of urea hydrolysis that increases the surrounding pH and in the presence of calcium leads to $CaCO_3$ precipitation. In this process, the negatively charged cell structures act as ideal nucleation sites for $CaCO_3$ formation [7].

More recently, researchers have suggested that MICP has a potential application in carbon capturing by converting supercritical CO_2 into calcium carbonate precipitates [6-8]. These findings have attracted a lot the attention of researchers since CO_2 content in atmosphere has been increasing from 280 ppm in preindustrial times to 388 ppm at the present time [9], and this trend is estimated to increase even further in the years to come with an increase rate of 2.11

ppm/year [9, 10]. Additionally, CO_2 is a greenhouse gas that absorbs solar radiation transmitted back from Earth in the infrared spectrum. This adsorbed energy is partially dissipated as heat, warming the atmosphere, land and sea. Up until now, plants have been described as the major players responsible for taking up CO_2 from the atmosphere. Oceans are also known to remove close to 40% of anthropogenic CO_2 [9]. Now, the MICP process has been shown as an alternative method for the CO_2 sequestration. However, no complete study has investigated the relationship amongst ureolytic activity, MICP, and CO_2 sequestration yet.

The overarching objective of this dissertation is to investigate the physiology and diversity of MICP by ureolytic microorganisms present in karstic environments. The overall hypothesis of this study is that ureolytic microorganisms present in karstic environment can convert CO_2 and calcium into calcium carbonates through the MICP process. This hypothesis was based on the fact that karstic environments have formations made of $CaCO_3$ precipitations and these environments are rich in calcium. These geological formations have recently been suggested to be induced by the presence of microbial activity, but little is known about the role of microorganisms in carbonate precipitation and the metabolism of karstic microorganisms involved in this reaction.

This dissertation is divided into 4 chapters. Chapter 1 includes a literature review of carbon dioxide sequestration including the traditional technologies and different carbon dioxide sequestration mechanisms done biologically, the role of microorganisms in calcium carbonate precipitation, the mechanism and importance of urea hydrolysis (or ureolysis) in calcium carbonate precipitation, the role of urease-positive (or ureolytic) microorganisms, current and new methods to determine the urease activity. Based on the literature, it was hypothesized that microorganisms in karstic environments, such as caves and travertines, can play an important

role in CO_2 sequestration through calcite precipitation. Therefore, to confirm this hypothesis, Chapter 2 investigates microbial consortia involved in MICP from a cave in Texas-USA and a travertine in Turkey grown in different growth media. The role of these consortia in MICP and CO_2 sequestration were investigated. The results of this chapter led to the following hypotheses: 1) different bacterial species in the consortia have different capabilities of calcite precipitation and therefore have different rates of CO_2 sequestration; 2) the environmental growth conditions play an important role in the CO_2 sequestration performance of different species involved in MICP. These hypotheses were investigated in Chapter 3. This chapter encompasses the isolation and identification of different species present in the consortia obtained in the Chapter 2, and determines the effects of different growth medium components in calcium carbonate precipitation and CO_2 sequestration. The results showed that the composition and concentration of the growth medium components played an important role in the biotic and abiotic CO_2 sequestration. Furthermore, we were able to link increase in urease activity with MICP and CO_2 sequestration. These results led us to hypothesize that CO_2 sequestration can be enhanced by optimization of the isolates' urease activity. In Chapter 4, we investigate the impact of changes in the concentrations of the most important parameters involved in urease activity and MICP, such as nickel, calcium and urea, to MICP and CO_2 sequestration using a model organism, *Sporosarcina pasteurii* ATCC 11859. This model organism has shown excellent urease activity and MICP performances. At the end of this dissertation, we discuss future directions for this study.

1.2 ROLE OF MICROORGANISMS IN CARBON DIOXIDE SEQUESTRATION

As the worldwide population continues to grow, there have been increasing concerns about global climate changes generated by increasing CO_2 production through anthropogenic

activities, such as land-use, deforestation, biomass burning, draining of wetlands, soil cultivation and fossil fuel combustion [11]. In fact, the concentration of atmospheric greenhouse gases has increased by 31% from 1850 to 2005, and is increasing at a rate of 0.46% per year [12]. Therefore, new technologies to mitigate or sequester the carbon dioxide involved in global climate change are of great need. In fact, three strategies of lowering CO_2 emissions to reduce climate change effects have been suggested so far, and they involve i) reducing the global energy use, ii) developing low or no-carbon fuel, and, iii) sequestering CO_2 from point sources or atmosphere through natural or engineering techniques [12].

The first option is really hard to implement due to the worldwide population growth rate. The second option is under investigation and can have some very high costs. The third option is also under investigation; however, it has been shown to have great potential as a strategy to lower CO_2 emissions. In nature, inorganic chemical transformation of CO_2 into $CaCO_3$, $MgCO_3$ and other minerals have been described, but are still not yet well understood. It is, however, known to occur at slow rates [10, 12].

The stoichiometric reactions of CO_2 sequestration and conversion to $CaCO_3$ are given below;

$$CO_{2(gas)} + H_2O \leftrightharpoons CO_{2(aq)} + H_2O \,, \qquad (1\text{-}1)$$

$$CO_{2(aq)} + H_2O \leftrightharpoons H_2CO_3 \,, \qquad (1\text{-}2)$$

$$H_2CO_3 \leftrightharpoons H^+ + HCO_3^- \,, \qquad (1\text{-}3)$$

$$HCO_3^- \leftrightharpoons H^+ + CO_3^{2-} \,, \qquad (1\text{-}4)$$

$$H_2CO_3 \leftrightharpoons 2\,H^+ + CO_3^{2-} \text{ ,and} \qquad (1\text{-}5)$$

$$Ca^{2+}{}_{(aq)} + CO_3^{-2}{}_{(aq)} \leftrightharpoons CaCO_3 \,. \qquad (1\text{-}6)$$

Sequestration of CO_2 has also been described to happen by two main processes [13]; a) abiotic sequestration, and b) biotic sequestration. Abiotic sequestration is based on physical and chemical reactions and engineering techniques without intervention of living organisms. For example, the injection of pure CO_2 at great depths in oceans, and the geological injection of CO_2 in coal seams, old oil wells, stable rock strata or saline aquifers. In biotic sequestration, higher plants and microorganisms are responsible for removing CO_2 from the atmosphere. A summary of these two sequestration pathways [12] can be seen in **Figure 1-1**.

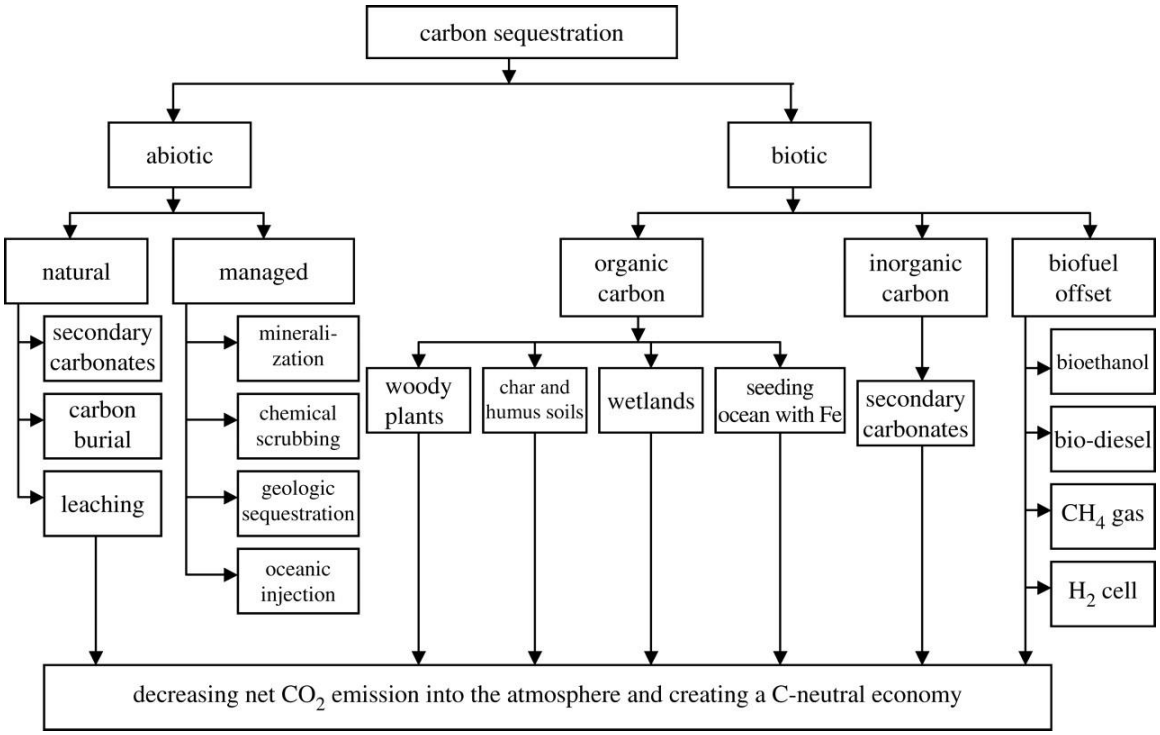

FIGURE 1-1 A WIDE RANGE OF PROCESSES AND TECHNOLOGIES FOR CARBON SEQUESTRATION IN AGRICULTURAL, INDUSTRIAL, AND NATURAL ECOSYSTEMS.

Within the abiotic CO_2 sequestration, carbonate ions precipitate as carbonate minerals, if counter ions are present and available. The most common counter ions that can form carbonate minerals are divalent cations, such as Ca^{2+}, Mg^{2+}, Mn^{2+}, Fe^{2+}, or Sr^{2+} [10]. Furthermore, researchers showed that the weathering of silicate minerals, such as olivine, serpentine, or wollastonite, can act as natural geochemical reactors with atmospheric CO_2 to form mineral carbonates. An

example of such type of reaction is the formation of calcite using wollastonite. The reaction is [10, 11]:

$$CaSiO_3 + CO_2 \rightarrow CaCO_3 + SiO_2 . \quad (1\text{-}7)$$

Even though this mechanism to capture CO_2 is geologically stable and environmentally safe, the reaction is extremely slow due to the slow dissolution rates of the minerals [11]. Therefore, identifying environments containing divalent cations and alkalinity to increase the chemical rate of mineral carbonate formations has been considered one of the main challenges for abiotic CO_2 sequestration [10]. Moreover, the acceleration of the reaction in an environmentally and economically viable way is critical for CO_2 mitigation by mineral carbonation. In the literature, there are also other abiotic approaches to sequester CO_2, such as use of chemical/physical solvents, adsorption onto solids, membranes, cryogenic/condensation systems, and deep ocean sequestration [9, 12]. However, the high cost of these approaches hinder their application for large scale CO_2 sequestration [14]. Alternatively, bio-mediated sequestration has been recently suggested.

In biotic sequestration, CO_2 can be successfully sequestered by microorganisms. Studies have shown that microorganisms can fix and transform atmospheric CO_2 through heterotrophic and autotrophic metabolic processes. Besides, photoautotrophic microorganisms that can fix atmospheric CO_2 in the presence of light, some microbial species have been described to produce minerals from gaseous carbon and nitrogen yielding organic cellular matter via various other autotrophic enzymatic processes. For instance, chemoautotrophs or chemolithotrophs, which are autotrophic bacteria capable of growth in the absence of light, are known to use inorganic substrates to derive energy for biosynthetic reactions using aerobic or anaerobic CO_2 assimilation [15]. Therefore, microbial CO_2 uptake from the atmosphere via these processes is

well known; however actual estimations of sequestration rates by these microbes are rare in literature.

Today, six pathways are well-known to be involved in sequestering CO_2 by microorganisms [13], which are i) the Calvin-Benson reductive pentose phosphate cycle, ii) the reductive citric acid (Arnon-Buchanan) cycle, iii) the reductive acetyl-CoA (Wood-Ljungdahl) pathway, iv) the hydroxypropionate (Fuchs-Holo) bi-cycle, v) the 3-hydroxypropionate/4-hydroxybutyrate cycles, and vi) the dicarboxylate/ 4-hydroxybutyrate cycles.

Amongst these pathways, The Calvin-Benson reductive pentose phosphate cycle (**Figure 1-2**) is the quantitatively most important and well-studied mechanism of photoautotrophic CO_2 fixation in nature. This pathway is centered on carbohydrates, and can primarily be found in organisms synthesizing large amounts of sugars, such as plants and photosynthetic organisms.

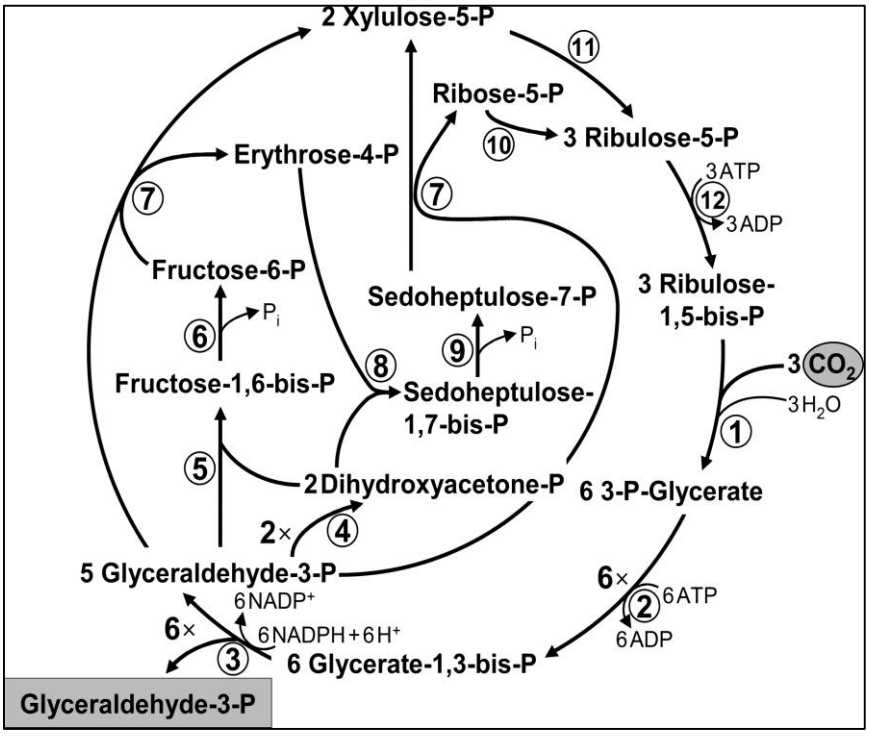

FIGURE 1-2 THE REDUCTIVE PENTOSE PHOSPHATE (CALVIN-BENSON) CYCLE [13].

The enzymes numbered in **Figure 1-2** are as following: 1, ribulose-1,5-bisphosphate carboxylase/oxygenase; 2, 3-phosphoglycerate kinase; 3, glyceraldehyde-3-phosphate dehydrogenase; 4, triose-phosphate isomerase; 5, fructose-bisphosphate aldolase; 6, fructose-bisphosphate phosphatase; 7, transketolase; 8, sedoheptulose-bisphosphate aldolase; 9, sedoheptulose-bisphosphate phosphatase; 10, ribose-phosphate isomerase; 11, ribulose-phosphate epimerase; and 12, phosphoribulokinase [13].

The key enzyme in this pathway is the ribulose-1,5-bisphosphate carboxylase/oxygenase (RubisCO). RubisCO catalyzes the electrophilic addition of CO_2 to the C5 sugar ribulose-1,5-bisphosphate. In prokaryotes, RubisCO can be found in carboxysomes, which are special carbon-fixing organelle-like micro-compartments. The Calvin-Benson cycle operates in plants, algae, cyanobacteria, and many aerobic or facultative aerobic *Proteobacteria* belonging to the alpha, beta, and gamma subgroups. For instance, it has been described in *Sulfobacillus* sp., an iron and sulfur-oxidizing member of the *Firmicutes* phylum; in some *Mycobacteria*, and green non-sulfur bacteria of the genus *Oscillochloris* (phylum *Chloroflexi*). The Calvin-Benson cycle not only functions in autotrophic CO_2 fixation, but is also required as an electron sink for photoheterotrophic growth of some purple bacteria (e.g., *Rhodobacter*, *Rhodospirillum*, and *Rhodopseudomonas*) [13].

Another cycle involved in CO_2 sequestration is the reductive citric acid (Arnon-Buchanan) cycle. This cycle was first proposed for the green sulfur bacterium *Chlorobium limicola* (*Chlorobi*) (**Figure 1-3**); however, in some other species, this cycle has further minor enzymatic modifications. This cycle has also been identified in anaerobic or microaerobic members of various other phyla, such as *Aquificae*, *Proteobacteria* (particularly in the delta and epsilon subdivisions), and *Nitrospirae* (e.g., *Nitrospira* and *Leptospirillum*). Although this cycle was first

discovered in *Chlorobium*, it has been more intensively studied in the thermophilic aerobic hydrogen-oxidizing bacterium *Hydrogenobacter thermophilus*. The primary CO_2 fixation product of the cycle is acetyl-CoA, which is further converted to other intermediates, such as pyruvate/phosphoenolpyruvate (PEP), oxaloacetate, and 2-oxoglutarate. Typically, bacteria using the rTCA cycle require the ferredoxin-dependent pyruvate synthase as an additional enzyme for the acetyl-CoA assimilation [13]. The pathway of acetyl-CoA assimilation to pyruvate, phosphoenolpyruvate (PEP), and oxaloacetate is shown in **Figure 1-3**.

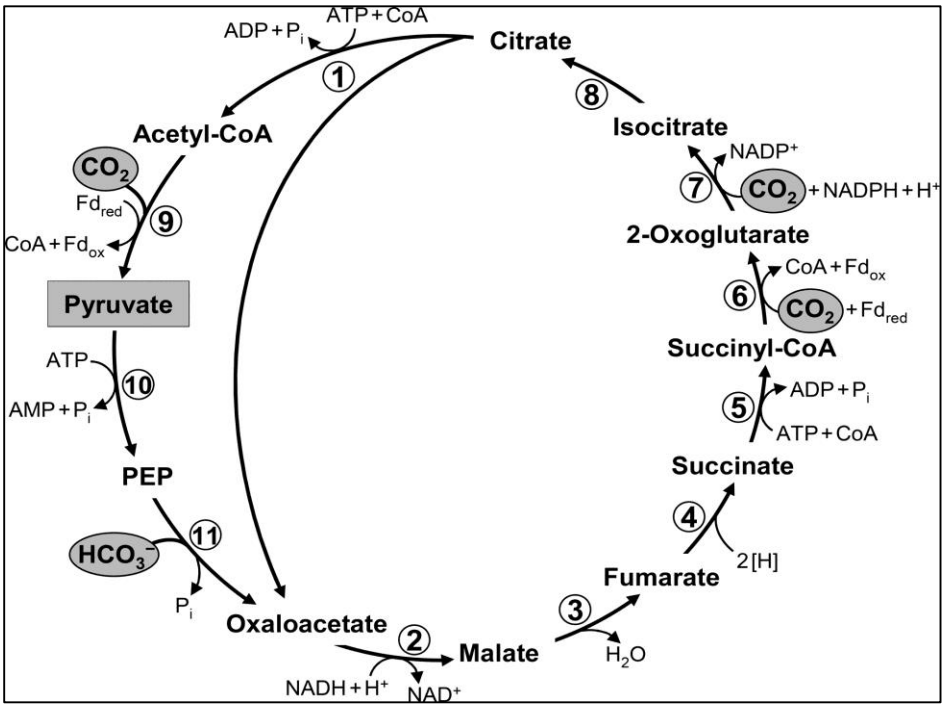

FIGURE 1-3 THE REDUCTIVE CITRIC ACID (ARNON-BUCHANAN) CYCLE IN GREEN SULFUR BACTERIA [13].

Enzymes numbered in **Figure 1-3** are as following; 1, ATP-citrate lyase; 2, malate dehydrogenase; 3, fumarate hydratase; 4, fumarate reductase (natural electron donor is not known); 5, succinyl-CoA synthetase; 6, ferredoxin (Fd)-dependent 2-oxoglutarate synthase; 7, isocitrate dehydrogenase; 8, aconitate hydratase; 9, Fd-dependent pyruvate synthase; 10, PEP synthase; 11, PEP carboxylase [13].

A third pathway involved in CO_2 sequestration is the reductive acetyl-CoA (Wood-Ljungdahl) pathway. This pathway is noncyclic and results in the fixation of two CO_2 molecules to form acetyl-CoA. One CO_2 molecule is bound to a tetrahydropterin coenzyme, while the other CO_2 molecule is reduced to carbon monoxide and then bound to nickel in the reaction center of CO-dehydrogenase enzyme (**Figure 1-4**). This enzyme also acts as an acetyl-CoA synthase. This pathway is typically found in acetogenic bacteria and methanogenic archaea.

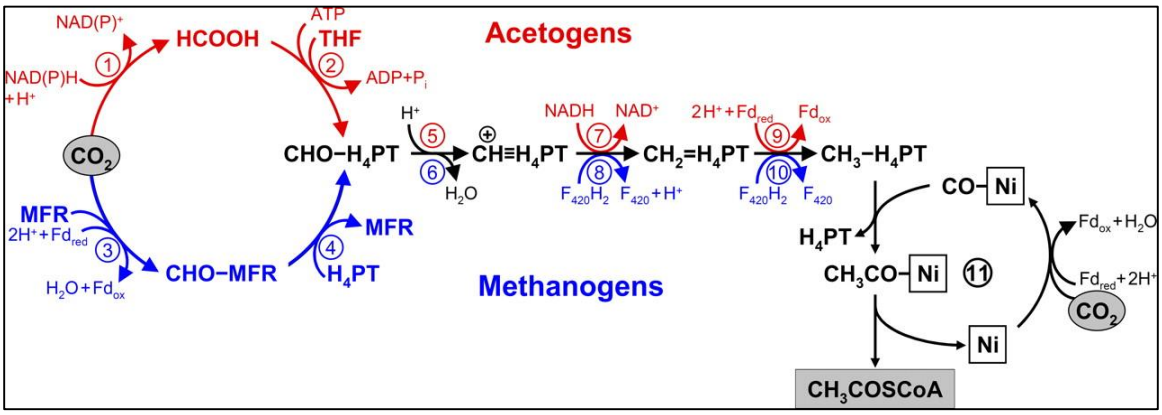

FIGURE 1-4 THE REDUCTIVE ACETYL-COA (WOOD-LJUNGDAHL) PATHWAY [13].

In **Figure 1-4**, the upper part (red) shows the variant of the pathway functioning in Acetogens, and the lower part (blue) depicts the pathway in Methanogens. In this figure, Fd represents ferredoxin; and the others are as following: THF, tetrahydrofolate; H4TPT, tetrahydropterin (THF in acetogens and tetrahydromethanopterin or tetrahydrosarcinopterin in methanogens); MFR, methanofuran; F420, coenzyme F420. The numbered enzymes in **Figure 1-4** are: 1, formate dehydrogenase; 2; formyl-THF synthetase; 3, formyl-MFR dehydrogenase; 4, formyl-MFR:tetrahydromethanopterin formyltransferase; 5, methenyl-THF cyclohydrolase; 6, methenyl-tetrahydromethanopterin cyclohydrolase; 7, methylene-THF dehydrogenase; 8, methylene-tetrahydromethanopterin dehydrogenase; 9, methylene-THF reductase; 10, methylene-tetrahydromethanopterin reductase; 11, CO dehydrogenase/acetyl-CoA synthase [13].

The fourth pathway involved in CO_2 sequestration is the hydroxypropionate (Fuchs-Holo) bi-cycle. This cycle was first discovered in *Chloroflexus aurantiacus*. The co-assimilation of numerous compounds (*i.e.*, acetate, propionate, and succinate) makes this pathway best suitable for mixotrophy. This pathway is commonly found in green non-sulfur phototrophs of the *Chloroflexaceae* family. An interesting feature of this cycle is the presence of a number of bi- and multifunctional enzymes (**Figure 1-5**): the pathway involves 19 steps and requires only 13 enzymes. Moreover, it does not contain oxygen-sensitive steps, and all of its enzymes can function under aerobic condition.

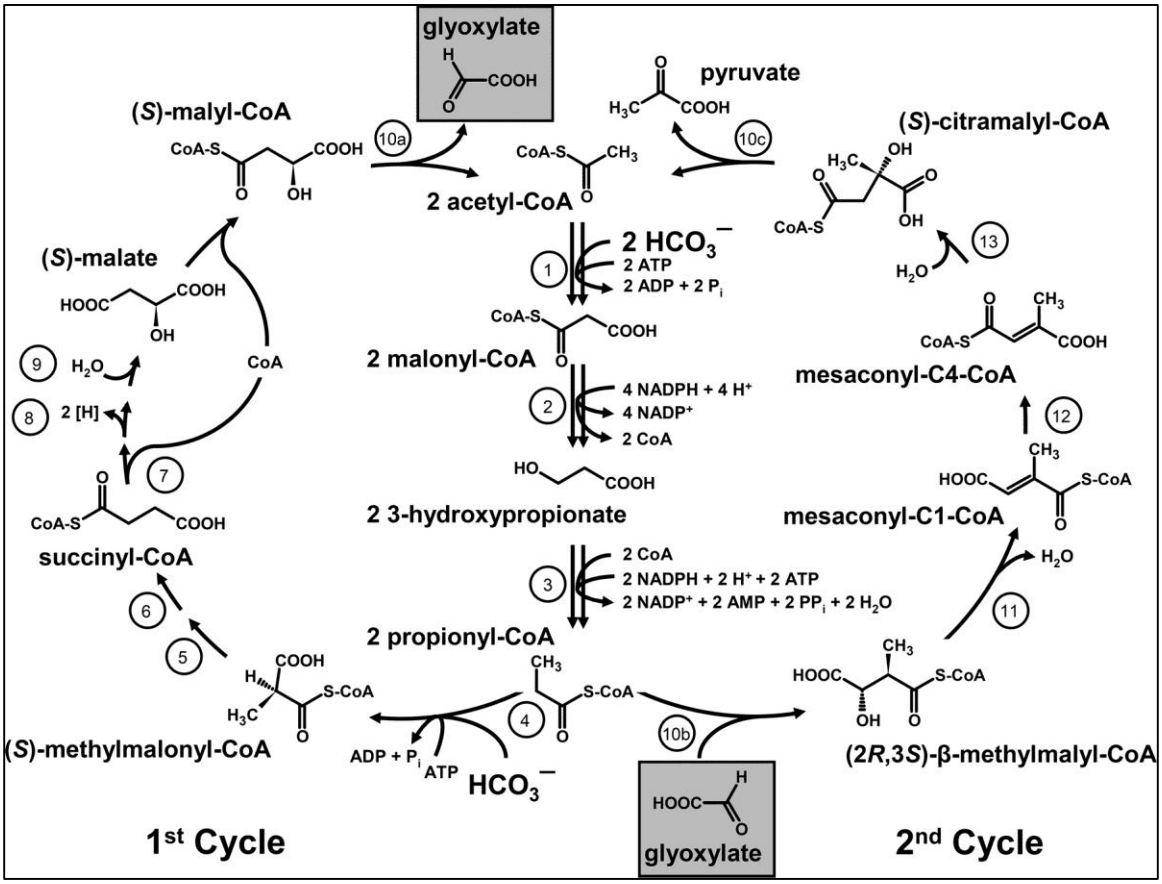

FIGURE 1-5 THE HYDROXYPROPIONATE (FUCHS-HOLO) BI-CYCLE [13].

Enzymes numbered in **Figure 1-5** are as following: 1, acetyl-CoA carboxylase; 2, malonyl-CoA reductase; 3, propionyl-CoA synthase; 4, propionyl-CoA carboxylase; 5, methylmalonyl-CoA

epimerase; 6, methylmalonyl-CoA mutase; 7, succinyl-CoA:(*S*)-malate-CoA transferase; 8, succinate dehydrogenase; 9, fumarate hydratase; 10a, 10b, and 10c, trifunctional (*S*)-malyl-CoA (a)/β-methylmalyl-CoA (b)/(*S*)-citramalyl-CoA lyase (c); 11, mesaconyl-C1-CoA hydratase; 12, mesaconyl-CoA C1-C4 CoA transferase; 13, mesaconyl-C4-CoA hydratase [13].

The fifth and the sixth cycles known to be involved in CO_2 sequestration are the 3-hydroxypropionate/4-hydroxybutyrate cycles (HP/HB) and the dicarboxylate/ 4-hydroxybutyrate cycles (DC/HB), respectively (**Figure 1-6**). These two cycles have been recently described in *Crenarchaeota*. In both cycles, acetyl-CoA and two inorganic carbons are converted to succinyl-CoA.

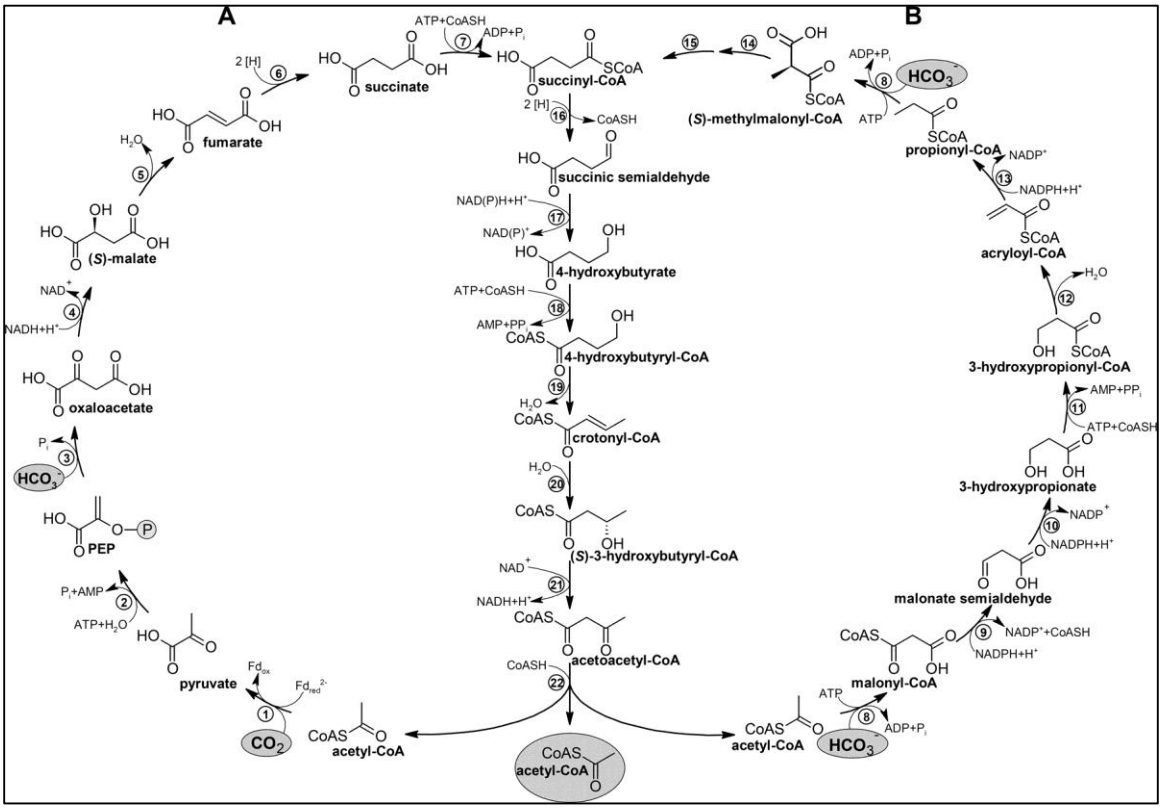

FIGURE 1-6 THE 4-HYDROXYBUTYRATE CYCLES OF AUTOTROPHIC CO_2 FIXATION [13].

In the HP/HB cycle, acetyl-CoA/propionyl-CoA carboxylase fixes two molecules of bicarbonate, and in the DC/HB cycle, pyruvate synthase and PEP carboxylase are the two

carboxylating enzymes. While both cycles produce acetyl-CoA, they differ with respect to how they are linked to the central carbon metabolism. The DC/HB cycle is anaerobic and uses pyruvate synthase to synthesize pyruvate. However, the HP/HB cycle is aerobic and requires another half turn of the cycle to make succinyl-CoA, which is oxidatively converted to oxaloacetate, pyruvate, and PEP. Consequently, the HP/HB cycle functions in (micro) aerobic *Sulfolobales*, and the DC/HB cycle is present in most of the anaerobic autotrophic representatives of *Thermoproteales* and *Desulfurococcales*.

In **Figure 1-6**, cycle-A shows the dicarboxylate/4-hydroxybutyrate cycle functions in *Desulfurococcales* and *Thermoproteales*; while cycle-B presents the 3-hydroxypropionate/4-hydroxybutyrate cycle functions in *Sulfolobales*. Note that succinyl-CoA reductase in *Thermoproteales* and *Sulfolobales* uses NADPH and probably reduced ferredoxin in *Desulfurococcales*. Enzymes numbered in **Figure 1-6** are as following: 1, pyruvate synthase; 2, pyruvate:water dikinase; 3, PEP carboxylase; 4, malate dehydrogenase; 5, fumarate hydratase; 6, fumarate reductase (natural electron acceptor is not known); 7, succinyl-CoA synthetase; 8, acetyl-CoA/propionyl-CoA carboxylase; 9, malonyl-CoA reductase; 10, malonic semialdehyde reductase; 11, 3-hydroxypropionate-CoA ligase; 12, 3-hydroxypropionyl-CoA dehydratase; 13, acryloyl-CoA reductase; 14, methylmalonyl-CoA epimerase; 15, methylmalonyl-CoA mutase; 16, succinyl-CoA reductase; 17, succinic semialdehyde reductase; 18, 4-hydroxybutyrate-CoA ligase; 19, 4-hydroxybutyryl-CoA dehydratase; 20, crotonyl-CoA hydratase; 21, (S)-3-hydroxybutyryl-CoA dehydrogenase (NAD^+); 22, acetoacetyl-CoA^+-ketothiolase. Fd, ferredoxin [13].

In addition to all these CO_2 sequestration pathways, it has been suggested that the carbonic anhydrase enzyme (CA) plays a role in CO_2 sequestration, especially associated with the autotrophic pathways (**Figure 1-7**). CA is a metalloenzyme containing Zn^{2+} ion in its active site,

and is widespread in animals, plants, and prokaryotes (bacteria and archaea) [14]. Two general roles have been suggested for known CA enzymes: i) transport of CO_2 or HCO_3^- and ii) to provide CO_2 or HCO_3^- for enzymatic reactions. The catalysis by CA is known to play important roles in various biological processes; such as, ion exchange, respiration, pH homeostasis, CO_2 acquisition, and photosynthesis. Moreover, in literature it can be seen that five different classes of CA have been identified so far in which three were characterized in bacterial systems and the two were identified in archaea [16-18]. However, in bacteria, α and β classes of CA are widespread [19, 20]. The prokaryotic CA has been purified from only five prokaryotes, since it was first identified in *Neisseria sicca* in 1963, and prokaryotic CA has not been studied extensively [18]. A recent study showed that *Serratia* sp., a chemolithoautotrophic bacterium, isolated from marble rocks can sequester CO_2 through its CA enzyme containing metabolism [16].

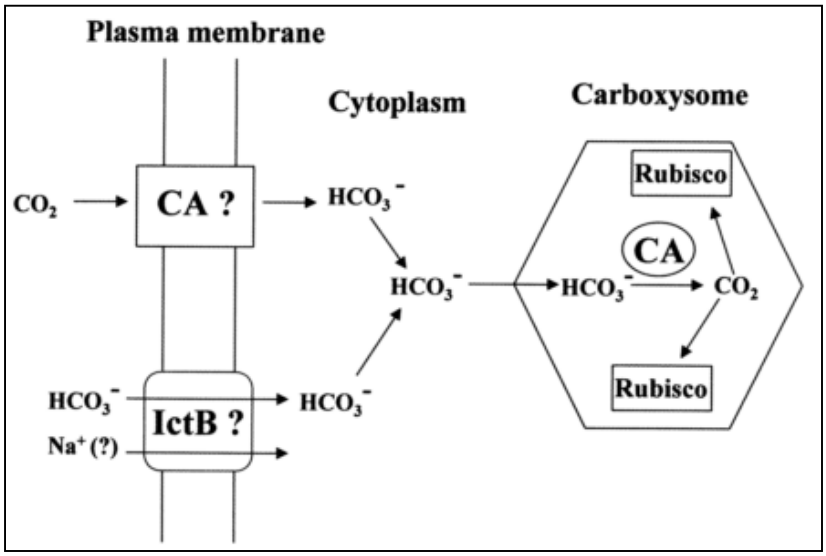

FIGURE 1-7 THE ROLE OF CARBONIC ANHYDRASE IN CYANOBACTERIA [18].

The prokaryotic CA enzyme is assumed to be located both in the cytoplasm and in the cell membrane [18]. The CO_2 required by the cell is typically transported into the cell by hydration reactions depending upon bicarbonate and CO_2 concentration. This transport is done by means of conversion of CO_2 into bicarbonate, and occurs very frequently. In autotrophic metabolisms,

however, CA has another main role in catalyzing the conversion of HCO_3^- into CO_2 (**Figure 1-7**) [18, 19]. All these are represented in **Figure 1-7**; i) active transport of inorganic carbon (CO_2 and HCO_3) into the cell by energy dependent transporters with resultant accumulation of HCO_3^- within the cell, and ii) generation of elevated CO_2 levels for efficient CO_2 fixation by Rubisco within the organelles termed carboxysome. In this second mechanism, bicarbonate freely diffuses into the carboxysomes where CA catalyzes its dehydration into CO_2 for consumption by Rubisco [18]. In **Figure 1-7**, the term IctB refers to a sodium-dependent bicarbonate transporting protein.

Besides the role of CA enzymes in the autotrophic cells, CA also plays an important role in ureolytic bacterial cells' pH regulation processes. For better understanding, this process was pictured in **Figure 1-8**, which explains the periplasmic buffering of *Helicobacter pylori*, a ureolytic bacterium [21].

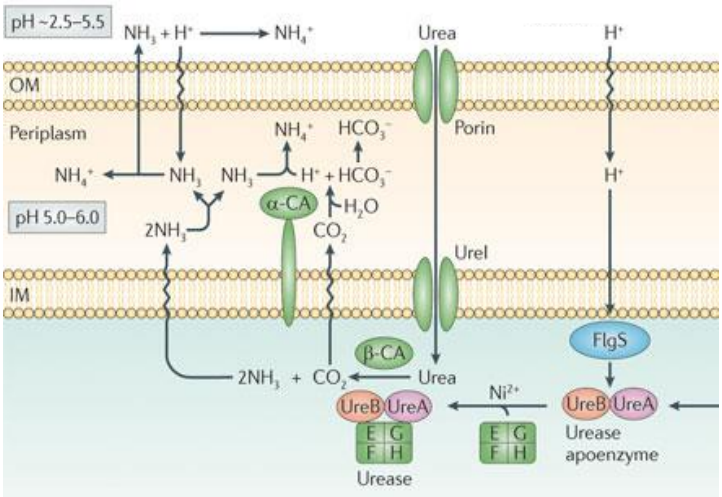

FIGURE 1-8 THE ROLE OF CARBONIC ANHYDRASE IN HELICOBACTER PYLORI [21].

In **Figure 1-8**, urea crosses the outer membrane (OM), and then the inner membrane (IM) through the acid-activated urea channel (UreI) at an external pH<6. Cytoplasmic urease forms NH_3 and H_2CO_3, and then the latter is converted to CO_2 by cytoplasmic β-carbonic anhydrase (β-CA). These cross the IM, and the CO_2 is converted to HCO_3^- by the membrane-bound α-carbonic

anhydrase (α-CA), thereby maintaining periplasmic pH at ~6.1. Exiting NH_3 neutralizes the H^+ that is produced by CA, as well as the entering H^+, and can also exit the OM to alkalize the medium. This process allows maintenance of a periplasmic pH that is much higher than the pH of the medium in *H. pylori* [21].

In addition to these pathways, in 1930s, Wood and Werkman claimed for the first time that carbon dioxide can be reduced during the fermentation of glycerol by propionic acid bacteria heterotrophically [22]. Afterwards, other researchers explained it further, and stated that active carboxylase enzymes in heterotrophs play a role in the intermediary metabolisms of cells. They also explained that 3-8% of the organic carbon in the heterotrophic bacteria may come from the CO_2 metabolized via carboxylation reactions. This can be done by chemoorganoheterotrophic microorganisms [23]. The CO_2 assimilation by carboxylation reactions of heterotrophs involve enzymes, such as pyruvate carboxylase, phosphoenol pyruvate carboxylase, carbamylphosphate synthetase, and acetyl CoA carboxylase, which can also be found in the autotrophic reactions described previously. Using ATP or similar molecules, most of these enzymes play a role in gluconeogenesis, fatty acid synthesis, and synthesis of nucleotides and some amino acids [23]. It was also found that the level of CO_2 assimilation depends on the organic substrates metabolized [24]. For example, a study with *Pseudomonas* sp. MS showed that cells assimilated 2.1% of the cell carbon from CO_2 when there was glucose in the growth medium, however, when cells were grown on methylamine, the assimilation went to up to 47.1%. Furthermore, researchers showed that the assimilation of CO_2 was also related to the variations of the concentration of CO_2 in the headspace [24]. These findings indicate that bacteria can be good candidates for biotechnological CO_2 capturing.

Recently, MICP has been shown to be an alternative, ecofriendly and economical method for CO_2 capturing [25]. The basic advantage of MICP is its ability to sequestrate atmospheric CO_2 through calcium carbonate formation [7]. In the next sections, the CO_2 sequestration through MICP will be discussed.

1.3 IMPORTANCE AND ORIGIN OF CALCIUM CARBONATE FORMATIONS

Calcium carbonate ($CaCO_3$) is estimated to be 4% of the Earth's crust. It is naturally found in the environment, such as sedimentary rocks, limestone, marble and calcareous sandstones [1]. It is used by several industries, such as construction, paint, plastic, rubber, ceramic, glass, steel, oil refining and paper industries, drinking and wastewater treatment, and fabrication of biocompatible composite materials for drug delivery and protein encapsulation [26-35]. Carbonate precipitation is essentially a function of carbonate alkalinity and the availability of free calcium ions. Precipitation of calcium carbonate occurs when concentrations of both free carbonate and calcium ions exceed saturation [36]. In nature, calcium carbonate precipitation occurs in a wide range of environments and are involved in the formation of microbioalites [37, 38], stromatolites [39], ooid and grains [40], ocean whiting events [40, 41], desert crust soils [36], soil precipitates [42], thrombolites, and hypersaline mats [43].

Calcium carbonate precipitation occurs with this chemical equation;

$$Ca^{2+} + 2HCO_3^- \rightarrow CaCO_3 + CO_2 + H_2O \ . \qquad (1\text{-}8)$$

However, this equation does not predict the mineralogy, morphology and crystal size of what will be formed. In fact, these are closely linked to the presence of other ions and molecules in the environment, and also depend on the microbiological activity in the precipitation of carbonated species [44]. Precipitated carbonates has different polymorphs, and the most common one is calcite, which is the most abundant and thermodynamically stable mineral at

surface conditions. Aragonite is another common mineral, which is found in shells of aquatic organisms, but is rare in soil profiles since it gradually recrystallises into ordered calcite at earth surface conditions. Vaterite, which also occurs in aquatic shells, has been rarely identified in soil as a precipitate produced by soil microorganisms [44].

In the literature, the following processes have been described to be related to $CaCO_3$ formation [4]: i) abiotic chemical precipitation; ii) external or internal skeleton synthesis by eukaryotes; iii) fungal mediation; and iv) bacterial mediation. These will be discussed in the following sections.

1.3.1 ABIOTIC CALCIUM CARBONATE PRECIPITATION

Abiotic precipitation is typically considered unrelated to biological activity to some extent. However, some organisms can play a synergistic role in carbonate precipitation in abiotic processes. This is especially true in near-surface environments where carbonate precipitation is tremendously complicated by the geochemical impacts of organisms [45].

In the abiotic process, minerals from water are fundamentally controlled by the thermodynamics of the carbonate systems [45]. The formation of $CaCO_3$ follows a typical homogeneous crystallization model, where the crystals grow until they reach micrometers size. The saturation state directly affects the structural progression of precipitates formed. Under high supersaturation conditions, there is a step-wise process to the crystallization followed by precipitation. Studies showed that by mixing $CaCl_2$ and Na_2CO_3 solutions will lead to the formation of an emulsion-like structure. This structure is decomposed of $CaCO_3$ nanoparticles, which then aggregates to form spheres having several micrometers in diameter. Finally, the spheres are transformed via dissolution and recrystallization to form distinct calcite structures [36]. For instance, in hard-water lakes, calcite precipitation is a prominent phenomenon that can

occur when the product of the calcium and carbonate ion activities exceeds calcite's solubility by creating an oversaturated environment [46]. In order for inorganic carbonates to precipitate at all, concentrations of calcium ions and carbonate ions must be elevated to the point that supersaturation is reached. At 25°C and 1 atm pressure, thermodynamic equilibrium for calcite is expressed as:

$$\alpha_{Ca^{2+}} \cdot \alpha_{CO_3^{2-}} = K_{calcite} = 10^{-8.48}, \quad (1\text{-}9)$$

where α refers to the activity of the ion, generally some fraction of the ion's concentration, and *K* is the thermodynamic constant for the mineral. When α is greater than $K_{calcite}$, the mineral is supersaturated. For this to occur, high levels of calcium, carbonate, or both are required. This occurs easily in evaporative concentration processes [45].

The abiotic precipitation depends on the following operating variables; such as pH of the solution, solute concentration, temperature of the reaction medium, and ionic strength of the media affect the crystal growth [47]. Moreover, the oversaturation depends on multiple factors; such as air exchange, photosynthesis, respiration, and decomposition of organic matter, which were previously shown as the factors affecting the rate of calcite precipitation. In the case of temperature, direct and indirect effects have been shown to affect the precipitation rate. As a direct effect of temperature, rising temperatures contribute to oversaturation by decreasing calcite's solubility while shifting the inorganic carbon equilibrium towards carbonate. On the other hand, the indirect effect of temperature occurs through biological processes of photosynthesis, and respiration and decomposition, as well as the air-water exchange of CO_2. These potentially change the carbonate ion concentration in the water and the degree of calcium carbonate saturation. Photosynthesis affects the CO_2 concentration by raising the local pH with an attendant shift of inorganic carbon speciation towards carbonate to induce abiotic

precipitation [46, 48]. It has also been found that increasing concentrations of dissolved CO_2 lowers the pH. Therefore, a continuous supply of biogenic CO_2 to surface waters can suppress the calcite precipitation, even if the calcium ion concentrations are high [49].

As described above, pH changes are assumed as a second common mechanism that induces the precipitation of inorganic carbonates. Dissolved inorganic carbon can be thought as dissolved CO_2, which in the water tends to form carbonic acid (H_2CO_3). The pH of the water, however, will ultimately determine the overall state of protonation of the carbonic acid: H_2CO_3 dominates low-pH water, HCO_3^- dominates neutral waters, and CO_3^{2-} is the dominant form only in very high-pH water (**Figure 1-9**). Ultimately, CO_3^{2-} is related to pH and P_{CO2} according to this relationship [45]:

$$\alpha_{CO_3{}^{2-}} = P_{\mathrm{CO2}}\, K_{\mathrm{H}}\, K_1\, K_2\, \alpha_{H^+}, \qquad (1\text{-}10)$$

where K_H=$10^{-1.5}$, and the dissociation constants of carbonic acid are K_1=$10^{-6.35}$ and K_2=$10^{-10.33}$. Thus, changes in P_{CO2} or pH have a direct impact on the α in Eq. 1-9. These mass balance relationships are essential in the control of inorganic carbonate precipitation [45].

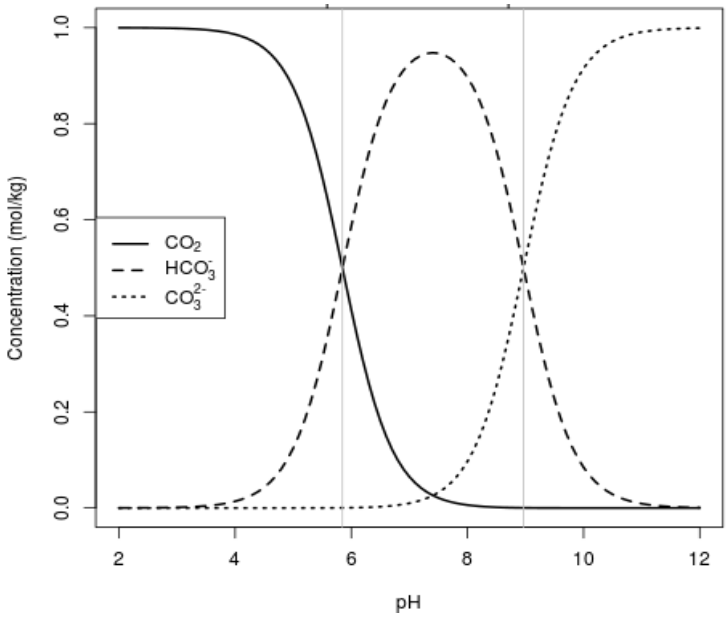

FIGURE 1-9 CARBONATE SYSTEM IN WATER [50].

1.3.2 BIOGENIC CALCIUM CARBONATE PRECIPITATION AND EXTERNAL OR INTERNAL SKELETON SYNTHESIS BY EUKARYOTES

Eukaryotes exert an exceptional control over the polymorphism, orientation and morphology of mineral produced through a series of biochemical processes generally called biomineralization [51]. In biomineralization processes, organic molecules and living eukaryotic and prokaryotic cells are involved [36]. For instance, the skeletal biomineralization is carried out in a controlled metabolic fashion and requires directed transport of calcium and carbonate, as well as molecular templates to guide mineral nucleation and growth [52].

It is generally recognized that the eukaryotic biomineralization involves the following steps; i) the fabrication of a hydrophobic solid organic substrate, ii) nucleation of crystalline materials associated with polyanionic molecules, iii) the crystal growth, and iv) the termination of the process by secretion of inhibitory molecules. These steps are commonly observed in the production of calcite, aragonite, vaterite, or amorphous calcium carbonate to form animal skeletons and shells. Well studied examples of eukaryotes doing biomineralization are corals and mollusk shells [51]. These organisms precipitate calcium carbonates as aragonite [53].

Besides aragonite, calcite and vaterite are also the most observed calcium carbonate polymorphs in eukaryotic organisms. All these biologically-controlled calcium carbonate precipitations are associated with photoautotrophic, heterotrophic or mixotrophic nutrition. In these precipitation reactions, organisms actively expel calcium ions through the ATPase pump to maintain low intracellular calcium concentrations. As calcium ion is pumped out of the cell, in exchange for two hydrogen ions pumped into the cell, the pH increases and calcium concentration heightens the calcium carbonate saturation state near the extracellular membranes, which in return induces or enhances calcification [54].

Examples of organisms producing calcite and vaterite are sponges, hydrozoans, algae, and foraminifers [54]. Species of earthworm also have been shown to produce calcium carbonate particles in the form of 0.1-2.5 mm. These granules of calcium carbonate have been observed as aggregates of individual calcite crystals arranged in radial, parallel or random pattern depending on earthworm species [44].

1.3.3 FUNGAL MEDIATION

In literature, researchers have shown that fungi also play a part in rock decay and diagenesis by biomineralization processes. Investigations in desert sediments and soils have shown that the microflora of fungi is very abundant and produces an appreciable amount of oxalic acid. The oxidation of oxalic acid leads to a pH increase and eventually to carbonate precipitation [55]. The oxalic acid produced reacts with the calcium carbonate, releasing carbonate ions available for secondary calcite precipitation. The calcium carbonate precipitates are typically light-colored calcite recrystallization rings, which contribute to harden the soft limestone [56]. A study investigating the role of the oxalate-carbonate pathway in calcite production demonstrated the potential long-term terrestrial sink for atmospheric CO_2 through this pathway. In that study, oxalate production by fungi and degradation by bacteria was associated with a strong local alkalinization and subsequent calcification. This calcification was mainly due to the pH shift caused by this synergistic reaction, which is required for calcification [57]. In another study, lichens were shown to produce calcium oxalate, which allowed the formation of crusts on rock surfaces. Optical analyses of these organic minerals showed that they are very similar to calcite [44]. These studies suggest that weddellite ($CaC_2O_4.2H_2O$) forms at the first stage of fungal filament mineralization. After which, more stable monohydrate crystals

are formed and calcium oxalate is transformed to calcium carbonate by bacteria, resulting in the formation of calcified fungi filaments [44].

1.3.4 BACTERIAL CARBONATE PRECIPITATION

Bacterial cells have been revealed to have cell size and cell structures that can serve as excellent nucleation sites during rock formations [58]; and to have the ability to change their surrounding environmental pH to favor calcium carbonate precipitation [59]. The high 'surface area to volume ratio' of bacteria and the presence of charged chemical functional groups on the bacterial cell surfaces make bacteria ideal for mineral nucleation [5]. In fact, bacterial cells are divided into two groups based on their cell wall structures; namely Gram-positive and Gram-negative. Each group has different chemical cell wall structure, but the main charged chemical constituents, which can be found in all bacterial cells (at neutral pH), are carboxyl, phosphoryl, and amino groups. At neutral pH, negatively-charged groups dominate over positively-charged ones, and give the cells an overall anionic charge [5, 60]. Furthermore, in some studies, extracellular polymeric substances (EPS) and gelatinous sheaths of many unicellular and filamentous bacteria have been found to be important for trapping abiotically formed $CaCO_3$ precipitates and enhancing the precipitation [36, 61, 62].

The production of calcium carbonate particles through bacterial mediation follows different pathways. One of them is autotrophy, which can produce calcium carbonates by non-methylotrophic methanogenesis, anoxygenic photosynthesis, and oxygenic photosynthesis [4]. All three autotrophic pathways use CO_2 as carbon source to produce organic matter and carbonates (**Figure 1-10**) [4]. Thus, they induce CO_2 depletion of the medium or of the immediate environment surrounding the bacteria. When calcium ions are present in the medium such depletion favors calcium carbonate precipitation [63].

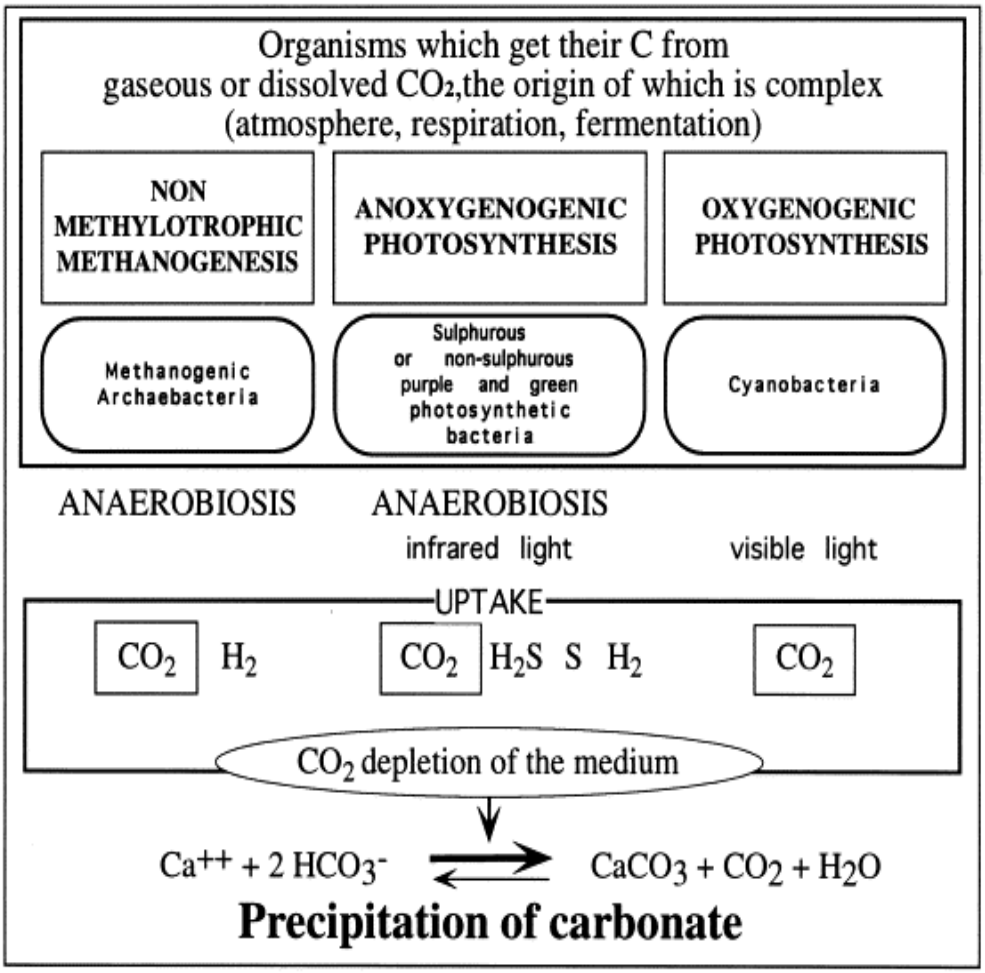

FIGURE 1-10 BACTERIAL $CACO_3$ PRECIPITATION IN AUTOTROPHY [4].

Another metabolism in bacterial mediation is heterotrophy. This one produces calcium carbonates by different bacterial metabolisms and typically involves the nitrogen and sulfur cycles. In the nitrogen cycle (**Figure 1-11**), precipitation can be induced by three pathways: i) the ammonification of amino-acids aerobically (in the presence of oxygen, organic matter and calcium), ii) the dissimilatory reduction of nitrate anaerobically or microaerophilically (in the presence of very low or no oxygen, organic matter, calcium and nitrate), and iii) the degradation of urea aerobically (in the presence of organic matter, calcium, and urea or uric acid).

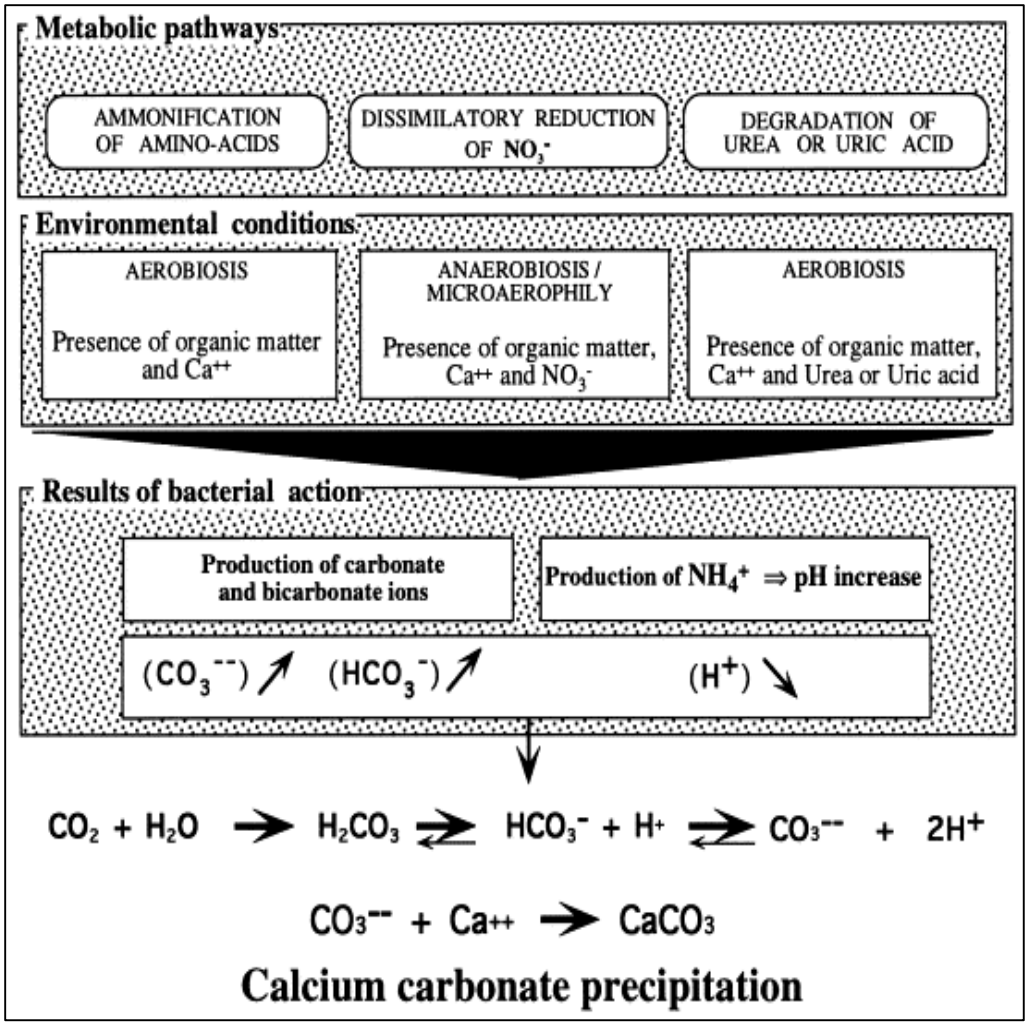

FIGURE 1-11 BACTERIAL PRECIPITATION OF $CACO_3$ IN THE NITROGREN CYCLE [4].

These three pathways of nitrogen cycle induce the production of carbonate and bicarbonate ions, and ammonia, which leads to pH increases. At high pH, the H^+ concentration decreases and the carbonate–bicarbonate equilibrium shifts towards the production of carbonate ions. If calcium ions are present, calcium carbonate precipitation occurs.

In the heterotrophic metabolism involving the sulfur cycle, the precipitation of calcium carbonate occurs through the dissimilatory reduction of sulphate in anoxic and organic matter-, calcium- and sulphate-rich environments (**Figure 1-12**). If calcium ions are present, the precipitation of calcium carbonate occurs [4].

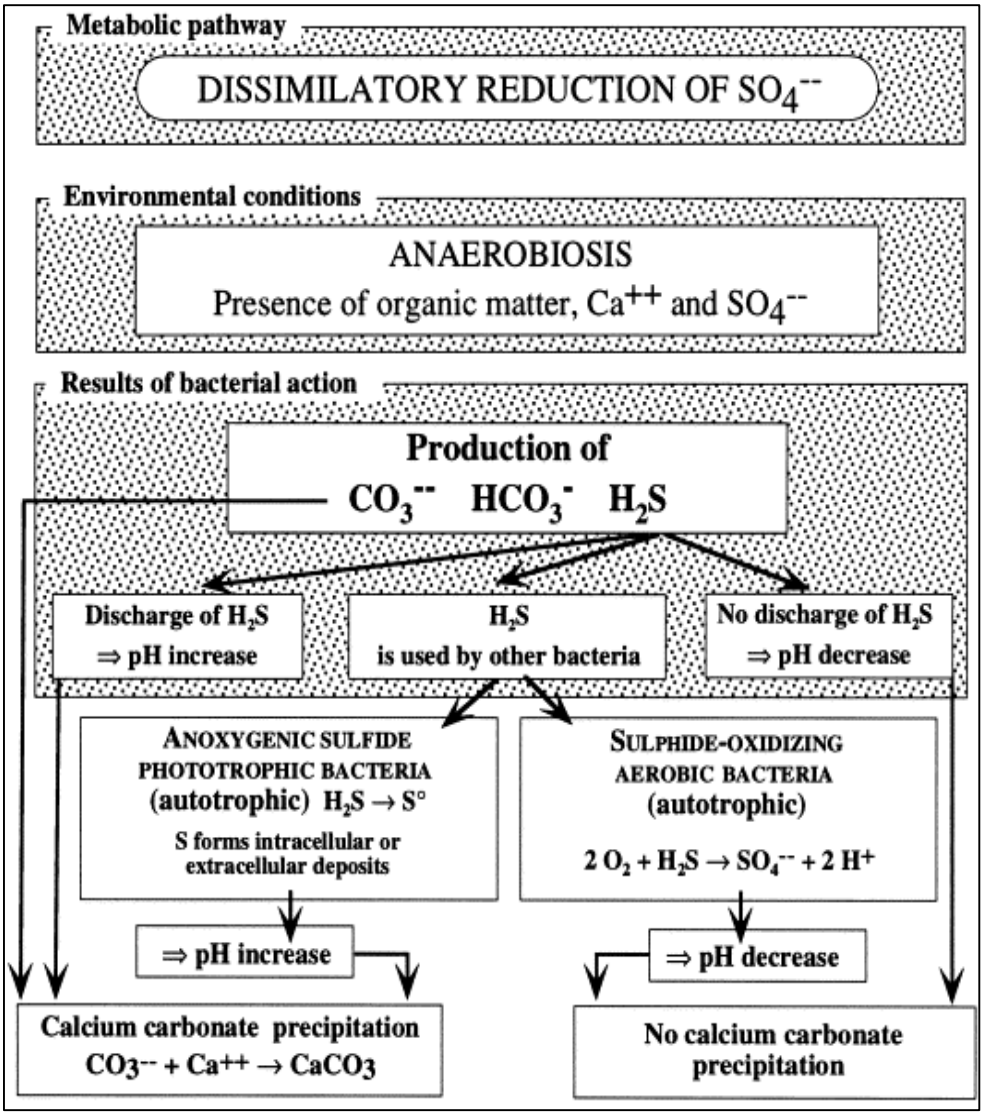

FIGURE 1-12 BACTERIAL PRECIPITATION OF $CACO_3$ IN THE SULPHUR CYCLE [4].

Based on this literature review, it is clear that the calcium carbonate precipitation is a common process frequently facilitated by microorganisms. This phenomenon has been extensively investigated with soil bacteria producing $CaCO_3$ crystals, but little is known about the karstic environments [64]. In these environments, the $CaCO_3$ crystals are found in five crystalline forms; calcite, aragonite, vaterite, monohydrocalcite and ikaite. Amongst them, calcite and aragonite are the two most common forms precipitated through bacterial mediation. Moreover, these crystalline forms are highly ordered and consist of the mineral only (such as, calcium and

carbonate). On the other hand, in the bacterial mediation, it is likely that few crystals are entirely inorganic. In fact, different types of organics, ranging from decaying organic matter to extracellular substances, have been implicated in the formation of biominerals having the size ranges from nanometers to microns [36]. Related to this, previous studies have shown that precipitated minerals are trapped in EPS, and specific portions of EPS were shown to serve as initiators or enhancers of the precipitation process [36, 65, 66].

Amongst the metabolic reactions associated with the bacterial $CaCO_3$ precipitation, urea hydrolysis by the urease enzyme is the simplest and has been the most extensively investigated mechanism [5, 6], but its role in carbon sequestration has not been fully explored. Therefore, in this dissertation, MICP with the ureolysis will be investigated.

1.4 THE IMPORTANCE AND ROLE OF UREOLYTIC BACTERIA IN CALCIUM CARBONATE PRECIPITATION

Urea is an organic nitrogenous compound occurring in natural environments. Urea is excreted in the urine of all mammals and is commonly used as an agricultural fertilizer. This compound is readily degraded by microorganisms in the environment due to the diverse population of urea-degrading (ureolytic) microorganisms in aquatic and terrestrial environments. Recently, the carbonate precipitation process through bacterial ureolysis has been adapted for mineral plugging and porous media cementing [58, 59, 67]. The precipitation of carbonates by ureolytic bacteria has been claimed to be the most straightforward and easily controlled mechanism to precipitate high amounts of calcites in a short period of time. Researchers, have therefore, mimicked nature to synthetically produce biocements from carbonate precipitates induced by microbes to protect and remediate building structures and materials [68], and a summary of these studies can be found in **Table 1-1**.

TABLE 1-1- OVERVIEW OF STUDIES WHERE MICROBIALLY INDUCED CALCITE PRECIPITATION WAS USED AS BIOCEMENT.

Inoculum	Method	Evaluation procedures	Authors
Culture in exponential phase: $10^7 – 10^9$ cells/mL	Spraying (5 times)	Water absorption, SEM analysis, surface roughness, colorimetric measurements, and plate count.	Le Metayer-Levrel et al., 1999.[69]
Overnight culture 10^6 cells/cm^2	Brushing on water saturated specimens, Wetting every day for 15 days	Water absorption, colorimetric measurements, and stone cohesion.	Tiano et al., 1999.[70]
2% inoculums	Immersion in growing bacterial culture (shaking or stationary conditions) for 30 days	Stone cohesion, weight increase, XRD and SEM analyses, porosimeter analysis.	Rodriguez-Navarro et al., 2003.[71]
1% inoculums	Immersion in growing bacterial culture (intermediate wetting) for 28 days	Water absorption and SEM analysis.	Dick et al., 2006.[72]
10^8 cells/mL	Spraying	Water absorption and drying due to evaporation, SEM and XRD analyses.	Anne et al., 2010.[73]
NA*	Immersion in test solution or spraying tests	Water absorption, colorimetric measurements, stone cohesion, staining of newly formed calcite.	Tiano et al., 2006.[74]
Overnight culture $10^7 – 10^9$ cells/mL	Immersion for 1 day	Water absorption, weight increase, gas permeability, chloride migration, carbonation, freezing and thawing, SEM and XRD analyses.	De Muynck et al., 2010.[75]

NA, not applicable.*

Other MICP studies aimed to gain a better understanding on the applicability of the MICP process for remediation of calcium ions, heavy metals and radionucleotides from soil and water [76], develop solutions for biodegradation of pollutants [77], sequester atmospheric CO_2 [50, 78], and modify the soil properties [79, 80]. Hence, it can be seen that the bacterial carbonates have been serving in many fields.

Microorganisms able to synthesize the urease enzyme are usually called urea-hydrolyzing bacteria, ureolytic bacteria, or urease-positive bacteria. Some of these microorganisms have been shown to play an important role in the MICP. The reactions involved in the MICP have been, however, described to be affected by various environmental factors, such as the presence of urea, calcium and nickel ions [75, 79, 81-85]. The stoichiometric reactions of urea hydrolysis are given below in Eqs. 1-11 to 1-13 [6, 72, 75, 84]:

$$H_2NCONH_2 \text{ (urea)} + H_2O \rightarrow 2NH_3 + CO_2 , \quad (1\text{-}11)$$

$$2NH_3 + CO_2 + H_2O \leftrightharpoons 2NH_4^+ + CO_3^{2-} , \text{ and} \quad (1\text{-}12)$$

$$Ca^{2+} + CO_3^{2-} \rightarrow CaCO_3 . \quad (1\text{-}13)$$

During the urea hydrolysis, the urease (urea amidohydrolase: EC 3.5.1.5), a nickel metalloenzyme produced by bacteria, is used and ammonium and bicarbonate ions are produced as byproducts (in Eqs. 1-11 and 1-12). This leads to an increase in pH, which accelerates the calcium carbonate precipitation (in Eq. 1-13) [80, 81, 86]. In the MICP by ureolytic microorganisms, the main role of bacteria has been ascribed to their ability to create an alkaline environment through their physiological activities. The bacterial surface has also been suggested to play an important role as nucleation sites for the precipitation of calcium carbonate, since the negatively charged functional groups found in the bacterial surfaces can bind to positively charged calcium ions (**Figure 1-13** and **Figure 1-14**) [34, 68, 75].

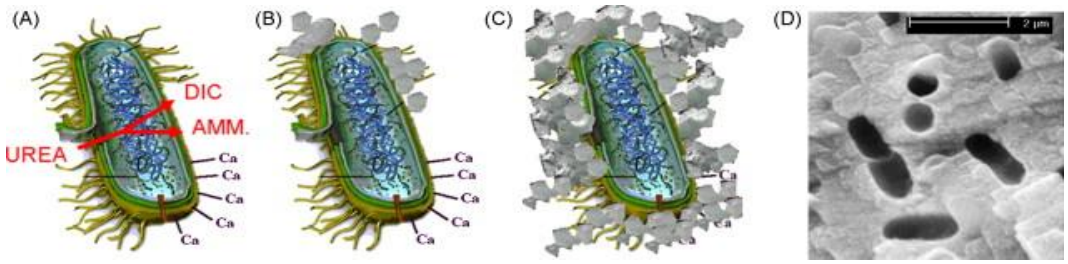

FIGURE 1-13 SIMPLIFIED REPRESENTATION OF THE EVENTS OCCURRING DURING THE UREOLYTIC INDUCED CARBONATE PRECIPITATION [75].

In **Figure 1-13** and **Figure 1-14**, calcium ions in the solution are attracted to the bacterial cell wall since the cell wall is negatively charged. Upon degradation of urea bacteria, dissolved inorganic carbon (DIC) and ammonium (AMM) are released in the micro-environment surrounding the bacteria (**Figure 1-13A**). In the presence of calcium ions, local supersaturation can occur resulting in calcium carbonate precipitation in the presence of the bacterial cell wall (**Figure 1-13B**). After a while, the whole cell becomes encapsulated (**Figure 1-13C**), limiting

nutrient transfer, resulting in cell death. **Figure 1-13D** shows the imprints of bacterial cells involved in this precipitation [75]. **Figure 1-14** shows the chemical process of ureolysis that leads to increase in pH level required for calcite precipitation [34].

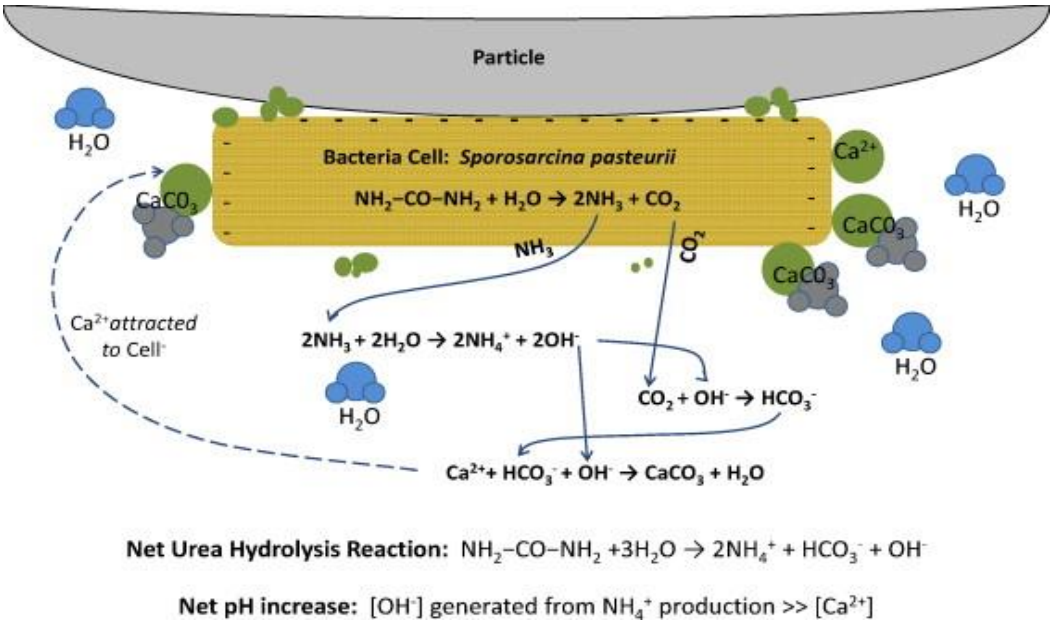

FIGURE 1-14- BACTERIA SERVING AS NUCLEATION SITE FOR $CACO_3$ PRECIPITATION [34].

In the literature, the most studied microorganism involved in MICP is *Sporosarcina pasteurii*. This bacterium was isolated from soil and has been reported many times to be able to precipitate calcite by ureolysis due to its high urease activity [59, 85]. The genus *Sporosarcina*, which belongs to the family *Bacillaceae*, has species that can be differentiated from other members of the *Bacillaceae* family by their coccoid or rod-shaped cells, motility, sporulation, and possession of MK-7 as the major menaquinone and A4α as the peptidoglycan variant [87].

So far, the MICP studies have focused on the mechanisms and kinetics of ureolysis and calcite precipitation as a function of temperature, inoculum size or different calcium and urea concentrations [85]. Besides *S. pasteurii*, other bacterial species have been described to be involved in the MICP, such as *Bacillus* sp. VS1 [79], *Bacillus cereus* [16], *Bacillus subtilis* [88],

Pseudomonas calcis [89], *Pseudomonas fluorescens* [16], *Pseudomonas denitrificans* [53], *Pseudomonas putida* [75], and *Myxococcus xanthus* [71]. Even though these microorganisms have been described to induce MICP, they have not been extensively investigated.

Besides microbial isolates, microbial communities have also been suggested to promote the ureolysis-driven calcite precipitation. These studies suggest that the microbial community must contain sufficient organisms with ureolytic activity [85]. However, very few studies are available describing the role of ureolytic microbial communities in the MICP process [50]. In order to stimulate natural indigenous ureolytic microbial communities, researchers have injected carbon or nitrogen substrates into the system to promote the biomass growth of ureolytic microorganisms [50, 76]. Alternatively, researchers have suggested the injection of urease positive organisms into the environment to provide the desired ureolytic activity [85].

In summary, several studies with MICP were done with ureolytic isolates, only one study so far was done *in situ* in a groundwater system [76]. Therefore, future studies should explore *in situ* assays of carbonate precipitation with complex microbial communities to gain a better understanding of the MICP process in the environment.

1.5 METHODS FOR THE SELECTION OF UREOLYTIC MICROORGANISMS

1.5.1 CURRENT METHODS

In the all the previous studies to obtain ureolytic microorganisms, traditional methods for urease activity determination have been used. The Stuart's broth is the quickest assay to determine whether a microorganism is urease-positive [90]. In this assay, bacteria are grown in the Stuart's broth, which consists of KH_2PO_4, K_2HPO_4, urea, yeast extract, and phenol red. Another common urease assay involves streaking the cultures on Christensen's agar plates [91], which contain peptone, dextrose, NaCl, KH_2PO_4, urea, phenol red, and agar (For detailed

protocols, please see Chapter 3). In both tests, the medium turns pink when there is urea hydrolysis (**Figures 1-15 and 1-16**) [92].

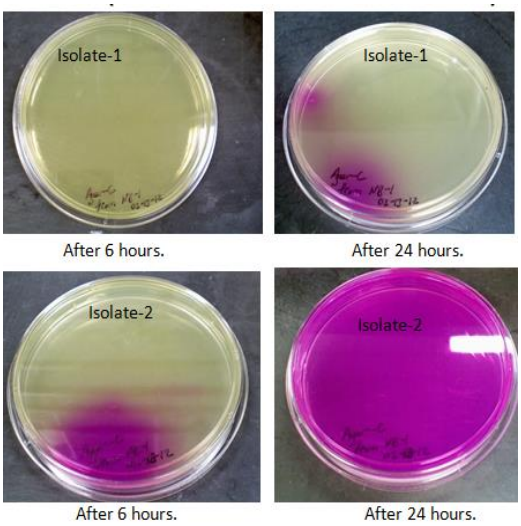

FIGURE 1-15- QUICK UREASE TEST WITH THE CHRISTENSEN'S UREA AGAR PLATES.

FIGURE 1-16- QUICK UREASE TEST WITH THE STUART'S BROTH.

The activity of the urease enzyme produced by the microorganisms includes assays that monitor ammonia release[81, 93, 94], $^{14}CO_2$ release[95], or increase in pH[81, 92]. The indophenol assay measures the amount of ammonia released to the medium. This method allows the reaction of ammonia with phenol-hypochlorite at higher pH to form indophenol, which generates an intense blue color that can be quantitatively measured by spectrophotometer. This method has the disadvantage of making measurements at a fixed-time-point, which requires multiple samplings for each assay. Moreover, several urease inhibitors were found to interfere with this method [92]. Another method employs glutamate dehydrogenase or horseradish peroxidase enzymes and measures the amount of ammonia released. This method can continuously

measure spectrophotometrically the reaction. The nonlinearity of the absorbance changes and the requirement of highly alkaline buffers are some of the drawbacks of this method [92].

The Nessler method is another technique, which has been extensively used in the literature. The Nessler method measures the ammonium concentration with the help of the Nessler's reagent (contains KI and HgI_2), which readily reacts with NH_3 in alkaline conditions to form colloidal dimercuric ammonium iodide (Nesslerization reaction). The product changes from yellow to orange-brown depending on the ammonium concentration. Darker colors indicate higher ureolytic activity. This method allows the calculation of the amount of ammonia produced [59, 85]. The method also requires collection and filtration of medium aliquots at regular time intervals to determine the reaction kinetics, and therefore tends to be expensive and laborious [96]. Due to the drawbacks of all these methods, a new high throughput, fast, quantitative and economical colorimetric method was developed within this dissertation to determine the urease activity.

1.5.2 THE NEW METHOD FOR UREASE ACTIVITY DETERMINATION

In this study we describe a rapid, high throughput, and quantitative colorimetric assay to determine urease activity of seven urease-positive (+) and two urease-negative (−) bacteria from diverse environmental sources (**Table 1-2**). All the chemicals used in this study were obtained from Sigma–Aldrich unless stated otherwise. All cultures were incubated for 24h at 150rpm (INNOVA 44, New Brunswick Scientific Co., USA) in their specific growth conditions as described in **Table 1-2**.

After 24h of growth, the cultures were washed and re-suspended in phosphate buffer solution (PBS; 0.01 M, pH 7.4) (Amresco). The bacterial cells were then adjusted to an optical

density of 0.5 at 600 nm with the Synergy MX Microtiter plate reader (BioTek, USA). The Stuart's broth (SB) was used for the proposed assay since it is commonly employed to distinguish urease-positive from urease-negative bacteria [90, 97].

TABLE 1-2- MICROORGANISMS, UREASE ACTIVITIES, ISOLATION SOURCES, AND GROWTH CONDITIONS

Bacteria	Urease activity	Source	Growth Conditions
Sporosarcina pasteurii ATCC 11859	+	Soil	ATCC 1832 medium[1], 27°C
Pseudomonas fluorescens ATCC 17575	+	Polluted seawater	TSB[2], 37°C
Sporosarcina sp. Strain TR1	+	Lake	ATCC 1832 medium[1], 27°C
Sporosarcina sp. Strain TR3	+	Lake	NB3[3], 27°C
Sporosarcina sp. Strain TR20	+	Lake	NB[4], 27°C
Stenotrophomonas sp. Strain TR16	+	Lake	1832-10X[5]
Sphingobacterium sp. Strain CV4	+	Cave	M2[6]
Escherichia coli MG 1655	-	Clinic	TSB[2], 37°C
Escherichia coli ATCC 11303	-	Clinic	TSB[2], 37°C

[1]ATCC 1832 medium contains 10 g/L tryptone, 5 g/L yeast extract, 4.5 g/L tricine, 5 g/L $(NH_4)_2SO_4$, 2 g/L glutamic acid, and 10 g/L urea (Alfa Aesar).
[2]TSB is Tryptic Soy Broth (Himedia).
[3]NB3 medium contains 1 g/L meat extract, 5 g/L peptone, 5 g/L NaCl, 2 g/L yeast extract, and 20 g/L urea.
[4]NB medium contains 3 g/L meat extract, 5 g/L peptone, and 20 g/L urea.
[5]1832-10X medium is 10 times diluted version of ATCC 1832 medium.
[6]M2 medium contains 6 g/L urea, 1 g/L NB, 0.84 g/L $NaHCO_3$.

Suspensions of 30 µL of each microorganism at OD_{600}=0.5 were inoculated in 300 µL of SB in triplicates in a flat bottom 96-well plate. The UV–visible spectrum scans of the plates were performed at 0, 1, 4 and 24 h to determine the wavelength corresponding to the appearance of the pink color in the SB. After the peaks were determined, a new plate was prepared and read at 430 nm and 560 nm every 30 min for 24 h. The color change rates (h^{-1}) were calculated as;

$$Rate = \frac{Absorbance\ at\ t_2 - Absorbance\ at\ t_1}{t_2 - t_1} . \qquad (1\text{-}14)$$

Within all the studies including the urease activity determination; a pure urease enzyme is used as a positive control and/or for the standard curve. For this reason, urease from jack bean

is highly preferred by researchers since this is the best studied urease. Moreover, this was the first enzyme to be crystallized and to be shown to contain nickel [92]. Therefore, the positive controls in the assays consisted of the urease enzyme (from Jack beans) and the negative controls were non-inoculated media. The Jack bean urease enzyme was also used to determine the standard curve of the bacterial enzyme activity (U/mL) for the new method. One unit of urease activity corresponds to the amount of enzyme that hydrolyzes 1 µM of urea per minute.

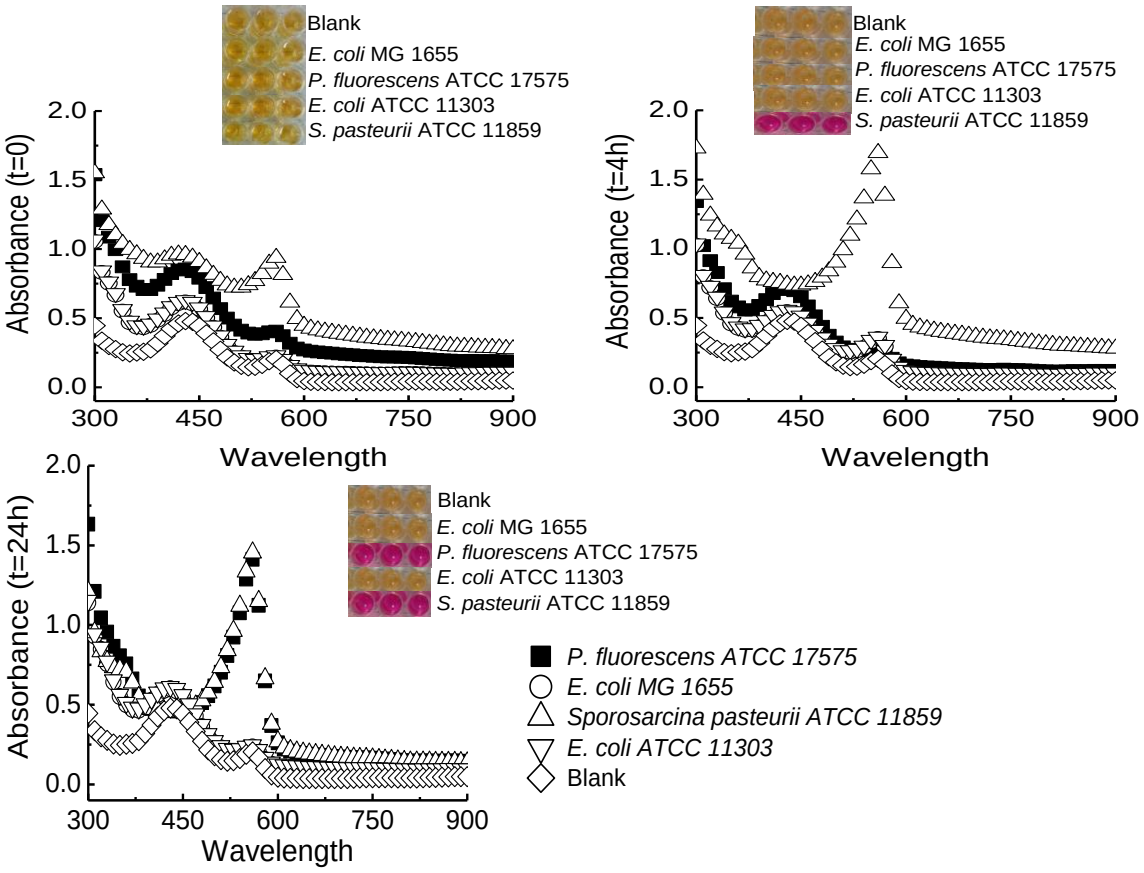

FIGURE 1-17- A REPRESENTATIVE IMAGE FOR THE UV-VIS SPECTRA OF E. COLI MG 1655, P. FLUORESCENS ATCC 17575, E. COLI ATCC 11303, AND S. PASTEURII ATCC 11859 IN STUART'S BROTH. THE BLANK WAS STUART'S BROTH WITH NO CELLS.

The **Figure 1-17** presents a visual and graphical representation of the color change in SB from yellow to pink. At time 0, a peak at OD_{430} was apparent due to the yellow color of the broth, which corresponded to 0 urease activity for all microorganisms. During the incubation, as

the pH changed, due to urea hydrolysis, the peak at 430 nm decreased as the peak at 560 nm appeared and increased over time for the urease positive microorganisms. Throughout the experiments the *E. coli* strains were not able to degrade urea, therefore the yellow color in the media remained the same throughout the experiments, and the absorbance at 430 and 560 nm did not change. These results for the *E. coli* strains were expected since they are well-known urease-negative bacteria [98]. To quantify the urease activity with this new method, the reaction rates (h^{-1}) were calculated from the absorbance data (**Figure1-18**) using Eq. 1-14 and they were correlated with the urease activity based on the standard curve of the urease enzyme (**Figure 1-19**).

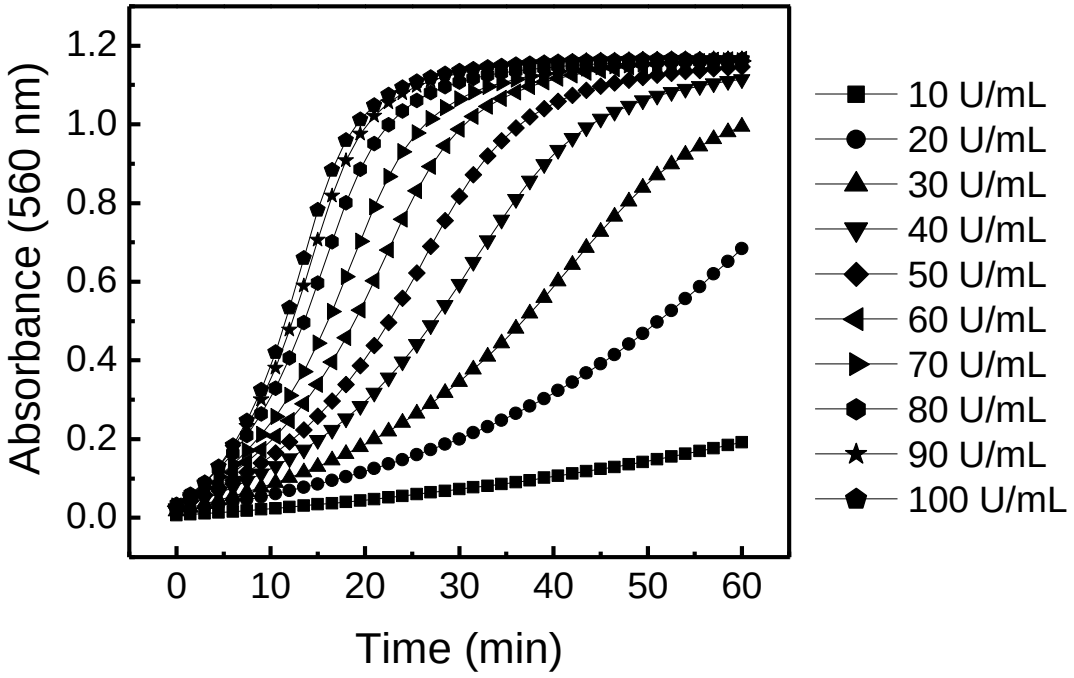

FIGURE 1-18- ABSORBANCE CURVES OF UREASE ENZYME ACTIVITIES (U/ML) IN THE STUART'S BROTH MEASURED AT 560 NM. THE SAMPLES WERE INCUBATED IN THE PLATE READER FOR 1 H AT 28OC IN A SLOW SHAKING MODE SET BY THE INSTRUMENT. ABSORBANCE WAS READ EVERY MINUTE AT 560 NM.

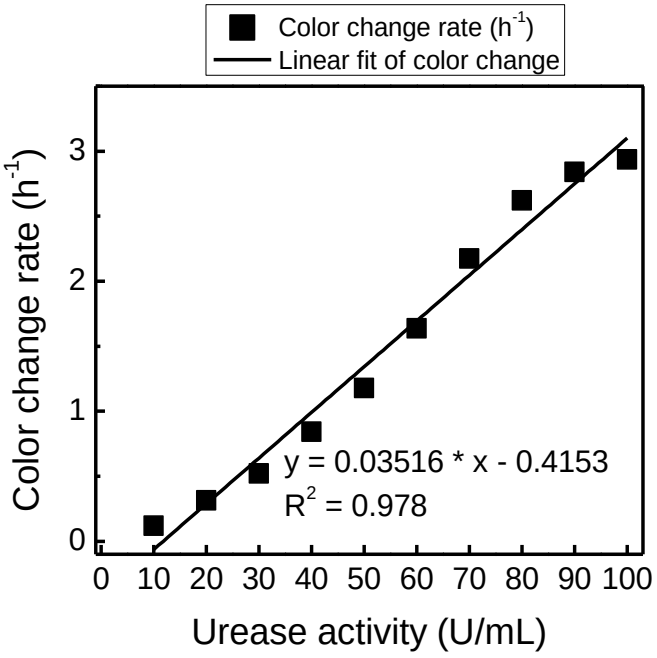

FIGURE 1-19- THE STANDARD CURVE BASED ON THE COLOR CHANGE RATES AND THE UREASE ACTIVITIES (10-100 U/ML).

The results of this method were compared to the standard Nessler method (**Table 1-3**). These two methods showed related but not identical values. It was described that the result and sensitivity of enzyme activity methods can be a function of concentration, reagents, operator, and incubation time [99]. The Nessler method requires sample collection and preparation steps before measurement of the enzyme activity, but the new method does not, which could explain the slightly different results.

TABLE 1-3- COMPARISON OF THE UREASE ACTIVITIES ACHIEVED BY THE NESSLER AND THE NEW METHOD

Bacteria	**Urease activity by Nessler (U/mL)**	**Urease activity by new method (U/mL)**
P. fluorescens ATCC 17575	6.59 ± 0.102	7.54 ± 0.045
E. coli MG 1655	1.54 ± 0.589	0.32 ± 0.009
E. coli ATCC 11303	0.92 ± 0.515	0.317 ± 0.01
S. pasteurii ATCC 11859	17.21 ± 0.55	14.86 ± 0.42
Sporosarcina sp. StrainTR1	4.17 ± 0.35	3.55 ± 0.12
Sporosarcina sp. Strain TR3	5.73 ± 0.02	3.49 ± 0.045
Sporosarcina sp. Strain TR20	9.16 ± 0.52	7.49 ± 0.093
Stenotrophomonas sp. Strain TR16	2.86 ± 0.297	1.913 ± 0.39
Sphingobacterium sp. Strain CV4	1.921 ± 0.34	1.739 ± 0.06

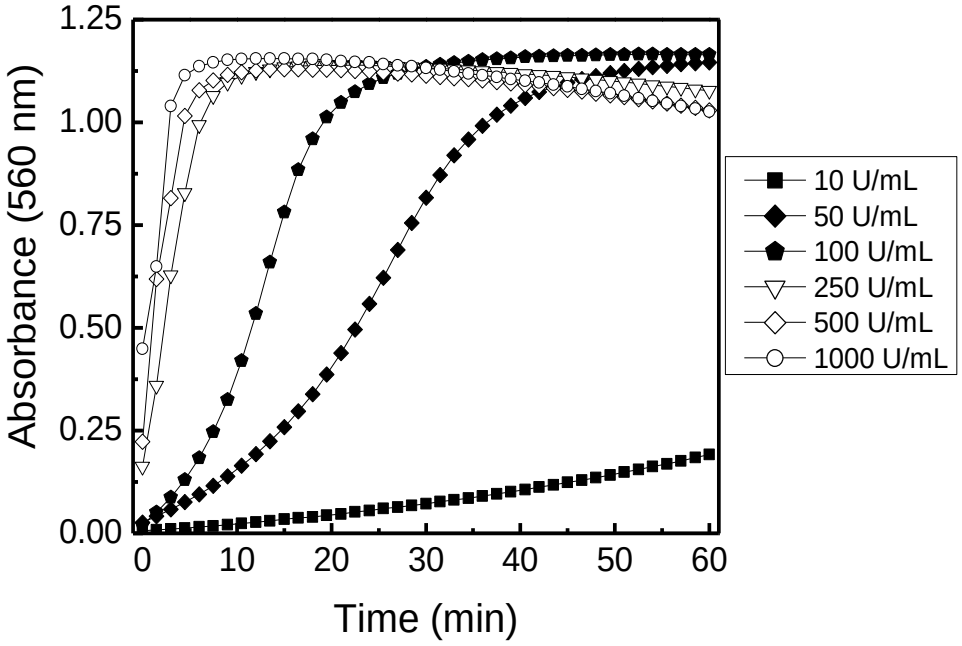

FIGURE 1-20- ABSORBANCE CURVES OF UREASE ENZYME IN THE STUART'S BROTH. THE SAMPLES WERE INCUBATED IN THE PLATE READER FOR 1 H AT 28OC IN A SLOW SHAKING MODE SET BY THE INSTRUMENT. ABSORBANCE WAS READ EVERY MINUTE AT 560 NM.

In addition, it was found that filtration affects the enzymatic activity, which might be another possible cause for the observed variation between the two results [100]. It is worth noting, however, that the new method was in closer agreement with the expected results for both *E. coli* strains than the Nessler method, *i.e.,* close to 0 enzymatic activities, since they are urease-negative bacteria. Additionally, this method has an upper detection limit of 100 U/mL (**Figures 1-20** and **1-21**). These results suggest that the new method is as sensitive as the Nessler method and more rapid. The correlation result between these two assays also represents this conclusion (**Figure 1-22**). In this figure, ρ represents the Spearman's rank correlation. In conclusion, the new method is high throughput, has decreased analysis processing, and a shorter assay work-up. These features make this method a good alternative to the Nessler method for rapid quantification and screening of urease activity.

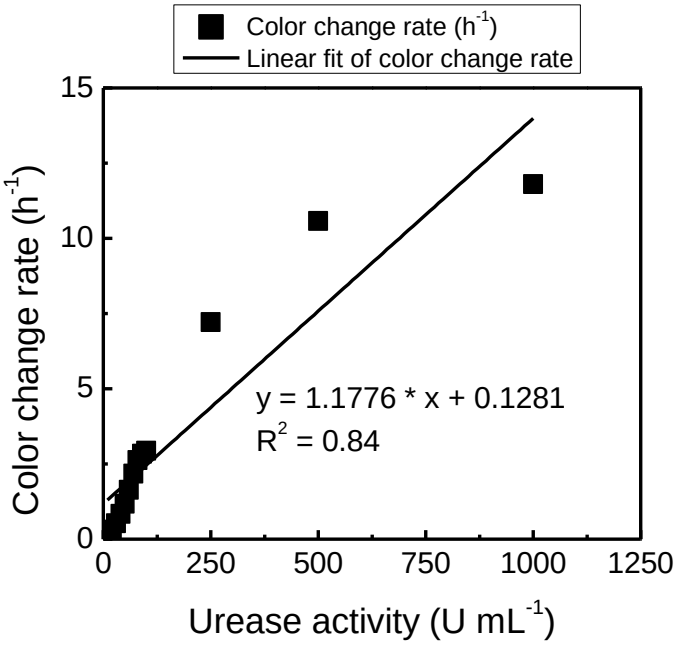

FIGURE 1-21- THE STANDARD CURVE BASED ON THE COLOR CHANGE RATES VERSUS THE UREASE ACTIVITIES. IN THIS GRAPH, ENZYME ACTIVITIES HIGHER THAN 100 U/ML WERE USED TO SHOW THE NON-LINEAR CURVE.

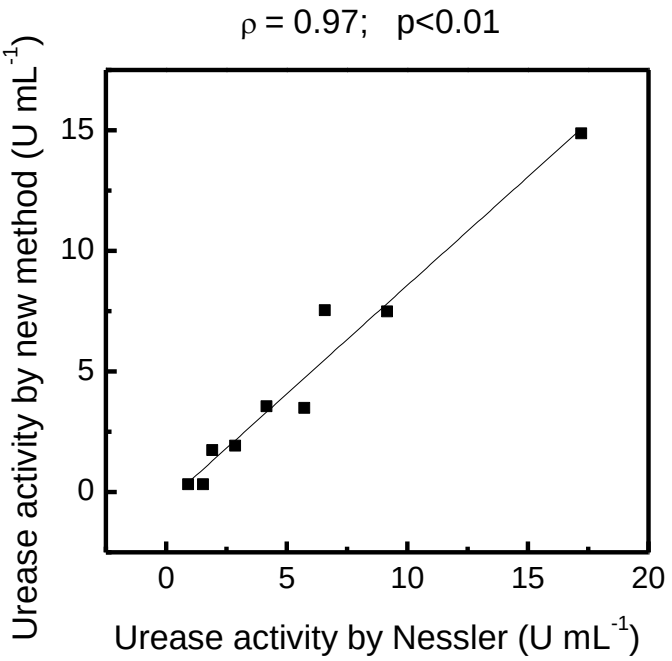

FIGURE 1-22- CORRELATION BETWEEN THE TWO UREASE ACTIVITY METHODS.

CHAPTER 2 CO_2 SEQUESTRATION BY MICROBIAL CONSORTIA DURING MICROBIALLY-INDUCED CALCIUM CARBONATE PRECIPITATION

2.1 RATIONALE AND OBJECTIVES

The increasing concern of global climate change due to increasing emissions of CO_2 has attracted scientists' attention for alternative mechanisms to sequester CO_2. One way for decreasing the atmospheric CO_2 concentrations is converting the CO_2 into carbonate minerals, because mineral carbonation has been presented as a geologically stable and environmentally safe way to store carbon [20]. The major issue with spontaneous chemical carbonate mineral formation is that this process tend to have slow reaction rates and is highly dependent on pH [11]. Biological mineral carbonation formations, called microbially-induced carbonate precipitation (MICP), on the other hand, have recently been suggested to participate in CO_2 sequestration [7, 101]. This biological process consists of a single step CO_2 sequestration process compared to other methods, such as geological and chemical sequestrations [20].

The MICP biological process has been extensively studied in soils [29, 34, 79, 102, 103], but very few studies so far have investigated this process in aquatic environments [67] or their potential role in CO_2 sequestration. The best model aquatic environmental systems to investigate the MICP are karstic environments, such as caves and travertines, since these environments have abundance in calcium ions [104] and are frequently contaminated by urea through different sources, such as through bats' and other mammals' urine [105], and from seasonal or continuous water infiltration from the surface [106-108]. Besides the urea and calcium, the presence of CO_2 has also been shown to play an important role in the MICP process [101].

The MICP process has been hypothesized to have two possible CO_2 sources for the calcium precipitation to happen: i) CO_2 from the air and ii) CO_2 from bacterial ureolysis and respiration. In the latter, the main question is whether the amount of CO_2 produced by bacterial metabolism

will exceed the bacterial capability to sequester CO_2 through MICP, which would lead to no significant CO_2 sequestration.

A recent study, published by our research group demonstrated that some isolates are able to sequester not only the CO_2 produced by their own microbial metabolism, but also excess of CO_2 present in the air [101]. In our study, we also demonstrated that different species had different capabilities of calcite precipitation and CO_2 sequestration; and that environmental conditions played an important role in the metabolism of these isolates and CO_2 sequestration. From this study, we hypothesized that the dominance and abundance of microbial populations involved in CO_2 sequestration in a consortium will determine whether a consortium can successfully sequester CO_2. The rationale for this hypothesis is that in a consortium some species will not be able to sequester CO_2 or will have poor MICP activity to sequester CO_2. These species will compete with the species involved in CO_2 sequestration; and therefore reduce the CO_2 sequestration, if a population non-capable of CO_2 sequestration in a consortium is greater than the population involved in CO_2 sequestration.

In order to investigate this hypothesis, 17 ureolytic consortia were obtained from the 'Cave Without A Name' and 'Pamukkale travertines' using 13 different growth media for ureolytic microorganisms. All consortia were deep sequenced using the Illumina MiSeq to determine their community diversity and structure. Then, community diversity and structure of the different consortia was correlated with CO_2 sequestration through MICP. This study is the first one to: i) employ high-throughput deep-sequencing to characterize ureolytic microbial consortia involved in MICP, ii) evaluate the potential CO_2 sequestration of ureolytic consortia involved in MICP, and iii) distinguish the biotic and abiotic factors affecting CO_2 sequestration during MICP. Lastly, this

investigation identifies genera that could be potentially involved in CO_2 sequestration during MICP in karstic environments.

2.2 MATERIALS AND METHODS

2.2.1 Sample collection and enrichment of consortia

Water samples were collected from two karstic locations; 'Pamukkale travertines' [109, 110], and 'Cave Without A Name' (Boerne, TX, USA). Calcite precipitating consortia were enriched by adding well-mixed aliquots of each water sample in 13 different growth media (10%, v/v). The medium compositions used in the enrichment process of this study are described in **Table 2-1** [50].

TABLE 2-1- MEDIA COMPOSITION AND INCUBATION TEMPERATURES USED FOR BACTERIAL ISOLATION.

Media	Ingredients	Used in the enrichment of
Nutrient Broth (NB)	3 g L^{-1} meat extract, 5 g L^{-1} peptone, 20 g L^{-1} urea, 0.1 g L^{-1} nickel (II) chloride.	Travertine
Nutrient Broth No.1 (NB1)	1 g L^{-1} D-glucose, 15 g L^{-1} peptone, 6 g L^{-1} NaCl, 3 g L^{-1} yeast extract, 20 g L^{-1} urea, 0.1 g L^{-1} nickel (II) chloride.	Travertine
Nutrient Broth No.3 (NB3)	1 g L^{-1} meat extract, 5 g L^{-1} peptone, 5 g L^{-1} NaCl, 2 g L^{-1} yeast extract, 20 g L^{-1} urea, 0.1 g L^{-1} nickel (II) chloride.	Travertine
ATCC 1832 Medium (1832)	10 g L^{-1} tryptone, 5 g L^{-1} yeast extract, 4.5 g L^{-1} tricine, 5 g L^{-1} $(NH_4)_2SO_4$, 2 g L^{-1} glutamic acid, 10 g L^{-1} urea, 0.1 g L^{-1} nickel (II) chloride.	Travertine
Medium 220 (M220)	17 g L^{-1} casein peptone, 2.5 g L^{-1} K_2HPO_4, 2.5 g L^{-1} D-glucose, 5 g L^{-1} NaCl, 3 g L^{-1} soy peptone, 20 g L^{-1} urea, 0.1 g L^{-1} nickel (II) chloride.	Travertine
Medium 2 (M2)	6 g L^{-1} urea, 1 g L^{-1} NB1, 0.1 g L^{-1} nickel (II) chloride, 0.84 g L^{-1} $NaHCO_3$.	Travertine and Cave
Tryptic Soy Broth (TSB)	17 g L^{-1} casein peptone-pancreatic, 2.5 g L^{-1} K_2HPO_4, 2.5 g L^{-1} D-glucose, 5 g L^{-1} NaCl, 3 g L^{-1} soy peptone-papain digest, 20 g L^{-1} urea, 0.1 g L^{-1} nickel (II) chloride.	Travertine
NB-10X	10X dilution of NB	Cave
NB1-10X	10X dilution of NB1	Cave
NB3-10X	10X dilution of NB3	Cave
1832-10X	10X dilution of 1832	Travertine and Cave
M220-10X	10X dilution of M220	Cave
TSB-10X	10X dilution of TSB	Cave

All experiments, including the initial consortium enrichments, were incubated aerobically at 150 rpm (INNOVA 44) for 3 d at 28°C and 20°C for travertine and cave samples, respectively. These temperatures were based on the local temperatures during sampling. TR and CV abbreviations correspond to travertine and cave consortia, respectively.

2.2.2 DNA extraction of consortia, 16S rRNA gene amplification, and sequencing

The total DNA of each consortium was extracted using a DNeasy® Blood and Tissue Kit (Qiagen, Valencia, CA). Triplicate extractions from each consortium were pooled and stored at -20°C until further analysis. DNA quantity and quality were determined with the Agilent 2100 Bioanalyzer (Agilent Technologies, Santa Clara, CA).

Amplicon preparation, library construction, and sequencing were carried out according to Illumina's instructions (16S Metagenomic Sequencing Library Preparation Rev. B, Illumina, San Diego, CA). Amplicons of 460 bp spanning the V3-V4 region of the 16S rRNA gene was amplified using the forward S-D-Bact-0341-b-S-17 (5'-CCTACGGGNGGCWGCAG-3') and reverse S-D-Bact-0785-a-A-21 (5'-GACTACHVGGGTATCTAATCC-3') primers [111]. These primers contained the following overhang sequences necessary for compatibility with Illumina index and sequencing adapters - forward overhang: 5'-TCGTCGGCAGCGTCAGATGTGTATAAGAGACAG -3' and reverse overhang: 5'- GTCTCGTGGGCTCGGAGATGTGTATAAGAGACAG -3'. The DNA was amplified in a 25 µl reaction containing 12.5 ng of DNA template, 2x KAPA HiFi HotStart ReadyMix (KAPA Biosystems, Wilmington, MA), and 0.2 µM of each primer (IDT, Coralville, IA). The following conditions were used for thermal cycling: initial denaturation at 98°C for 20 s and 95°C for 3 min; 25 cycles of 95°C for 30 s, 55°C for 30 s, 72°C for 30 s; and a final elongation step at 72°C for 5 min.

The PCR products were immediately purified using Agencourt AMPure XP beads (Beckman Coulter, Indianapolis, IN). The index PCR was performed in a 50 µl reaction volume containing 5 µl DNA template (from the previous magnetic bead-based PCR clean-up step), 5 µl of each index primer (Illumina Nextera XT Index Kit, 24 index kit), and 25 µl of 2x KAPA HiFi HotStart ReadyMix (KAPA Biosystems). The following conditions were used for thermal cycling: initial denaturation at 98°C for 20 sec and 95°C for 3 min; 8 cycles of 95°C for 30 sec, 55°C for 30 sec, 72°C for 30 sec; and a final elongation step of 72°C for 5 min. The samples were purified using the same magnetic bead-based clean-up procedure used after the 16S rRNA gene PCR step.

After purification, all samples were quantified using a Qubit 2.0 Fluorometer (Life Technologies, Carlsbad, CA) using the Qubit dsDNA BR assay kit (Life Technologies) and diluted 1:50 to validate the library size on an Agilent 2100 Bioanalyzer. Libraries were normalized to 4 nM prior to pooling. The pooled library and PhiX DNA (Illumina PhiX Control Kit v3) were denatured and diluted to 4 pM, combined (using a 5% PhiX spike-in), and denatured again just prior to loading using an Illumina MiSeq Reagent Kit v3 (2x150 bp paired-end reads). Sequencing of the library pool was conducted at the NASA JSC Microbiology Laboratory (Johnson Space Center, Houston, TX). The data obtained was deposited in the NCBI database under the BioProject ID: PRJNA273158.

2.2.3 Sequencing analysis and calculation of diversity indices

Illumina MiSeq Reporter software was used for quality control, trimming, and mapping. The diversity of each consortium was determined using the 16S Metagenomics v1.0 application on Illumina's BaseSpace cloud-computing platform for the species richness (S_{obs}) and the Shannon diversity index (*H'*). EstimateS software [112] was used to calculate the ACE (S_{ace}), Chao1 (S_{chao1}), JackKnife ($S_{jack.k}$), and Simpson (*D*) indices, as well as Shannon (*J'*) and Simpson evenness (E_D).

Coverage of the species was determined by rarefaction curves generated by "iNEXT online: interpolation and extrapolation (Version 1.3.0)" software (http://glimmer.rstudio.com/tchsieh /inext/).

2.2.4 Determination of urease activity

The urease activity for each consortium was determined as previously described [113]. Briefly, the optical density (OD) of each consortium at 560 nm was measured every 30 min for 24 h with a 96-well plate reader (Biotek). The data obtained was used to calculate the enzymatic activity (U mL^{-1}) for each consortium with a standard curve obtained from the purified Jack Bean urease enzyme.

2.2.5 Determination of calcium carbonate precipitation

Each consortium was grown in 39-mL serum bottles containing 9 mL of its respective medium (**Table 2-1**) supplemented with 6.9 g L^{-1} $CaCl_2$, which was found to be the optimum calcium concentration for MICP [3]. The serum bottles were incubated for 96 h at 150 rpm and the calcium ion concentrations in the supernatants were measured for 96 h using atomic absorption spectroscopy (AAS, Perkin Elmer AAnalyst™ 200) after samples were centrifuged at 12857 *g* for 10 min and filtered with 0.2 µm syringe filters. Negative controls, without bacteria, served to determine non-biological calcite precipitations.

2.2.6 Determination of CO_2 sequestration

Overnight grown cultures were centrifuged at 12857 *g* for 10 min, the pellets were collected, washed with sterile phosphate buffer solution (PBS, 0.01M, pH=7.4), and resuspended to an $OD_{600\,nm}$ of 0.5. A 1 mL volume of suspended cells was inoculated in 39-mL serum bottles containing 9 mL of growth medium with 6.9 g L^{-1} $CaCl_2$. The bottles were capped with butyl rubber stoppers and aluminum seals. Pure CO_2 gas was injected into each serum bottle to obtain

10% of CO_2 gas in the headspace. The serum bottles were then incubated for 24 h. After 24 h, triplicate serum bottles were analyzed for headspace CO_2 concentration using the 180C Gas Analyzer containing a non-dispersive infrared (NDIR) CO_2 sensor (Columbus Instruments). Negative controls contained the respective growth medium for each consortium, but no cells.

2.2.7 Determination of abiotic and biotic CO_2 sequestration

Bacterial ureolysis tends to increase the growth medium pH from 7 to 9.5, depending on the consortium composition. The fact that the dissolution of CO_2 in aquatic systems depends on the pH of the water, led us to investigate the abiotic CO_2 sequestration in each consortium's growth medium. For the abiotic CO_2 sequestration experiment, 9 mL of sterile growth medium with adjusted pH to the final pH value found in the growth medium after growing the consortia (**Table 2-3**) was added into 39-mL serum bottles. After pH adjustments, all the serum bottles were capped, sealed, injected with CO_2, and incubated as described in the previous section. After 24 h, CO_2 concentrations in the headspaces and the final pH of the solutions were measured. For the biotic CO_2 sequestration, the amount of CO_2 sequestered by the abiotic process was subtracted from the total CO_2 sequestration results found in the previous section (**Figure 2-1**).

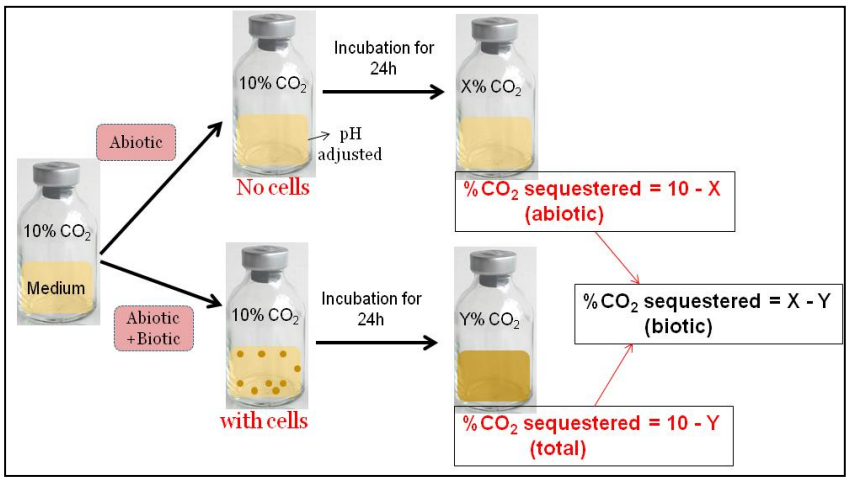

FIGURE 2-1- SCHEMATIC FOR ABIOTIC AND BIOTIC CO_2 SEQUESTRATION EXPERIMENTS.

2.2.8 Statistical analyses

All urease activity, MICP and CO_2 sequestration experiments were repeated three times in three different days to take into consideration daily variations. All results were averaged and their respective standard deviations were calculated. ANOVA statistical analyses were performed using GraphPad Prism 6.04. Excel was used to calculate the Spearman's rho to assess the relationship between urease activity, MICP, CO_2 sequestration, and diversity analyses results [114]. To perform this procedure, we first ranked the results we obtained from all analyses from smallest to largest and assigned ranks from 1 to *n*. Since we have 15 consortia, in our case *n*=15. Afterwards, all the ranks were used to calculate the Spearman's rho, as previously described [114]. We used the following table to make assessment of the correlations:

Value of ρ	Strength of relationship
-1.0 to -0.5 or 1.0 to 0.5	Strong
-0.5 to -0.3 or 0.3 to 0.5	Moderate
-0.3 to -0.1 or 0.1 to 0.3	Weak
-0.1 to 0.1	None or very weak

2.3 RESULTS AND DISCUSSION

2.3.1 Impact of growth media on the diversity of ureolytic consortia

In the present study, we obtained 17 consortia using 13 different enrichment media. Through this investigation, we determined the impact of growth medium on the diversity of ureolytic consortia. The results clearly show that different growth media led to consortia with different community structures (**Figure 2-2** and **Figure 2-3**).

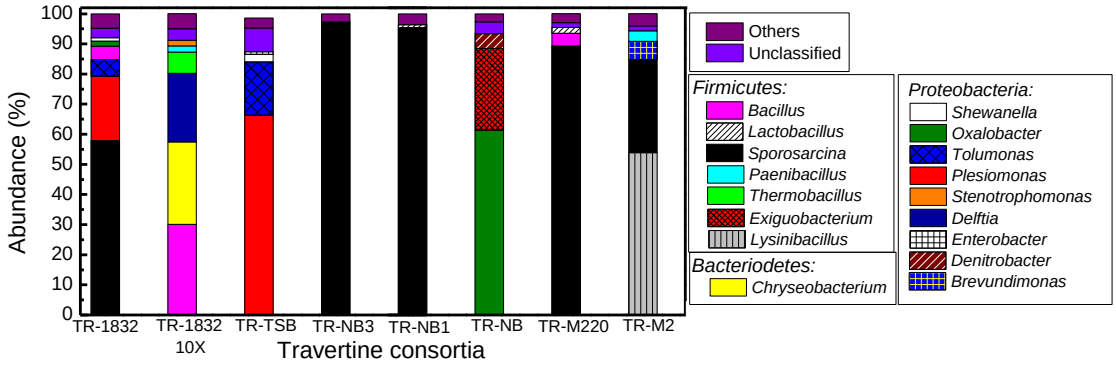

FIGURE 2-2- 16S PHYLOGENETIC COMPOSITION OF THE TR CONSORTIA AT GENUS LEVEL. ONLY THE RESULTS HAVING >1% ABUNDANCE WERE USED TO PLOT THIS GRAPH. GENERA HAVING LESS THAN 1% ABUNDANCE WERE INCLUDED IN 'OTHERS'.

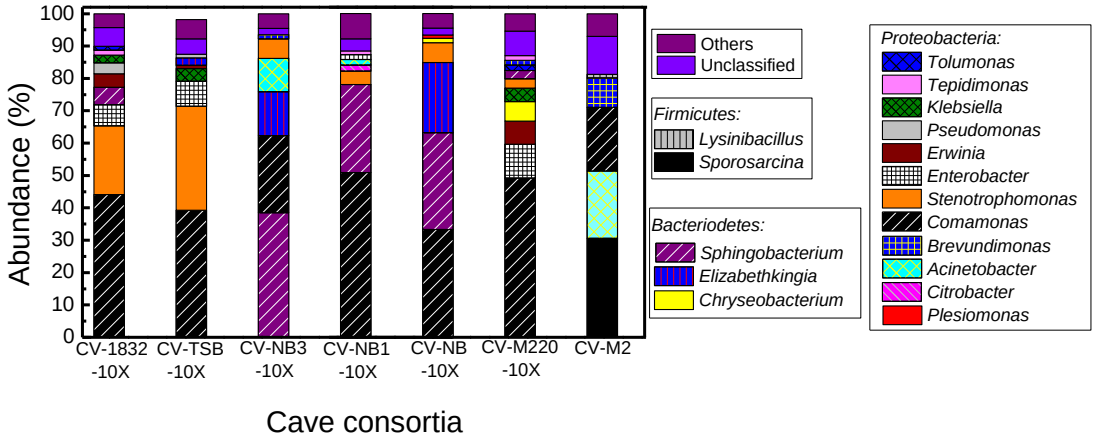

FIGURE 2-3- 16S PHYLOGENETIC COMPOSITION OF THE CV CONSORTIA AT GENUS LEVEL. ONLY THE RESULTS HAVING >1% ABUNDANCE WERE USED TO PLOT THIS GRAPH. GENERA HAVING LESS THAN 1% ABUNDANCE WERE INCLUDED IN 'OTHERS'.

To compare the diversity of the different consortia obtained in this study, analyses of species richness (S_{obs}) and evenness were performed [115-118] with the EstimateS software using the results of the 16S rRNA gene deep sequencing data [112]. The results indicated that each consortium was composed of a different number of OTU (Operational Taxonomix Units), S_{obs}, between 350 and 685 OTU (**Table 2-2**). Among all the travertine consortia, the highest number of OTU (685) was obtained with the 1832-10X medium, while NB1 resulted in the lowest diversity (350). For the cave consortia, the highest and lowest S_{obs} were obtained with the TSB-

10X (587) and M2 (404) media, respectively. However, it is important to point out that the richness in natural environments is typically higher than consortia grown in the laboratory [117]. This study, however, does not aim at reporting the real microbial diversity of caves and travertines. Future metagenomics study will permit us to better assess the true microbial diversity of these two habitats and relate to its ureolytic population.

TABLE 2-2- BACTERIAL 16S RRNA GENE-BASED DIVERSITY INDICES OF TRAVERTINE AND CAVE COMMUNITIES.

Consortia	Number of species (S_{obs})	ACE (S_{ace})	Chao1 (S_{chao1})	JackKnife ($S_{jack.k}$)	Shannon (H')	Shannon evenness (J')	Simpson (D)	Simpson evenness (E_D)
TR-1832	495	617	619	495	0.637	0.103	0.794	0.128
TR-1832-10X	685	876	876	685	0.943	0.144	0.629	0.096
TR-TSB	464	665	670	464	0.525	0.086	0.781	0.127
TR-NB3	563	757	760	563	0.439	0.069	0.833	0.132
TR-NB1	350	521	526	350	0.672	0.115	0.690	0.118
TR-NB	406	537	541	406	1.175	0.196	0.407	0.068
TR-M220	427	605	609	427	0.496	0.082	0.840	0.139
TR-M2	603	782	785	603	1.135	0.177	0.510	0.080
CV-1832-10X	478	606	609	477	1.447	0.235	0.437	0.071
CV-TSB-10X	587	768	772	587	1.304	0.205	0.495	0.078
CV-NB3-10X	410	490	493	410	1.519	0.253	0.358	0.060
CV-NB1-10X	492	694	699	492	1.231	0.199	0.500	0.081
CV-NB-10X	405	531	535	405	1.367	0.228	0.402	0.067
CV-M220-10X	541	715	719	540	1.419	0.225	0.442	0.070
CV-M2	404	547	551	404	1.509	0.251	0.377	0.063

In the present study, we also investigated the consortia richness, evenness, and dominance using the Shannon diversity index (H'), Shannon evenness (J'), Simpson index (D), and Simpson evenness (E_D), respectively (**Table 2-2**). The results of these indices showed that among all the consortia investigated, TR-NB and CV-NB3-10X consortia were the most diverse with evenly

distributed OTU of similar dominance. Besides these indices, the ACE, Chao1 and Jackknife diversity estimators were also calculated. The results of these indices showed that TR-1832-10X and CV-TSB-10X consortia exhibited the highest S_{ace}, S_{chao1}, and S_{jack} than all the other travertine and cave consortia, respectively, which can be explained by a much higher S_{obs} in these two consortia (**Table 2-2**). Rarefaction curves indicated that the sequencing coverage barely approached saturation (**Figure 2-4**), since the curves did not reach a plateau, with the exception of CV-M2.

These diversity results showed that not only the different medium compositions, but also the strength of the growth media, impacted the composition, abundance and diversity of OTUs in the consortia. For instance, in TR-1832 and TR-1832-10X consortia (**Figure 2-2**), *Sporosarcina* sp. and *Bacillus* sp. were the predominant OTU, respectively. Also, in the TR-1832-10X consortium, the S_{obs} was higher than in the TR-1832 consortium. These results suggest that a less rich medium is more suitable to obtain a more diverse consortium from karstic environments. Our results are corroborated by a previous study that also demonstrated that relatively low nutrient concentrations resulted in an increase in diversity [119].

When analyzing the composition of the consortia obtained from these two environments, we observed that *Proteobacteria, Bacteriodetes, and Firmicutes* were the most frequent-phyla found (**Figure 2-2** and **Figure 2-3**). Other studies with karstic samples also observed similar phyla [64, 120, 121]. In the phylum *Firmicutes*, the *Sporosarcina* genus was observed in high abundances in a number of travertine consortia, such as TR-1832, TR-NB1, TR-NB3, TR-M220, and TR-M2 (**Figure 2-2**). This genus is well known to have high urease activity and to have species involved in the MICP process [3, 85]. This genus was also present in all cave consortia, but CV-M2 exhibited the greatest proportion (>1%) of this genus (**Figure 2-3**).

In the phylum *Bacteriodetes*, one of the most abundant genera was *Chryseobacterium,* which was mostly observed in TR-1832-10X (**Figure 2-2**) and CV-M220-10X (**Figure 2-3**) consortia. This genus also has urease-positive species [122]. Two other abundant genera from the *Bacteriodetes* phylum identified in the consortia were *Sphingobacterium* and *Elizabethkingia*. These two genera have also been described to be urease-positive [123]. In the phylum *Proteobacteria*, the genera *Oxalobacter*, *Plesiomonas*, and *Delftia* were the most abundant in the travertine consortia (**Figure 2-2**). While *Comamonas*, *Stenotrophomonas*, *Enterobacter* and *Acinetobacter* were the most abundant in the cave consortia (**Figure 2-3**). Amongst these genera, *Delftia* [124], *Comamonas* [125], *Stenotrophomonas* [126], and *Enterobacter* [127] are urease-positive. The other genera found in the consortia have not been described to be urease-positive. These results show that the growth media used are not selective for only ureolytic microorganisms, since non-ureolytic genera were also obtained. The role of these non-ureolytic microorganisms, in the MICP process, however, is unclear.

Deep sequencing also revealed the following phyla: *Actinobacteria*, *Tenericutes*, *Acidobacteria*, *Verrucomicrobia*, *Chlorobi*, *Cyanobacteria*, *Chlamydiae*, *Spirochaetes*, *Chloroflexi*, *Planctomycetes*, *Thermi*, *Nitrospirae*, *Fusobacteria*, *Thermotogae*, *Synergistetes*, and *Deferribacteres*. These phyla were shown as 'Others' in **Figure 2-2** and **Figure 2-3** due to their low abundances in the consortia (<1%). Their low abundance in the consortia does not mean that they are in low abundance in these environments. Amongst these phyla, *Actinobacteria* [128], *Tenericutes* [129], *Acidobacteria* [130], *Verrucomicrobia* [131], *Cyanobacteria* [132], *Spirochaetes* [133], *Chloroflexi* [134], *Planctomycetes* [135], *Thermi* [136], *Nitrospirae* [137], *Fusobacteria* [138], and *Deferribacteres* [139] contain species described to be urease-positive; a trait that has been shown to be essential for MICP.

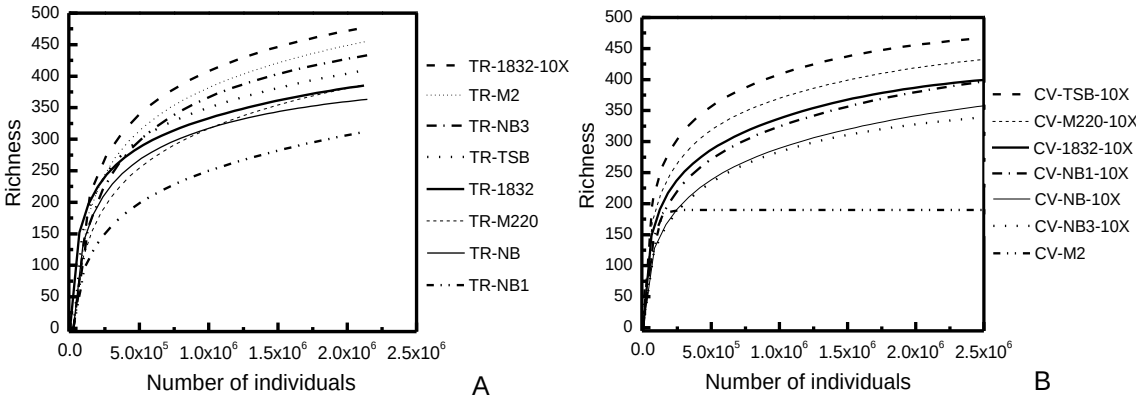

FIGURE 2-4- SAMPLE-SIZE-BASED RAREFACTION CURVES OF TRAVERTINE (A) AND CAVE (B) CONSORTIA.

2.3.2 Relationship between urease activity and consortia microbial composition

As described in the previous section, a number of urease-positive genera were identified in the different consortia. Hence, the urease capabilities of the consortia were further investigated. The results in **Figure 2-5** demonstrated that each consortium possessed different urease activities ranging between 12.2 U mL^{-1} and 0.3 U mL^{-1}. The ANOVA analyses showed that the diverse consortia had statistically significant different urease activities ($p<0.001$). The travertine consortia containing *Sporosarcina* sp., as the dominant OTU (TR-1832, TR-NB1, TR-M220, and TR-NB3) exhibited greater urease activities (12.2, 6.4, 6.3, and 2.3 U mL^{-1}, respectively) than others. This is not surprising, since *Sporosarcina* species have typically high urease activities [3]. In the case of the cave consortia, the CV-M2 consortium, which had *Sporosarcina* sp. as the predominant OTU (30.6%), also presented the highest urease activity (2 U mL^{-1}) among the cave consortia. In this study, CV-1832-10X (0.3 U mL^{-1}) and CV-TSB-10X (0.3 U mL^{-1}) presented the lowest urease activity among all the consortia (**Figure 2-5**). *Comamonas* was the predominant genus in these two consortia (**Figure 2-3**). This genus has species that are ureolytic, but their urease activities are typically lower than *Sporosarcina* species, which would explain the lower urease activity of these two consortia [95, 125].

In case of TR-NB1 and TR-NB3 consortia, the abundance of the *Sporosarcina* genus was found to be very similar (95.4% and 97.3%, respectively), but the latter presented 2.8 times lower urease activity (ANOVA, $p<0.0001$). This could be due to the difference in the growth medium composition, since researchers also observed differences in urease activity when growing *Sporosarcina* in different media [93]. Hence, both the microbial composition and the growth medium of the consortia seem to influence the functionality of the consortia in relation to urease activity.

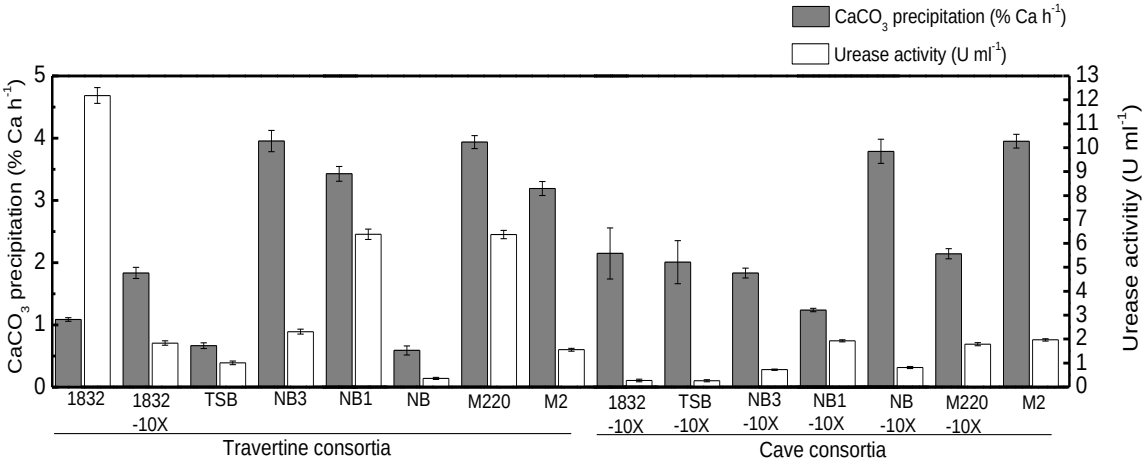

FIGURE 2-5- $CACO_3$ PRECIPITATION RATES (GRAY) AND UREASE ACTIVITIES (WHITE) OF TRAVERTINE AND CAVE CONSORTIA. ALL CONSORTIA WERE CULTURED IN THEIR SPECIFIC GROWTH CONDITIONS. ALL EXPERIMENTS WERE DONE IN TRIPLICATE AND THE ERROR BARS CORRESPOND TO STANDARD DEVIATIONS.

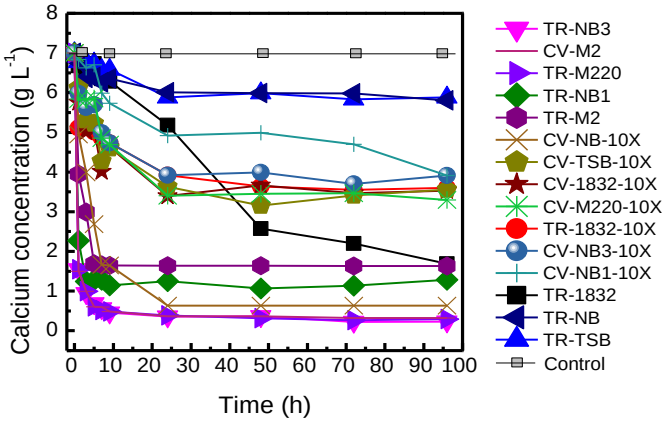

FIGURE 2-6- THE CALCIFICATION GRAPH SHOWING THE CALCIUM CONCENTRATIONS (g L^{-1}) DETERMINED BY THE AAS IN THE GROWTH MEDIUM FOR EACH CONSORTIUM.

2.3.3 Relationship among MICP, urease activity and consortia diversity

Previous studies with pure cultures of ureolytic microbes demonstrated that MICP directly correlates with urease activity [140]. It is, however, unclear whether non-ureolytic microbes, present in a consortium, will impact the urease activity and calcite precipitation of the ureolytic microorganisms. To investigate that, we performed MICP assays to determine the amount of dissolved calcium in each medium during microbial growth. The **Figures 2-5** and **2-6** showed that each consortium had different capability to induce precipitation of calcium carbonate (ANOVA, $p<0.001$). Results also showed that the most diverse consortia (*i.e.*, TR-1832- 10x and CV-TSB-10x) did not present the highest $CaCO_3$ precipitation or urease activity (**Figures 2-2**, **2-3**, and **2-5**). When comparing the least diverse consortia (*e.g.*, TR-NB1 and CV-M2) with the most diverse, we observed that the least diverse consortia presented higher urease activity and $CaCO_3$ precipitation.

Upon further investigation of the correlation between diversity and urease activity, as well as microbial diversity and calcite precipitation using Spearman's rho, we observed diversity and urease activity have a negative moderate relationship (ρ=-0.56; $p<0.05$). This negative correlation suggests that more diverse populations will have lower urease activity. In the case of the correlation analysis between diversity and MICP, we observed a very weak correlation (ρ=-0.028; $p<0.05$) (**Table 2-3**). Contrary to previous investigations with isolates that have determined that the urease activity and MICP rates were strongly related; this investigation shows that in consortia, this correlation does not seem to strongly apply [81]. Besides the diversity, we observed that the dominance of OTU also played a role on the urease activity and $CaCO_3$ precipitation. In consortia presenting similar OTU dominance, the precipitation rates were also similar.

TABLE 2-3- CORRELATION RESULTS.

	Spearman's rho	**p-values**		**Spearman's rho**	**p-values**
Urease Activity & MICP	0.315	0.03	Simpson evenness & Urease activity	0.614	0.01
Urease Activity & Total CO_2 sequestration	0.558	0.03	Simpson evenness & MICP	0.067	0.05
Urease Activity & Abiotic CO_2 sequestration	0.585	0.02	Simpson evenness & Total CO_2 sequestration	0.308	0.02
Urease Activity & Biotic CO_2 sequestration	0.215	0.02	Simpson evenness & Abiotic CO_2 sequestration	0.415	0.1
Urease Activity & pH	0.604	0.01	Simpson evenness & Biotic CO_2 sequestration	-0.160	0.05
MICP & Total CO_2 sequestration	0.714	0.002	Simpson evenness & pH	0.411	0.1
MICP & Abiotic CO_2 sequestration	0.638	0.002	Richness & Urease activity	-0.082	0.07
MICP & Biotic CO_2 sequestration	0.663	0.007	Richness & MICP	-0.156	0.05
MICP & pH	0.814	$2x10^{-4}$	Richness & Total CO_2 sequestration	-0.144	0.05
pH & Total CO_2 sequestration	0.949	$7x10^{-8}$	Richness & Abiotic CO_2 sequestration	-0.029	0.07
pH & Abiotic CO_2 sequestration	0.955	$3x10^{-8}$	Richness & Biotic CO_2 sequestration	-0.215	0.02
pH & Biotic CO_2 sequestration	0.724	0.002	Richness & pH	-0.064	0.05
Shannon index & Urease activity	-0.557	0.03	ACE & Urease activity	-0.007	0.07
Shannon index & MICP	-0.028	0.01	ACE & MICP	-0.064	0.07
Shannon index & Total CO_2 sequestration	-0.298	0.02	ACE & Total CO_2 sequestration	-0.176	0.04
Shannon index & Abiotic CO_2 sequestration	-0.383	0.08	ACE & Abiotic CO_2 sequestration	-0.054	0.03
Shannon index & Biotic CO_2 sequestration	0.131	0.05	ACE & Biotic CO_2 sequestration	-0.250	0.001
Shannon index & pH	-0.357	0.06	ACE & pH	-0.039	0.02
Simpson index & Urease activity	0.614	0.01	Chao1 & Urease activity	0.014	0.002
Simpson index & MICP	0.067	0.09	Chao1 & MICP	-0.067	0.05
Simpson index & Total CO_2 sequestration	0.308	0.03	Chao1 & Total CO_2 sequestration	-0.167	0.04
Simpson index & Abiotic CO_2 sequestration	0.415	0.1	Chao1 & Abiotic CO_2 sequestration	-0.049	0.03
Simpson index & Biotic CO_2 sequestration	-0.160	0.05	Chao1 & Biotic CO_2 sequestration	-0.240	0.01
Simpson index & pH	0.411	0.1	Chao1 & pH	-0.036	0.01
Shannon evenness & Urease activity	-0.568	0.02	JackKnife & Urease activity	-0.082	0.06
Shannon evenness & MICP	-0.014	0.07	JackKnife & MICP	-0.156	0.05
Shannon evenness & Total CO_2 sequestration	-0.276	0.05	JackKnife & Total CO_2 sequestration	-0.144	0.05
Shannon evenness & Abiotic CO_2 sequestration	-0.358	0.06	JackKnife & Abiotic CO_2 sequestration	-0.029	0.01
Shannon evenness & Biotic CO_2 sequestration	0.163	0.05	JackKnife & Biotic CO_2 sequestration	-0.215	0.02
Shannon evenness & pH	-0.339	0.05	JackKnife & pH	-0.064	0.05

This phenomenon was observed with the travertine consortia, TR-NB3 and TR-M220, which were dominated by *Sporosarcina* sp., and therefore showed similar $CaCO_3$ precipitation rates (**Figure 2-5**). On the other hand, the CV-NB-10X consortium was mainly composed by *Comamonas*, *Sphingobacterium*, and *Elizabethkingia*, and presented very low urease activity but very high $CaCO_3$ precipitation. These results clearly show that the urease activity is not necessarily linked to MICP as previously suggested by studies with pure cultures [141]. These results were further analyzed for correlation, which confirms the moderately low relationship between MICP and urease activity (ρ=0.315; $p<0.01$).

2.3.4 Relationship among biotic and abiotic CO_2 sequestration capabilities and MICP

Previous studies suggested that microorganisms involved in MICP process can facilitate CO_2 sequestration [7]. In order to determine CO_2 sequestration by the different consortia, we added 10% CO_2 to the headspace of sealed serum bottles and determined how much of these 10% CO_2 were removed from the headspace (**Figure 2-7**). In this investigation we determined the biotic and abiotic CO_2 removal. The abiotic sequestration was also investigated since CO_2 can dissolve in water. The dissolution depends directly on the pH and chemical composition of the water [9, 12]. The simultaneous investigation of biotic and abiotic processes is important to determine the real contribution of microorganisms in the CO_2 sequestration, specially since microorganisms can change the pH of their surrounding environment during their metabolic activities.

For instance, during the MICP process, it is commonly observed the increasing in the medium pH, due to the production of ammonia. This increase in pH can lead to CO_2 dissolution and formation of carbonates in water. In the growth medium, CO_2 dissolution can be altered even more, due to increasing viscosity caused by different concentrations of nutrients in the growth medium [142, 143]. Moreover, it was found that CO_2 solubility depended on environmental

factors such as pH, temperature and pressure, and other parameters such as salinity, sugar, fat, and protein content [144]. Therefore, determining how much of the CO_2 sequestration during MICP process is biotic or abiotic is vital to gain a better understanding of the role of microbial populations in the environment and in the MICP process.

In this study, we determined the abiotic CO_2 sequestration by quantifying the CO_2 content in the headspace of the serum bottles having only media (no cells) (**Figure 2-1**). In this investigation, each sterile medium had its pH adjusted to the final pH observed after microbial growth for 24 h. The goal was to determine the amount of CO_2 left in the headspace after incubation for 24 h in the growth media with adjusted pH values (**Table 2-4**). The results showed that the abiotic CO_2 sequestration was dependent on both pH and the type of growth medium. The correlation between pH and abiotic CO_2 sequestration was further confirmed by the Spearman's rho correlation analysis (ρ=0.955; p-value<0.01). When pH>8.5, greater abiotic CO_2 uptake was observed. The media 1832, NB3, M220, and NB1 showed the highest abiotic CO_2 uptakes with 5.8, 4.4, 4.2 and 3.5%, respectively, out of the initial 10% CO_2 present in the headspace. In the control vials, which did not have the pH adjusted, little or no CO_2 dissolution was observed (**Table 2-5**). In the growth media, which were diluted 10X, less abiotic CO_2 uptake was observed (**Figure 2-7**). The data suggest that both the concentration and composition of the growth media appeared to play a role in the abiotic CO_2 sequestration during the MICP process.

The biotic CO_2 uptake during the MICP was also determined: the results from the abiotic assays were subtracted from the total CO_2 sequestered from the headspace during MICP (**Figure 2-1**). Among the 15 consortia investigated, four of them (TR-TSB, TR-NB, CV-NB1-10X and CV-M220-10X) were found to not be able to sequester CO_2 biotically (**Figure 2-7**). In fact, the consortia that could not sequester CO_2 increased the CO_2 concentration in the headspace (**Table**

2-4), possibly due to cellular respiration [145]. The pH results measured in these four consortia after 24 h of incubation were the lowest amongst all consortia. The strong correlation between biotic CO_2 sequestration and pH, was confirmed by the Spearman's rho analysis (ρ=0.724; p-value<0.01). Interestingly, these consortia contained the following most abundant genera: *Plesiomonas*, *Tolumonas*, *Oxalobacter*, *Exiguobacterium*, *Comamonas*, and *Sphingobacterium*. It is probable that these genera are not involved in CO_2 sequestration through MICP. Furthermore, these cells could be producing organic acids during growth, which could have caused the decrease in the pH of the growth media and inhibit the MICP process [102]. The other 11 consortia, on the other hand, decreased the headspace CO_2 content by at least 0.9% to up to 8.6% from the initial 10% CO_2 present in the headspace.

TABLE 2-4- THE CHANGES OF CO_2 CONCENTRATION IN HEADSPACE AND PH OF GROWTH MEDIA AFTER 24 H INCUBATION WITH AND WITHOUT BACTERIAL CONSORTIA TO DETERMINE THE BIOTIC AND ABIOTIC CO_2 SEQUESTRATION.

Consortia	Initial CO_2 in the headspace (%)	Initial pH	Final CO_2 in the headspace (%) (Abiotic+Biotic)	Final pH	CO_2 at abiotic** bottles (%) (Abiotic)	Biotically sequestered CO_2 (%)
TR-1832	10	7	2.29	9	4.19	1.90
TR-1832-10X	10	7	8.89	7.12	9.34	0.45
TR-TSB	10	7	11.60	6.77	9.69	NA*
TR-NB3	10	7	1.36	9.28	5.65	4.29
TR-NB1	10	7	1.46	9.08	6.55	5.09
TR-NB	10	7	11.08	6.75	9.02	NA*
TR-M220	10	7	1.63	9.25	5.79	4.16
TR-M2	10	7	3.57	8.74	9.11	5.54
CV-1832-10X	10	7	8.99	7.13	9.34	0.35
CV-TSB-10X	10	7	6.20	7.42	9.17	2.97
CV-NB3-10X	10	7	4.24	7.09	9.64	5.40
CV-NB1-10X	10	7	10.49	7.04	9.64	NA*
CV-NB-10X	10	7	4.47	8.4	9.15	4.68
CV-M220-10X	10	7	10.76	7.08	9.17	NA*
CV-M2	10	7	2.26	9.02	9.1	6.84

*NA is not applicable. ** Abiotic bottles have no cells, and represents CO_2 dissolution.

TABLE 2-5- A REPRESENTATIVE TABLE SHOWING CO_2 CONCENTRATIONS IN HEADSPACE VOLUMES OF SERUM BOTTLES CONTAINING ONLY MEDIA (NO CELLS) WITH SPECIFIED PH.

Media	Initial CO_2 (%)	CO_2 (%) at initial pH (pH=7)	CO_2 (%) at pH=7.3	CO_2 (%) at pH=8.3	CO_2 (%) at pH=9.3
ATCC 1832	10	8.9±0.2	8.6±0.7	6.2±0.5	2.3±0.1
NB3	10	9.8±0.1	9.7±0.8	9.1±0.7	4.5±0.3
NB	10	9.7±0.3	9.2±0.6	8.4±0.7	6.1±0.5
NB-10X	10	9.8±0.2	9.1±0.6	9.1±0.7	9.1±0.7
ATCC 1832-10X	10	9.9±0.3	9.6±0.6	9.6±0.7	8.6±0.6

Similarly to the abiotic CO_2 sequestration, the biotic CO_2 uptake also showed a relatively strong correlation with MICP and pH (ρ=0.663 and 0.724, respectively). The consortia that showed the greatest CO_2 uptake results were CV-M2 and TR-M2 consortia with 6.8% and 5.5% of CO_2 sequestered, respectively. The CV-M2 consortium consisted mainly of *Sporosarcina*, *Acinetobacter*, *Comamonas*, *Brevundimonas*, and *Lysinibacillus*; and TR-M2 consortium was predominantly composed of *Lysinibacillus*, *Sporosarcina*, *Brevundimonas* and *Paenibacillus*. The CV-1832-10X and TR-1832-10X consortia, on the other hand, had the lowest CO_2 sequestration amounts, with 0.3% and 0.5%, respectively. The consortium CV-1832-10X was mainly composed of *Comamonas*, *Stenotrophomonas*, *Enterobacter*, *Sphingobacterium*, *Erwinia*, *Pseudomonas*, *Klebsiella*, *Tepidimonas* and *Tolumonas*; while the most abundant genera in TR-1832-10X were *Bacillus*, *Chryseobacterium*, *Delftia*, *Thermobacillus*, *Paenibacillus* and *Stenotrophomonas*. In summary, when considering the consortia that demonstrated a high level of biotic CO_2 sequestration (CV-NB3-10X, TR-NB1, CV-NB-10X, and TR-NB3) and no biotic CO_2 sequestration (TR-TSB, TR-NB, CV-NB1-10X and CV-M220-10X), it can be seen that the presence of the genera *Comamonas*, *Plesiomonas* and *Oxalobacter* correlated well with reduced CO_2 uptake in the consortia, and the genera *Sporosarcina*, *Lysinibacillus*, *Sphingobacterium*, *Acinetobacter* and *Elizabethkingia* correlated well with greater CO_2 uptake.

When comparing the diversity of the consortia with the CO_2 sequestration, we observed that the most diverse consortia in both the cave and travertine (TR-1832-10X and CV-TSB-10X) sequestered less CO_2 than the least diverse cave and travertine consortia (TR-NB1 and CV-M2). The results also show that the relationship between CO_2 sequestration and MICP or urease activity was not completely linear (**Figures 2-5** and **2-6**). In the case of CO_2 sequestration and MICP, even though the relationship was not completely linear, the correlation was still somewhat strong (ρ=0.663; p-value<0.001). This result suggests that the majority of the CO_2 was sequestered through MICP. In the case of the biotic CO_2 sequestration and urease activity the correlation was very weak (ρ=0.215; p-value<0.05), which suggests that other mechanisms of biotic CO_2 sequestration than urease activity through MICP could probably be happening.

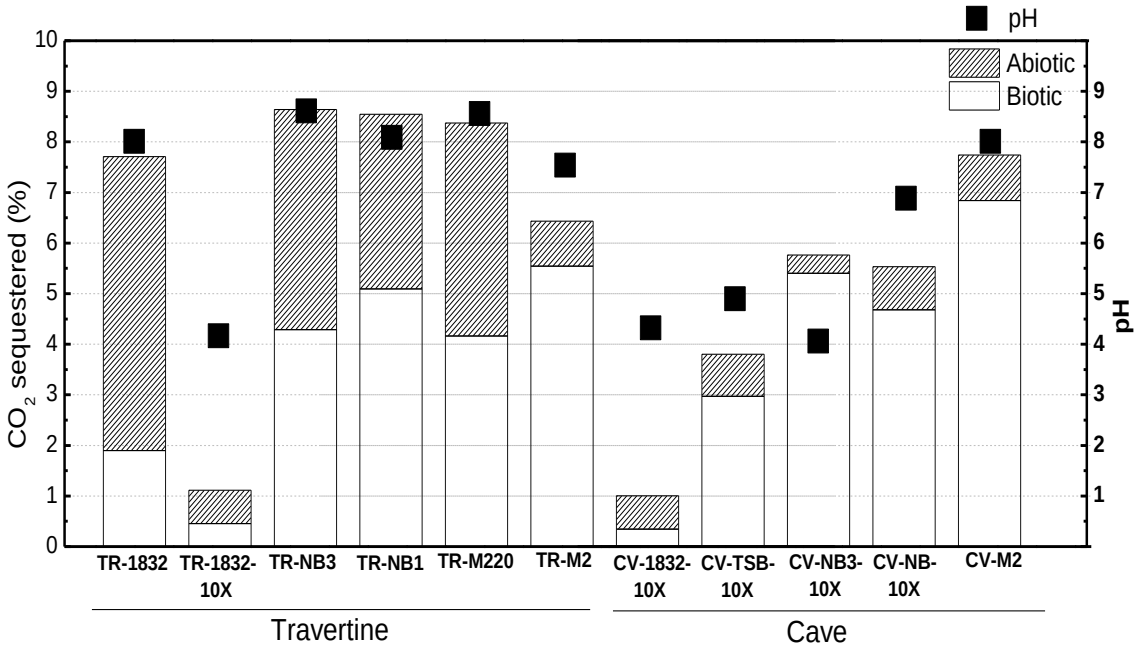

FIGURE 2-7- THE COMPARISON OF SEQUESTERED CO_2 (%) BY THE TRAVERTINE AND CAVE CONSORTIA GROWN IN DIFFERENT GROWTH MEDIA, AND THE FINAL PH OF CONSORTIA AFTER 24 H INCUBATION. THE WHITE COLOR AND PATTERNS IN EACH COLUMN STAND FOR ABIOTIC AND BIOTIC CO_2 SEQUESTRATION RESULTS, RESPECTIVELY.

2.3.5 The biotic CO_2 sequestration involves other sequestration mechanisms than MICP

To quantitatively determine the differences in biotic CO_2 sequestration and $CaCO_3$ precipitation, we calculated stoichiometrically the amount of CO_2 sequestered during the MICP process. The results demonstrated that more CO_2 was sequestered than we could account for in the MICP process (**Tables 2-6** and **2-7**). This means that in each consortium we observed higher amounts of CO_2 sequestered than the amount of $CaCO_3$ precipitated. It is possible that due to the high microbial diversity in the consortia, there may be microorganisms with different CO_2 uptake mechanisms than the MICP process.

Previous studies have determined that the Calvin-Benson reductive pentose phosphate cycle, the reductive citric acid (Arnon-Buchanan) cycle, the reductive acetyl-CoA (Wood-Ljungdahl) pathway, the hydroxypropionate (Fuchs-Holo) bi-cycle, the 3-hydroxypropionate/4-hydroxybutyrate and dicarboxylate/4-hydroxybutyrate cycles could play an important role in CO_2 sequestration [13]. In fact, related genes involved in these cycles have been detected in a previous study done with cave bacteria [146].

In our study, we observed the presence of microorganisms from the phyla *Cyanobacteria*, *Chloroflexi*, *Proteobacteria* (*e.g,. Thioalkalimicrobium*, *Hydrogenophilus, Magnetospirillum*, *Rhodobacter* and *Rhodospirillum*), *Firmicutes* (*e.g., Sulfobacillus*), and *Actinobacteria* (*e.g., Mycobacterium*), which have been associated with the Calvin-Benson cycle for CO_2 sequestration. In the case of the Arnon-Buchanan cycle, *Chlorobi*, *Nitrospirae*, and *Proteobacteria* phyla (*Deltaproteobacteria*, such as *Desulfobacter*, and *Epsilonproteobacteria* subdivisions) were also detected in the consortia. Microorganisms involved in the The Wood-Ljungdahl pathway, such as *Planctomycetes*, and *Moorella* (phylum *Firmicutes*) and *Desulfobacter* (phylum *Proteobacteria*), were also found in our consortia. Finally, *Chloroflexus*

aurantiacus (phylum *Chloroflexi*), *Nitrosobacter* (phylum *Proteobacteria*), and *Chloroherpeton thalassium* (phylum *Chlorobi*), were also observed in our study and have been described to have the Fuchs-Holo bi-cycle pathway for CO_2 sequestration [13, 147, 148]. We did not identify, however, any microorganisms that could be associated with the 3-hydroxypropionate/4-hydroxybutyrate and dicarboxylate/4-hydroxybutyrate cycles. Typically these two cycles are associated with *Pyrolobus*, *Sulfolobales*, *Thermoproteales* and *Desulfurococcales* [13].

Recently, researchers have identified the enzyme carbonic anhydrase (CA) in certain species; such as, *Enterobacter* sp., *Citrobacter freundii*, *Bacillus subtilis*, *Stenotrophomonas acidaminiphila*, *Proteus vulgaris, Neisseria gonorrhoeae*, and *Staphylococcus* sp.. This enzyme was reported to assist in CO_2 fixation [19, 20]. Some of these genera were also observed in our consortia, which could also explain the biotic CO_2 sequestration observed in our study. The authors, however, mentioned that the CO_2 fixing process through CA enzyme has a limiting step, which is CO_2 dissolution [20].

In this investigation, we were able to demonstrate that ureolytic microorganisms can increase the pH of the surrounding environment and increase CO_2 dissolution in the media. Therefore, it is possible that the combination of the CA process with MICP in the consortia could have resulted in a greater rate and magnitude of CO_2 sequestration by some consortia. The results of this study indicate that in addition to the MICP, these consortia may have other biotic mechanisms of CO_2 sequestration that require further investigation.

TABLE 2-6- Ca^{2+} CONCENTRATIONS TO COMPARE THE REAL SEQUESTERED CO_2 AND STOICHIOMETRIC AMOUNTS. BASED ON THESE RESULTS, IT CAN BE SEEN THAT THE MICP WAS NOT THE ONLY CO_2 SEQUESTRATION METHOD IN CONSORTIA.

Consortia	Dissolved Ca^{2+} (g/L) at T=0	Dissolved Ca^{2+} (g/L) at T=96 h	Ca^{2+} precipitated (g/L)	Ca^{2+} precipitated (mol)	Stoichiometric amount for CO_2 sequestration (mol)	Total CO_2 sequestered (%)	Total CO_2 sequestered (mg/mL)	Total CO_2 sequestered (mg)	Total CO_2 sequestered (mol)
TR-1832	6.9	1.686	5.214	0.0013	0.0013	7.71	77.1	2313	0.0526
TR-1832-10X	6.9	3.599	3.301	0.0008	0.0008	1.11	11.1	333	0.0076
TR-TSB	6.9	5.880	1.020	0.0003	0.0003	0	0	0	0
TR-NB3	6.9	0.230	6.670	0.0017	0.0017	8.64	86.4	2592	0.0589
TR-NB1	6.9	1.285	5.615	0.0014	0.0014	8.54	85.4	2562	0.0582
TR-NB	6.9	5.801	1.099	0.0003	0.0003	0.92	9.2	276	0.0063
TR-M220	6.9	0.293	6.607	0.0016	0.0016	8.37	83.7	2511	0.0571
TR-M2	6.9	1.630	5.270	0.0013	0.0013	6.43	64.3	1929	0.0438
CV-1832-10X	6.9	3.530	3.370	0.0008	0.0008	1.01	10.1	303	0.0069
CV-TSB-10X	6.9	3.558	3.342	0.0008	0.0008	3.8	38	1140	0.0259
CV-NB3-10X	6.9	3.915	2.986	0.0007	0.0007	5.76	57.6	1728	0.0393
CV-NB1-10X	6.9	3.915	2.986	0.0007	0.0007	0	0	0	0
CV-NB-10X	6.9	0.630	6.270	0.0016	0.0016	5.53	55.3	1659	0.0377
CV-M220-10X	6.9	3.299	3.601	0.0009	0.0009	0	0	0	0
CV-M2	6.9	0.323	6.577	0.0016	0.0016	7.74	77.4	2322	0.0528

TABLE 2-7- TITRATION RESULTS OF CARBONATES IN THE GROWTH MEDIA ENRICHED WITH 10% CO_2.

	Initial			After 24 h incubation (with Ca^{2+})			After 24 h incubation (no Ca^{2+})		
Consortia	pH	$[CO_3^{-2}]$ (mol)	$[HCO_3^{-1}]$ (mol)	pH	$[CO_3^{-2}]$ (mol)	$[HCO_3^{-1}]$ (mol)	pH	$[CO_3^{-2}]$ (mol)	$[HCO_3^{-1}]$ (mol)
TR-1832	7	0	4.40E-05	9	7.12E-04	2.03E-04	8.8	9.12E-04	9.42E-04
TR-1832-10X	7	0	8.00E-06	7.1	0	2.50E-05	7.1	0	2.30E-05
TR-TSB	7	0	4.10E-05	6.8	0	3.30E-05	6.8	0	3.10E-05
TR-NB3	7	0	3.00E-05	9.3	5.85E-04	5.42E-04	9.1	8.42E-04	1.89E-04
TR-NB1	7	0	4.70E-05	9.1	5.51E-04	1.95E-04	9.1	8.21E-04	3.47E-04
TR-NB	7	0	7.40E-05	6.8	0	7.27E-04	6.7	0	7.62E-04
TR-M220	7	0	6.60E-05	9.3	2.33E-04	1.12E-04	9.2	5.44E-04	1.55E-04
TR-M2	7	0	1.70E-05	8.7	9.90E-05	1.70E-05	8.5	1.88E-04	4.40E-05
CV-1832-10X	7	0	8.00E-06	7.1	0	4.70E-05	7.1	0	2.42E-04
CV-TSB-10X	7	0	9.00E-06	7.4	0	3.88E-04	7.3	0	6.66E-04
CV-NB3-10X	7	0	1.10E-05	7.1	0	2.44E-04	7.2	0	7.12E-04
CV-NB1-10X	7	0	9.00E-06	7	0	1.96E-04	7.1	0	1.99E-04
CV-NB-10X	7	0	1.20E-05	8.4	0	2.50E-05	7.3	0	2.70E-05
CV-M220-10X	7	0	8.00E-06	7	0	4.70E-05	7	0	2.42E-04
CV-M2	7	0	1.70E-05	9	1.63E-04	4.20E-05	8.8	2.11E-04	1.28E-04

2.4 CONCLUSIONS

The present study shows that in the consortia, the $CaCO_3$ precipitation does not directly correlate to urease activity, as previously observed in studies with pure cultures. Additionally, this study also demonstrates that bacterial populations in caves and travertines were able to sequester different amounts of CO_2, using the MICP process and probably other pathways not investigated in this study. The results also suggested that CO_2 sequestration through MICP process is directly related to bacterial community composition and also abiotic factors, such as pH and growth media. In consortia with low diversity, the CO_2 sequestration was much higher than in very diverse consortia. Finally, this study shows for the first time that species from the genera *Sporosarcina*, *Lysinibacillus*, *Sphingobacterium*, *Acinetobacter* and *Elizabethkingia* seem to play an important role in CO_2 sequestration.

CHAPTER 3 CO_2 SEQUESTRATION BY MICROBIAL ISOLATES DURING MICROBIALLY-INDUCED CALCIUM CARBONATE PRECIPITATION

3.1 RATIONALE AND OBJECTIVES

Carbon sequestration consists in transferring and storing atmospheric carbon dioxide (CO_2) into other forms of carbon or by injecting into non-atmospheric reservoirs. The conversion of CO_2 into other forms of carbon is a process that can occur through natural and anthropogenic processes [12]. For many years, plants and photosynthetic microorganisms were considered to be the only natural sinks for CO_2. More recently, researchers have identified some microorganisms capable of sequestering CO_2 through carbonate precipitation process, which has been called biomineralization or "microbially-induced carbonate precipitation (MICP)" [7, 8]. Researchers suggest that MICP occurs as a by-product of urea hydrolysis with urease enzymes produced by ureolytic bacteria [4, 5, 10, 34, 75]. The suggested chemical reactions for MICP through ureolysis for CO_2 sequestration are presented as follows [78]:

Ureolysis:

$$CO(NH_2)_2 + 2H_2O \rightarrow 2NH_4^+ + CO_3^{2-} , \quad (3\text{-}1)$$

CO_2 dissolution in aquatic systems:

$$CO_2 + H_2O \leftrightharpoons H_2CO_3 , \quad (3\text{-}2)$$

$$H_2CO_3 \leftrightharpoons HCO_3^- + H^+ , \quad (3\text{-}3)$$

$$HCO_3^- \leftrightharpoons CO_3^{2-} + H^+ , \text{ and} \quad (3\text{-}4)$$

Overall Ureolysis and $CaCO_3$ precipitation:

$$NH_2CONH_2 + 2H_2O + Ca^{2+} \rightarrow 2NH_4^+ + CaCO_3 . \quad (3\text{-}5)$$

In the ureolysis reaction, urea is degraded by ureolytic microorganisms, resulting in the production of ammonium (NH_4^+), dissolved inorganic carbon, and increasing in pH (Eq. 3-1), which will favor $CaCO_3$ precipitation in the presence of calcium ions (Eq. 3-5). At alkaline pH values generated by the ammonium production, the CO_2 from the air will dissolve in water and get converted to carbonates (Eqs. 3-2 to 3-4). These carbonates can, then, react with calcium ions and precipitate as calcium carbonates.

In the MICP process, there are two possible CO_2 sources for the calcification reaction to happen: i) CO_2 from the air and ii) CO_2 from the bacterial ureolysis and respiration. However, little is known about how much of the CO_2 can really be sequestered by these ureolytic microorganisms in aquatic environments and what are the real roles of microorganisms in the CO_2 sequestration during MICP.

Studies investigating MICP have been done mostly with microorganisms from soil. In soils, several species have been described to be able to perform MICP, such as *Sporosarcina pasteurii* [80], *Pseudomonas calcis* [89], *Bacillus* sp. VS1 [79], *Pseudomonas denitrificans* [53]. However, the presence of these microorganisms in pristine aquatic environments, such as caves and travertines, as well as their roles in calcification and CO_2 sequestration has not been fully investigated.

Recent studies suggested that the formation of stalactites and stalagmites in natural karst landscapes, such as caves and travertines could involve microorganisms active in MICP [64]. In such habitats, it has been hypothesized that the presence of CO_2, high calcium concentrations and the presence of urea provide optimal environmental conditions for biomineralization and therefore formation of stalactites and stalagmites and CO_2 sequestration [149]. The fact that these formations have been in these karstic environments for several thousands of years and continue

to grow every year, suggest that, if MICP is truly involved in the production of these formations, it could be a very promising natural long-term carbon sequestration process.

In these karstic environments, calcium comes originally from the rocks and surrounding soils [104]. Urea, on the other hand, is brought into caves and travertines through different sources: in the case of caves, urea is frequently introduced through mammals' urine [105], such as bats, and from seasonal or continuous water infiltration from the surface [106-108].

Compared to caves, travertines are outdoors, more prone to urea contamination from diverse sources, such as recreational human activities, animal excretions, municipal, or agricultural wastewater infiltration [150, 151]. The fact that urea and calcium are present in these habitats, allows us to hypothesize that microorganisms involved in MICP could also be present in these aquatic environments and be playing an important role in calcium carbonate precipitation and carbon sequestration.

Vis-a-vis the importance of ureolytic microorganisms in the MICP process and the fact that ten percent of the Earth's surface is occupied by karst landscapes, the presence of ureolytic microorganisms were investigated in two natural karstic environments, the Pamukkale travertines in Denizli, Turkey and the 'Cave Without A Name' in Texas, United States. In this study, we isolated and identified ureolytic microorganisms and determined their role in MICP and CO_2 sequestration. The effects of growth conditions on the carbon sequestration by these microorganisms were also investigated to better understand their physiology and roles in carbon sequestration during MICP.

3.2 MATERIALS AND METHODS

3.2.1 Sample collection and characterization

Water samples were collected aseptically in sterile 1L polyethylene containers from the Pamukkale travertine ponds in Denizli, Turkey (37°54'59" N, 29°07'02" E), and a pond in the 'Cave Without A Name' in Boerne, TX, USA (29°47'40" N, 98°43'55" W) in December 2011 and March 2012, respectively. The samples were kept at 4°C until they were processed. The physicochemical characteristics of the water samples were measured in triplicate according to the Standard Methods of water analysis [152] and presented in **Table 3-2** in the results. Water samples were stored at 4°C until brought to the laboratory for further analyses.

3.2.2 Growth conditions for enrichment and isolation of calcifying bacteria

Well-mixed aliquots of the water samples were inoculated (10%, v/v) in 13 different growth media as described in **Table 3-1**, and incubated aerobically at 150 rpm (INNOVA 44, New Brunswick Scientific Co., USA) for 3 days at 28°C and 20°C for travertine and cave samples, respectively. These temperatures were based on the local temperatures during sampling. For the bacterial isolation, serial dilutions were done in phosphate buffer solution (PBS, 0.01 M, pH=7.4), and samples were plated in triplicates onto agar plates prepared with 15 g/L of agar with their respective original growth broth (**Table 3-1**). The plates were incubated for 24 h at 28°C and 20°C for the travertine and cave samples, respectively. Different colonies in each plate were selected based on colony morphology. The selected colonies were streaked at least three times under the same conditions to ensure purity.

The isolates were then investigated for urease activity using the Stuart's broth and the Christensen's agar plates. The Stuart's broth contained 0.1 g L^{-1} yeast extract, 9.1 g L^{-1} KH_2PO_4,

9.5 g L^{-1} K_2HPO_4, 20 g L^{-1} urea, and 0.01 g L^{-1} phenol red [90]. The Christensen's agar plates contained 1 g L^{-1} peptone, 1 g L^{-1} dextrose, 5 g L^{-1} NaCl, 2 g L^{-1} KH_2PO_4, 20 g L^{-1} urea, 0.012 g L^{-1} phenol red, and 16 g L^{-1} agar [91]. All the urease-positive isolates were also investigated for calcium carbonate precipitation, according to Hammes and collaborators [82].

All the calcifying isolates were stored in 50% glycerol (v/v) and kept at -80°C as stock cultures for future experiments. In all experiments, unless indicated otherwise, the travertine and cave isolates were grown in their specific isolation medium as described in **Table 3-1** under 150 rpm at 28°C and 20°C, respectively.

TABLE 3-1- MEDIA COMPOSITION AND INCUBATION TEMPERATURES USED FOR BACTERIAL ISOLATION

Media	Ingredients	Isolate	Incubation temperature (°C)
Nutrient Broth (NB)	3 g L^{-1} meat extract, 5 g L^{-1} peptone, 20 g L^{-1} urea, 0.1 g L^{-1} nickel (II) chloride. pH 7.0.	TR9, TR20	28
Nutrient Broth No.1 (NB1)	1 g L^{-1} D-glucose, 15 g L^{-1} peptone, 6 g L^{-1} NaCl, 3 g L^{-1} yeast extract, 20 g L^{-1} urea, 0.1 g L^{-1} nickel (II) chloride. pH 7.0.		
Nutrient Broth No.3 (NB3)	1 g L^{-1} meat extract, 5 g L^{-1} peptone, 5 g L^{-1} NaCl, 2 g L^{-1} yeast extract, 20 g L^{-1} urea, 0.1 g L^{-1} nickel (II) chloride. pH 7.0.	TR3, TR11	28
ATCC 1832 Media (ATCC1832)	10 g L^{-1} tryptone, 5 g L^{-1} yeast extract, 4.5 g L^{-1} tricine, 5 g L^{-1} $(NH_4)_2SO_4$, 2 g L^{-1} glutamic acid, 10 g L^{-1} urea, 0.1 g L^{-1} nickel (II) chloride. pH 8.3.	TR1	28
Medium 220 (M220)	17 g L^{-1} casein peptone, 2.5 g L^{-1} K_2HPO_4, 2.5 g L^{-1} D-glucose, 5 g L^{-1} NaCl, 3 g L^{-1} soy peptone, 20 g L^{-1} urea, 0.1 g L^{-1} nickel (II) chloride. pH 7.0.		
Media 2 (M2)	6 g L^{-1} urea, 1 g L^{-1} NB1, 0.1 g L^{-1} nickel (II) chloride, 0.84 g L^{-1} $NaHCO_3$. pH 7.0	CV4	20
Tryptic Soy Broth (TSB)	17 g L^{-1} casein peptone-pancreatic, 2.5 g L^{-1} K_2HPO_4, 2.5 g L^{-1} D-glucose, 5 g L^{-1} NaCl, 3 g L^{-1} soy peptone-papain digest, 20 g L^{-1} urea, 0.1 g L^{-1} nickel (II) chloride. pH 7.0.		
NB-10X	10X dilution of NB	CV1	20
NB1-10X	10X dilution of NB1	CV2	20
NB3-10X	10X dilution of NB3		
ATCC1832-10X	10X dilution of ATCC1832	TR6, TR12, TR16, TR28	28
M220-10X	10X dilution of M220	CV3	20
TSB-10X	10X dilution of TSB		

3.2.3 DNA extraction and Amplified ribosomal DNA restriction analysis (ARDRA)

The total DNA of each isolate was extracted with the DNeasy® Blood and Tissue Kit as described by the manufacturer [153]. DNA quantification (O.D. 260) and quality (ratio A_{260}/A_{280})

was determined with the Take3 plate of the Synergy MX Microtiter plate reader (BioTek, USA). Total DNA extracted from each isolate was stored at -20^{o}C until further analyses.

The ARDRA experiment was performed with the universal eubacterial primers for the 16S rRNA genes. The primers were 27f (5'-AGAGTTTGATCMTGGCTCAG-3') and 1401r (5'-CGGTGTGTACAAGACCC-3') [154]. Triplicate PCR reactions of 50 µL for each isolate were performed using 1X AmpliTaq Gold® Fast PCR Master Mix (Applied Biosystems), 0.2 µM of each primer, and 50 ng/µL of the DNA template in the Applied Biosystems Veriti™ thermal cycler. The PCR amplification conditions were performed as previously described [154]. All replicate experiments contained negative controls without DNA and positive controls containing DNA from *E. coli*.

In order to verify the successful PCR amplification, aliquots of 10 µL of the PCR products were mixed with 5 µL of loading dye (Thermo Scientific), and loaded onto 1% agarose gel (Omnipur Agarose, EMD Millipore) containing SYBR Safe DNA gel stain (Invitrogen) (5 µL SYBR Safe stain per 50 mL TAE buffer), using 1X TAE buffer (Fermentas) as the running buffer. The agarose gel electrophoresis was run at 150 V for 30 min. The DNA in the gel was visualized and photographed with a Compact Digimage System UVDI, Major Science. The DNA fragment sizes were estimated using a 100 bp DNA ladder (Thermo Scientific). The remaining 40 µL of amplified PCR products were purified for further analyses using the QIAquick PCR Purification Kit (Qiagen), as described by the manufacturer [155].

The triplicate products for each isolate were combined in a single tube for purification. The purified products were quantified and their concentrations were adjusted to 100 ng μL^{-1} using the Take3 plate.

The 16S rRNA gene amplicons were then digested with *Hha*I (GCG'C) and *Msp*I (C'CGG) (New England Biolabs). Briefly, for each isolate, 10 µL of the purified PCR products were digested individually with each restriction enzyme in a reaction mixture containing 1 µL of restriction enzyme (20 µM), 2 µL of Buffer-4 (New England Biolabs), 6.8 µL of nuclease free water (Thermo Scientific), and 0.2 µL of bovine serum albumin (Thermo Scientific). All digestions were incubated at 37°C for 3 h, followed by a denaturation step at 65°C for 20 min. The restriction fragments were separated by electrophoresis in 3% (w/v) agarose gel at 60 V for 4 h, and visualized as previously described [156]. ARDRA patterns were analyzed using the PyElph 1.3 software that automatically extracts the data from the gel images, computes the molecular weights, and compares the DNA patterns using the Neighbor Joining method to determine the percent similarity among the isolates [157].

3.2.4 16S rRNA phylogenetic analyses

The purified PCR fragments were sequenced by the MD Anderson Genetic Laboratories (Houston, TX). Both the forward and reverse primers were used to sequence the whole length of the PCR products. The sequences were assembled using MEGA 5.1 software. The sequences obtained were compared to similar sequences available at the National Center for Biotechnology Information (NCBI) using BLASTn [158]. Similar sequences to the isolates were retrieved from GenBank and aligned against the DNA sequences of the isolates using MEGA 5.1 [159]. A phylogenetic tree was also constructed using MEGA 5.1 through the Neighbor joining method [160]. Bootstrap analysis based on 500 replications of the Neighbor joining dataset was also generated. The nucleotide sequences determined in this study were deposited in the NCBI database under accession numbers KM009125 to KM009137.

3.2.5 Determination of physiological properties of calcifying isolates

Physiological properties of the isolates were determined by measuring the growth rate of each isolate at different pH values and temperatures in their specific isolation medium. A plate reader was used to obtain the microbial growth rates in each experiment by measuring the absorbance at 600 nm for 24 h in each well. To determine the pH range that isolates were able to grow, 96-well plates were prepared for each isolate containing 300 µL of its specific growth medium in triplicate with pH values of 2, 3, 4, 5, 6, 7, 8, 9, 10, 11, and 12. For the pH experiments, the incubation temperature was kept at 28°C and 20°C for the travertine and cave isolates, respectively. For the temperature experiments, each isolate was grown in its specific isolation media at 15, 20, 25, 30, 35, and 40°C. The pH was kept at 7 ± 0.3 for the temperature experiments. All conditions were performed in triplicate. The growth rates for each condition and isolate were calculated as previously described [3]. The growth rate results were used to determine the optimum pH and temperature for each isolate. The triplicate results were averaged and the standard deviations were also calculated.

3.2.6 Determination of urease activity, calcification and CO_2 sequestration

Urease activities of calcifying isolates were determined as previously described [113]. Briefly, color change in the Stuart's broth was measured at 560 nm every 30 min for 24 h using the 96-well plate reader. At the end of the incubation, the color change rates (h^{-1}) were calculated for each isolate. A standard curve with the purified Jack Bean urease enzyme was used to determine the enzymatic activity (U mL^{-1}) of each isolate. One unit of urease activity corresponds to the amount of enzyme that hydrolyzes 1 µM of urea per min.

The rates of calcification and CO_2 sequestration were determined with five environmental isolates. Among these five isolates, three of them presented the highest urease activities (TR1, TR3 and TR20), while the other two showed the lowest urease activities (TR12 and CV1). TR and CV abbreviations correspond to travertine and cave isolates, respectively. For the calcification assay, these five isolates were incubated in their respective isolation medium supplemented with 6.9 g L^{-1} calcium chloride, which was found to be the optimum calcium concentration for calcification in *Sporosarcina pasteurii* ATCC 11859 [3]. The remaining calcium ions in the medium, after calcification, were measured by atomic absorption spectroscopy (Perkin Elmer AAnalyst™ 200) after centrifuging at 10000 rpm for 10 min and filtering the supernatant through 0.2 µm syringe filters. Negative controls, which had no bacterium, were used to determine whether there were non-biological calcite precipitations throughout the experiment.

In order to confirm the CO_2 sequestration, headspace CO_2 concentrations were measured in sealed serum bottles using a gas analyzer containing a non-dispersive infrared (NDIR) CO_2 sensor (Columbus Instruments Model 180C Gas Analyzer, Columbus, OH). For this experiment, overnight grown cultures were centrifuged at 10000 rpm for 10 min, and cells were collected, washed with sterile PBS, and the absorbance of the cell suspensions were adjusted to 0.5 at 600 nm. Subsequently, 39 mL serum bottles containing 9 mL of growth medium (with or without 6.9 g L^{-1} $CaCl_2$) were inoculated with 10% of the washed cell suspensions. The bottles were capped with butyl rubber stoppers and aluminum seals. Pure CO_2 gas was injected into each serum bottle to obtain 10% of CO_2 gas in the headspace. The serum bottles were then incubated for 24 h at 150 rpm and 20 or 28°C, depending on the isolate origin. After 1, 3.5, 6.5, 9, 21.5, and 24 h, duplicate serum bottles were analyzed for CO_2 concentration in the headspace. All experiments were repeated three times in three different days to take into consideration daily variations.

Abiotic controls, which had no cells, were included in each experiment as negative controls. All results were averaged out and their respective standard deviations were also calculated.

3.2.7 Abiotic effects of pH on CO_2 sequestration

Since bacteria can change the pH during growth, the abiotic effect of pH on calcium carbonate precipitation and CO_2 sequestration was also determined in growth medium with adjusted pH and without bacteria (**Table 3-5**). Briefly, similarly to the bacterial CO_2 sequestration experiment, 9 mL of non-inoculated growth medium was placed into 39 mL serum bottles. The pH of the different growth media used in this investigation were adjusted to 7.3, 8.3, 8.9, 9.2, and 9.3. The selection of the pH to do the abiotic experiment in each growth medium depended on the final pH after growing the bacteria in their specific growth medium (**Table 3-4**). After adjusting the pH, all the bottles were capped, sealed, injected with CO_2, and incubated as described in the previous section. After 24 h incubation, CO_2 concentrations in the headspace and the final pH of the solutions were measured.

In order to determine whether the CO_2 in the air was converted to carbonate and/or bicarbonate ions in the different growth media at different pH values, titrations of the media were done according to the Standard methods (**Table 3-12**) [152]. Before starting the incubations, the prepared growth media were titrated with 0.1 N H_2SO_4 with the help of phenolphthalein and methyl orange to determine the initial concentrations of the carbonate ions in the solution. At the end of the incubation periods with or without bacteria, the media were titrated again. These experiments allowed us to distinguish the biotic (*i.e.,* bacteria) and abiotic (*i.e.,* pH) effects on the CO_2 sequestration. All experiments were performed in triplicate in three different days. The results were averaged and the standard deviations were calculated.

3.2.8 Determination of dry cell weight

In order to normalize the CO_2 sequestration results by dry cell biomass, dry cell weights were determined for the five isolates (TR1, TR3, TR20, TR12 and CV1). Each isolate was grown overnight under its specific growth conditions, and a volume of 10 mL from each suspension was filtered through 0.2 µm pore-size sterile filters (Whatman). After filtration, the filter membranes containing the bacteria were dried at 60°C for 24 h and kept in the desiccator until measured. The dried biomass was determined by calculating the difference in the filter mass before and after filtering the cells in the filter membranes.

Experiments for each isolate were conducted in triplicate and the average biomass of dried cells per filter was compared with the control filter membranes after filtration of the media without bacteria. This procedure allowed us to determine any mass change in the filter caused by the media constituents retained in the filter membranes.

3.2.9 Scanning electron microscopy and energy dispersive X-ray spectroscopy

The calcification was confirmed using scanning electron microscopy (SEM) and energy dispersive X-ray spectroscopy (EDS) analyses (JEOL JSM-6010LA). The five isolates (TR1, TR3, TR20, TR12 and CV1) were incubated for 96 h with sterile glass slides in their original isolation medium (**Table 3-1**) with 6.9 g L^{-1} calcium. At the end of the incubation time, the glass slides were removed with a sterile spatula and washed with sterile distilled water to remove dissolved salts and loosely attached cells. The glass slides were dried at 60°C overnight and sputter coated (Denton Desk V) with gold at 5 mA for 30 s using 0.00016 mbar Argon prior to the SEM-EDS analysis. All experiments were done in triplicates and repeated three times in different days.

3.2.10 Growth medium components affecting the CO_2 sequestration

The growth medium components affecting microbial CO_2 sequestration were investigated following the Plackett–Burman design using the Design Expert software [161]. In the design, a total of 11 components commonly found in the medium for MICP microorganisms (tryptone, yeast extract, tricine, ammonium sulfate, glutamic acid, urea, meat extract, peptone, sodium chloride, nickel (II) chloride, and glucose) were selected for the CO_2 sequestration investigation. The experimental design is shown in **Table 3-5**, where each row represents one experiment and each column represents an independent variable. In all the Plackett-Burman design experiments, 6.9 g L^{-1} calcium chloride was added to the media. The optimum concentrations of the medium constituents were determined to enhance the CO_2 sequestration for the five isolates (TR1, TR3, TR20, TR12, and CV1). In order to confirm the CO_2 sequestration optimization results, experimental assays were performed under the optimum conditions determined by the Design Expert software and CO_2 sequestration yields were calculated. All experiments were performed in triplicate and the results were averaged out and standard deviations were calculated.

3.2.11 Statistical analyses

With the Design Expert software, the analysis of variance (ANOVA) was employed to determine the statistical significance of the results. The quality of the experiments was determined statistically by the coefficient of determination R^2, and the F-test. To assess the relationship between urease activity, MICP, and CO_2 sequestration results, Excel was used and the Spearman's rank correlation was calculated [114].

3.3 RESULTS AND DISCUSSION

3.3.1 Isolation of calcifying bacteria and water sample analysis

In this study, 13 different media (**Table 3-1**), commonly used in MICP studies, were used for the first time to obtain calcifying microorganisms from water samples collected in Pamukkale travertines from Turkey and 'A Cave Without a Name' from the United States. The different media yielded different numbers of isolates with distinct morphological characteristics, such as size, shape, and color. It is important, however, to point out that some growth media did not allow the growth of any microorganisms from these habitats; this observation was especially true for the cave sample. For instance, the nutrient rich media did not allow isolation of microorganisms from the cave sample. In total, 6 and 28 isolates from the cave and the travertine pond, respectively, were obtained.

After isolation, the microorganisms were investigated for urease activity and calcification and it was determined that all these isolates were capable of MICP. The chemical analyses of water samples can be seen in **Table 3-2** below.

TABLE 3-2- PHYSICOCHEMICAL CHARACTERISTICS OF THE WATER SAMPLES BASED ON TRIPLICATE ANALYSES

Analyses	**Concentrations (mg L^{-1})**	
	Travertine water	**Cave water**
TOC	No detectable	No detectable
Phosphate (PO_4^{-3})	0.09±0.003	0.06±0.001
Nitrate (NO_3^- - N)	0.2±0.015	0.2±0.042
Nitrite (NO_2^-)	1±0.17	1±0.22
Ammonia (NH_3-N)	0.44±0.03	0.07±0.002
Chlorine (Cl_2)	0.02±0.001	0.02±0.008
Calcium (Ca^{2+})	51.2±0.5	49.1±0.3
pH	7±0.1	7.4±0.1

3.3.2 Genetic fingerprinting and phylogenetic classification of isolates

The isolates were further investigated for identical band patterns by digestion with *Hha*I and *Msp*I restriction enzymes of the amplified 16S rRNA genes. The different band patterns were then subjected to cluster analysis. The ARDRA results with the *Hha*I and *Msp*I enzymes could distinguish 17 (**Figure 3-2**) and 13 (**Figure 3-1**) different strains, respectively. These results showed that the *Msp*I enzyme was more stringent than *Hha*I in this study. The isolates presenting 100% identical band patterns were considered to be clonal isolates and were no further investigated. The isolates (4 isolates from cave and 9 isolates from travertine) presenting distinct band patterns for *Msp*I with a similarity lower than 60% (**Figure 3-1**) were further sequenced for identification.

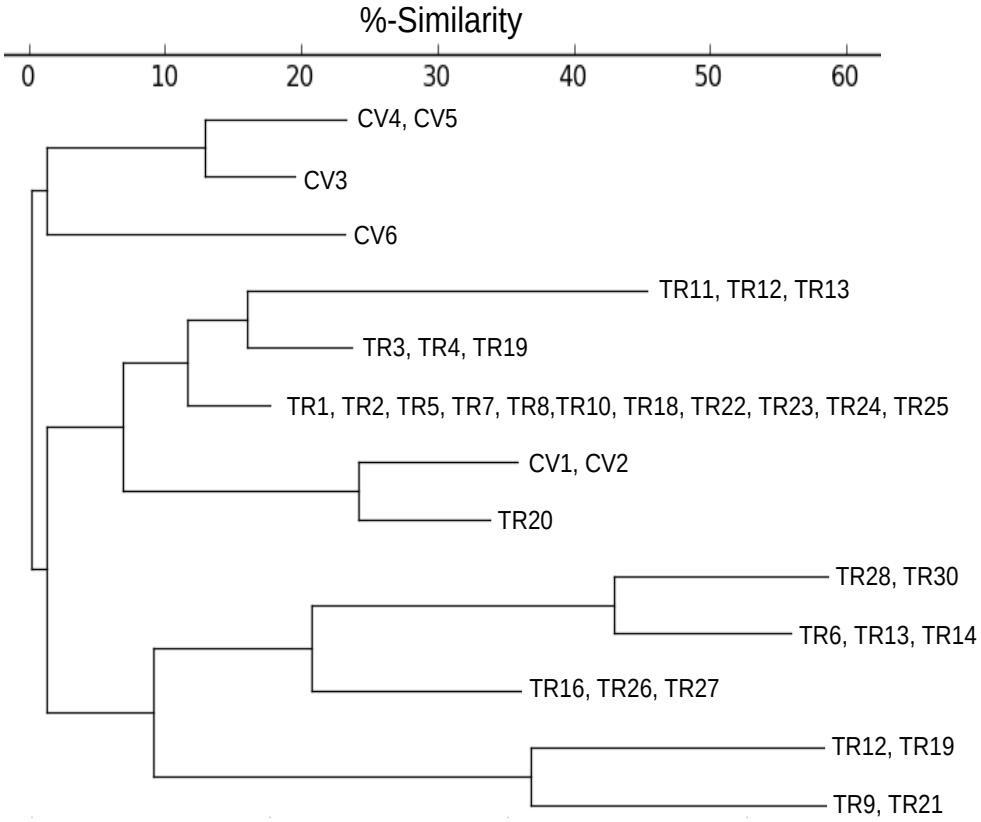

FIGURE 3-1- ARDRA DENDOGRAM OF CALCIFYING ISOLATES FROM TRAVERTINE AND CAVE AFTER DIGESTION OF THE 16S RRNA GENES WITH MSPI ENZYME.

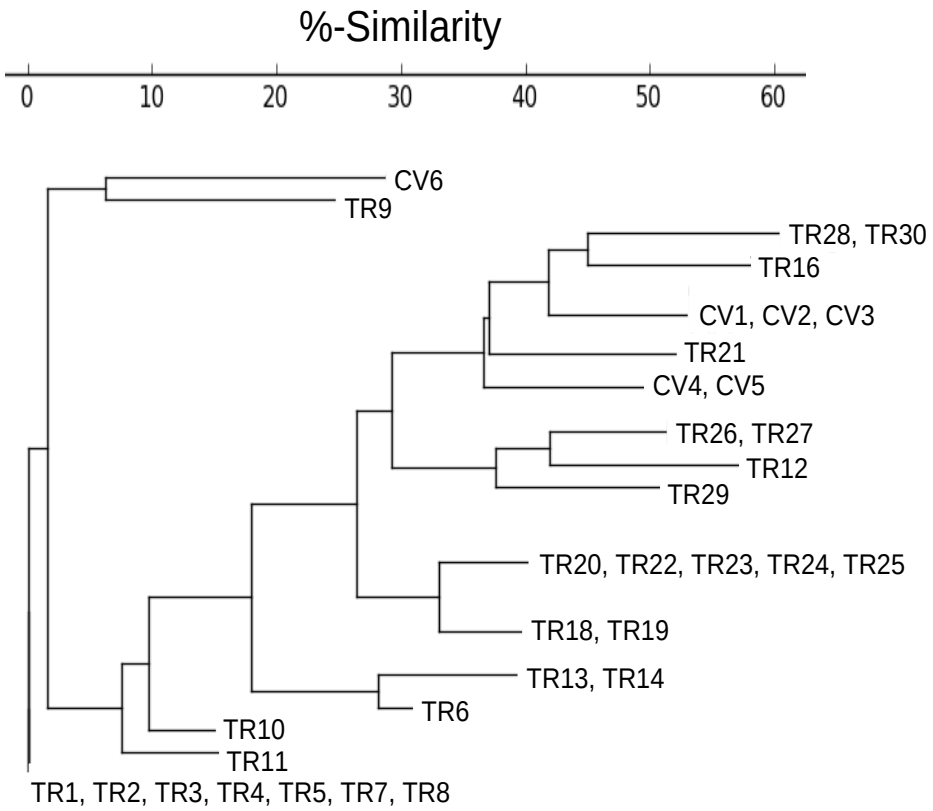

FIGURE 3-2- ARDRA DENDOGRAM OF CALCIFYING ISOLATES FROM TRAVERTINE AND CAVE AFTER DIGESTION OF THE 16S RRNA GENES WITH HHAI ENZYME. PERCENTAGES OF SIMILARITY WERE SHOWN ABOVE THE DENDOGRAM.

The sequencing results (**Figure 3-3**) showed that the majority of the isolates belonged to two genera, *Sporosarcina* and *Sphingobacterium.* The isolates with high similarity to *Sporosarcina* were CV1 (92%), TR1 (92%), TR20 (91%), and TR3 (91%), while CV4 (87%), CV3 (88%), and CV2 (83%) had high similarity to *Sphingobacterium*. The isolates TR11 (99%), TR6 (96%), TR28 (94%), TR9 (94%), TR12 (96%), and TR16 (99%) presented high similarity to *Bacillus*, *Brevundimonas*, *Chryseobacterium*, *Alcaligenes*, *Acinetobacter*, and *Stenotrophomonas*, respectively (**Figure 3-3**). Based on these results, we were able to isolate more diverse MICP microorganisms in the travertine samples than in the cave. It is possible; however, that other types of medium, not investigated in this study, could be more appropriated for the isolation of a more diverse microbial population in the cave.

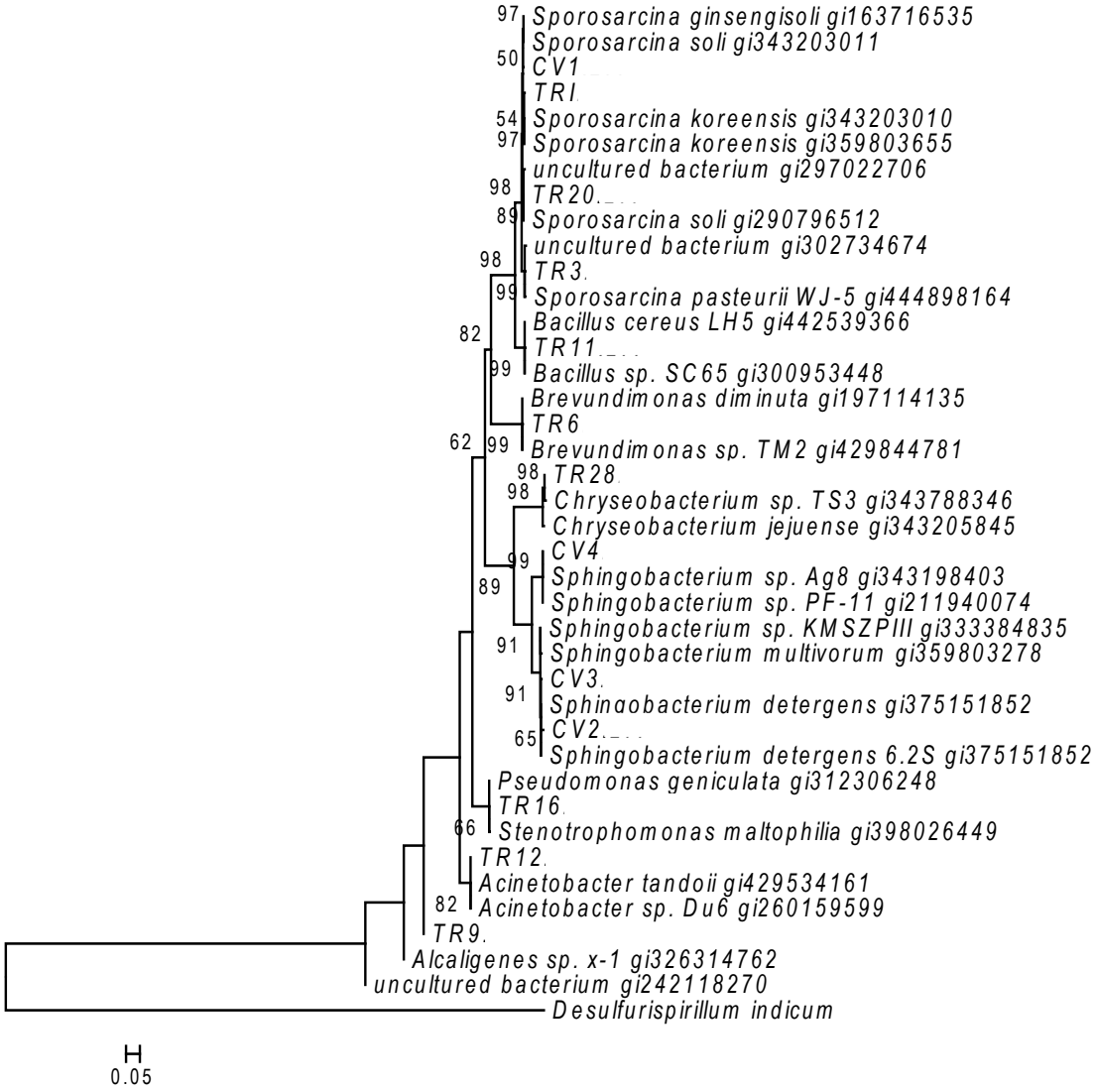

FIGURE 3-3- PHYLOGENETIC TREE BASED ON 16S RRNA GENE SEQUENCES SHOWING THE RELATIONSHIP AMONG CALCIFYING ISOLATES OBTAINED FROM THE PAMUKKALE TRAVERTINES AND THE 'CAVE WITHOUT A NAME' WITH THEIR CLOSEST RELATIVES ACCORDING TO NCBI.

The comparison of the results obtained in **Figure 3-1** and **Figure 3-3** showed that the ARDRA dendogram obtained with the *Msp*I enzyme is very similar to the 16S rRNA phylogenetic tree. Therefore, it can be concluded that *Msp*I seems to be a better restriction enzyme to identify and cluster calcifying isolates than *Hha*I. Additionally, the phylogenetic results (**Figure 3-3**) showed that some isolates, even though they had different band patterns in the ARDRA results (**Figure**

3-1), they still presented 99% similarity in their 16S rRNA gene sequences. This was the case for some isolates, such as TR6 and TR11, TR1, TR28, CV4 and TR 20. The 16S rRNA phylogenetic tree also showed that the isolates were clustered in six different classes: *Bacilli* (CV1, TR1, TR20, TR3, TR11), α-*Proteobacteria* (TR6), *Flavobacteria* (TR28), *Sphingobacteria* (CV4, CV3, CV2), γ-*Proteobacteria* (TR16, TR12), and β-*Proteobacteria* (TR9). In this study, the most abundant and diverse number of isolates belonged to *Bacilli*.

3.3.3 Effect of growth media on bacterial isolation

In the present study, rich and mineral media were investigated. The different types of media used allowed the isolation of diverse microorganisms in the two sites. In the case of the cave, isolates were only obtained in more oligotrophic media, such as the M2 medium (minimal medium) and the 10X diluted-rich media. In the case of the travertine, isolates were obtained from both types of media. The rich media, however, allowed the isolation of 5 distinct bacteria, while 8 distinct bacteria were obtained in the mineral or diluted-rich media. Among the media investigated, ATCC-1832-10X medium was the best to obtain the highest number of isolates from the travertine (**Table 3-1**).

3.3.4 Physiological properties of the calcifying isolates

The physiology of these microorganisms was determined by measuring their pH and temperature growth ranges, as well as their optimum temperature and pH for growth. The results show that the isolates were able to grow in a wide range of pH values and presented optimum pH values between 6 and 9 (**Table 3-3**). It is important to point out that the isolates (TR1, TR3, and TR20) presenting the highest urease activities among the isolates (**Figure 3-4**) preferred alkaline conditions for growth. In contrast, the isolates with optimum growth at pH values equal or below 7, presented lower urease activities.

TABLE 3-3- THE PH AND TEMPERATURES AT WHICH THE ISOLATES ARE ABLE TO GROW, AND THEIR OPTIMUM VALUES

Isolate	Isolation growth media	pH range of growth	Optimum pH	Temperature range (°C)	Optimum growth temperature (°C)
TR1	ATCC 1832	3-11	9	15-40	35
TR3	NB3	3-12	8	15-40	30
TR6	ATCC 1832-10X	3-12	7	15-40	35
TR9	NB	4-12	7	15-40	35
TR11	NB3	3-12	7	15-40	30
TR12	ATCC 1832-10X	4-12	7	15-30	25
TR16	ATCC 1832-10X	4-12	8	15-40	25
TR20	NB	2-12	9	25-40	30
TR28	ATCC 1832-10X	4-11	7	30-40	35
CV1	NB-10X	4-11	6	15-35	35
CV2	NB3-10X	4-12	7	15-25	20
CV3	M220-10X	4-11	7	15-30	30
CV4	M2	4-11	8	15-35	35

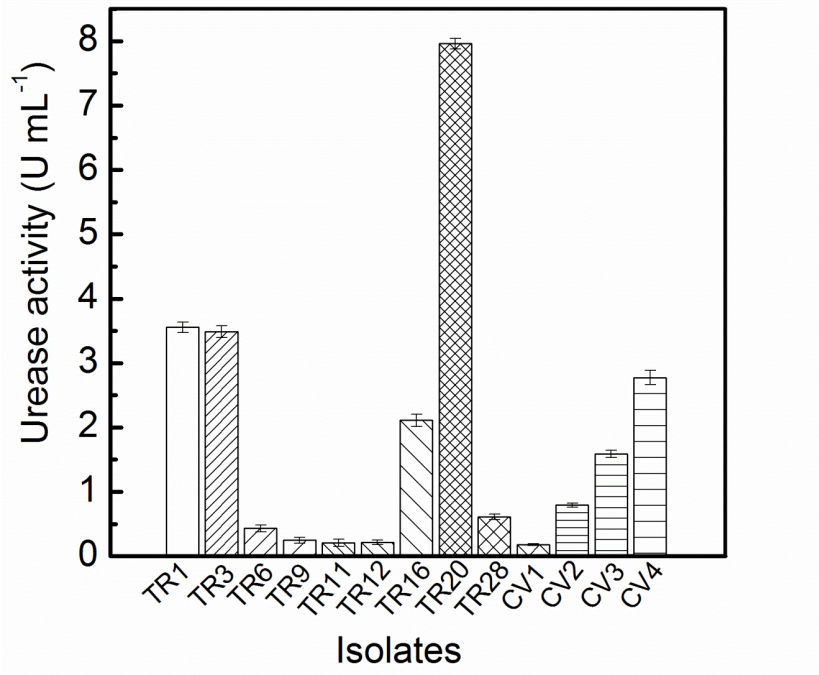

FIGURE 3-4- UREASE ACTIVITIES OF TRAVERTINE (TR) AND CAVE (CV) ISOLATES. ALL ISOLATES WERE CULTURED IN THEIR SPECIFIC GROWTH CONDITIONS. ALL EXPERIMENTS WERE DONE IN TRIPLICATE AND THE ERROR BARS CORRESPOND TO STANDARD DEVIATIONS.

In the case of the temperature, the average annual temperature in our sampling cave is nearly 20°C [162]. Hence, all the cave isolates were able to grow at this temperature; however only the isolate CV2 showed an optimum growth at 20°C, the others all had higher optimum

growth temperatures. Considering that Texas has very warm temperatures, it is possible that the isolates could have come from an external source other than the cave, which would have explained the preference of these isolates for higher temperatures than the normal cave temperature.

In the Pamukkale travertines, the average annual temperature is 35^{o}C at the exit point, where the spring water comes from the underground [163]. Our sampling site was, however, far from the spring point. Therefore, the water temperature was around 28^{o}C. The different water temperatures at different points in the travertine would explain the different optimum temperature preferences of the isolates. In all cases, however, the travertine isolates had optimum growth temperatures in the range of the temperatures found in the site.

Besides investigating the optimum pH and the temperature for the growth of the isolates, we also investigated their urease activities; the 13 isolates showed different urease activities ranging between 8 and 0.2 U mL^{-1} (**Figure 3-4**). The top three performing isolates, TR20, TR1 and TR3, having 8, 3.6 and 3.5 U mL^{-1} urease activities, respectively; and the two worst performing isolates, TR12 and CV1, having 0.22 and 0.18 U mL^{-1} urease activity, respectively, were selected for the calcification investigations and CO_2 sequestration. In these investigations, the goal was to determine whether the urease activity was linked to calcification and CO_2 sequestration; and then determine whether changes in the medium concentration components would allow the enhancement of the CO_2 sequestration even by the worst ureolytic microorganisms.

In the calcification assays, we determined the amount of calcium left in the medium (**Figure 3-5**) and analyzed all the precipitates formed during the microbial growth. The quantifications of the calcium ions left in the bacterial media showed that each isolate had different calcification capabilities (**Figure 3-5**).

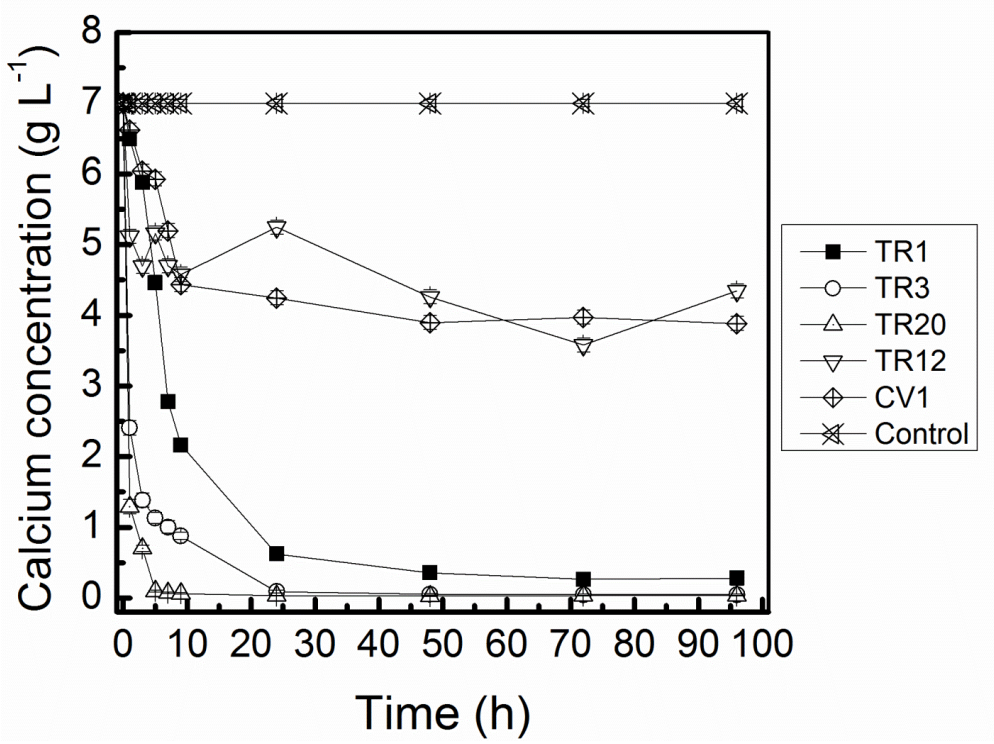

FIGURE 3-5- THE CALCIUM CONCENTRATIONS IN THE GROWTH MEDIA DURING MICROBIAL GROWTH.

The isolate presenting the highest calcium carbonate precipitation was TR20, which precipitated almost 100% of the calcium carbonate within 6 h. The isolates TR1 and TR3, on the other hand, precipitated 69% and 87% of calcium carbonate, respectively, in the same period of time (**Figure 3-5**). No changes in the calcium ions in the medium were observed in the control samples, which had no bacteria.

In order to further corroborate the calcium ion precipitation from the media, SEM and EDS analyses of the precipitates were performed. The results showed that the particles precipitated by the microorganisms during MICP were $CaCO_3$ mineral precipitates. In **Figure 3-6**, the SEM results demonstrated that the precipitates are composed mostly by calcite and a few vaterites [64]. Elemental analysis of the precipitates with EDS (**Figure 3-6**) confirmed the presence of $CaCO_3$.

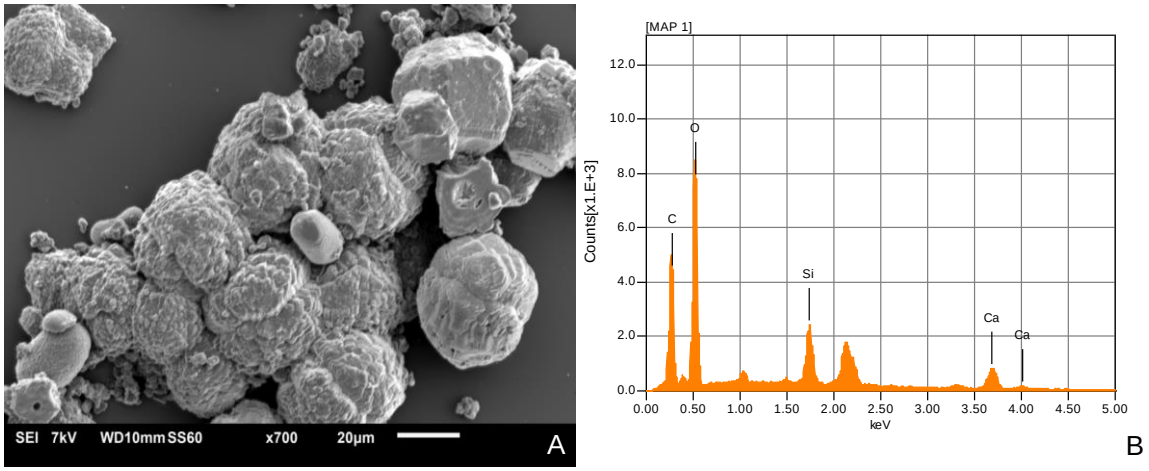

FIGURE 3-6- (A) REPRESENTATIVE SEM IMAGE OF PRECIPITATED CACO3 PARTICLES OF SPOROSARCINA SP. TR20 ON A GLASS SLIDE. (B) EDS RESULT OF PRECIPITATED CALCIUM CARBONATE. SCALE BAR: 20 µM

3.3.5 Effects of pH on biotic and abiotic CO_2 sequestration

In aquatic systems, the carbonate system plays an essential role in the abiotic CO_2 sequestration [12]. The carbonate system is also directly linked to pH, which can lead to the formation of carbonate and/or bicarbonate in the water or growth medium [9]. Microorganisms also play an important role in changing the pH of their surrounding environment and producing CO_2 during growth. At the same time, MICP microorganisms have also been described to facilitate calcite precipitation to store CO_2 [7]. However, no study so far has done a systematic investigation to determine how much of the CO_2 sequestration during the MICP process is really biotic or abiotic.

In this work, the abiotic CO_2 uptake was determined by quantifying the CO_2 in the headspace of the serum bottles by a gas analyzer and by titration of the media to determine the amounts of carbonate (CO_3^{2-}) and bicarbonate (HCO_3^-) ions present in the growth media. In this investigation, sterile growth media had their pH adjusted to the same final pH of the media that typically the microorganisms induce after growth for 24 h (**Table 3-4**). The goal was to determine whether the 10% CO_2 in the headspace got dissolved in the growth media at the

specific pH generated by the bacteria through abiotic processes. The results (**Table 3-4**) showed that the medium NB-10X had the lowest abiotic CO_2 uptake from the headspace (0.9%). The medium ATCC 1832, on the other hand, had the highest abiotic CO_2 uptake (5.4%).

TABLE 3-4- THE CHANGES OF CO_2 CONCENTRATION IN HEADSPACE AND PH OF GROWTH MEDIA AFTER 24 H INCUBATION WITH AND WITHOUT BACTERIAL CELLS TO DETERMINE BIOTIC AND ABIOTIC CO_2 SEQUESTRATION.

Medium (with bacteria cells)	Initial CO_2 in the headspace (%)	Initial pH	Final CO_2 in the headspace (%)	pH after 24 h incubation	CO_2 (%) in abiotic bottles*
TR1 in ATCC 1832	10	7.6	2.1	8.9	4.6
TR3 in NB3	10	7.5	2.6	9.2	6.1
TR20 in NB	10	7.3	3.6	9.3	6.1
CV1 in NB-10X	10	7.3	6.4	8.3	9.1
TR12 in ATCC 1832-10X	10	7.3	6	7.3	9.1

*Abiotic bottles had no cells and their pH values were adjusted to the same pH as the biotic experiments after 24 h incubation.

The biotic uptake by the MICP process was also determined by growing the isolates in their respective growth medium and measuring the amount of CO_2 left in the headspace. The results from the abiotic assays were subtracted from the assays with the bacteria to determine the biotic CO_2 uptake by the microorganisms. The results showed that all isolates were able to sequester CO_2. The isolates that showed the highest and the lowest biotic CO_2 uptake were TR3 and TR1 with a capability of sequestering 3.5% and 2.4% of CO_2, respectively (**Table 3-4**). Besides, we also investigated the sterile growth media at specific pH values (**Table 3-5**) in order to better understand the abiotic CO_2 sequestration.

TABLE 3-5- CO_2 CONCENTRATIONS IN HEADSPACE VOLUMES OF SERUM BOTTLES CONTAINING ONLY MEDIA WITH SPECIFIED PH AND NO BACTERIA

Media (No bacteria)	Initial CO_2 (%)	CO_2 (%) at pH=7.3	CO_2 (%) at pH=8.3	CO_2 (%) at pH=9.3
ATCC 1832	10	8.6±0.7	6.2±0.5	2.3±0.1
NB3	10	9.7±0.8	9.1±0.7	4.5±0.3
NB	10	9.2±0.6	8.4±0.7	6.1±0.5
NB-10X	10	9.1±0.6	9.1±0.7	9.1±0.7
ATCC 1832-10X	10	9.6±0.6	9.6±0.7	8.6±0.6

In summary, in the MICP process, we were able to observe two CO_2 sequestration phenomena happening: abiotic and biotic CO_2 uptake. Briefly, most of the isolates increased the pH of the media, which led to an increase in abiotic CO_2 uptake by the growth media, but also the cells induced the calcite precipitation that also sequestered CO_2. It is worth point out, that if no cells were grown in the media, there would not be any pH increase and therefore no CO_2 removal from the headspace. But, if we changed the pH chemically or biologically to a pH higher than 7, we started to observe CO_2 sequestration when we only had excess amounts of CO_2 (10%) in the serum bottles.

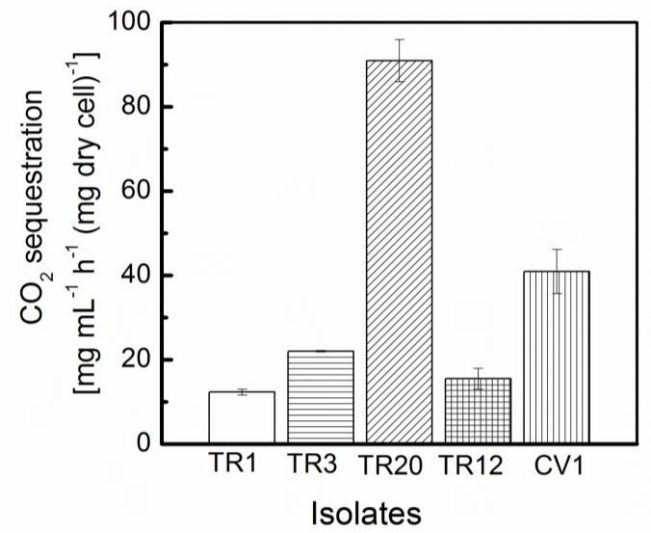

FIGURE 3-7- NORMALIZED CARBON DIOXIDE SEQUESTRATION RATES FOR EACH ISOLATE.

In addition to the headspace and titration measurements, the CO_2 uptake rates were determined and normalized by the dry cell weight (**Figure 3-7**). Among the isolates, a faster CO_2 sequestration was achieved by the isolate TR20, with a sequestration rate of 90.9 mg mL^{-1} h^{-1} (mg dry cell)$^{-1}$. However, TR1 showed the slowest CO_2 sequestration rate with 12.3 mg mL^{-1} h^{-1} (mg dry cell)$^{-1}$. The comparison of the CO_2 sequestration rates (**Figure 3-7**), with the urease activity results (**Figure 3-4**), showed that the urease activity and the CO_2 sequestration rates were not directly proportional, but were somehow connected (**Table 3-12**). For instance, the

isolates having the lowest urease activities and calcification rates (TR12 and CV1), presented significant CO_2 sequestration rates. Based on these results, one could hypothesize that the urease-positive bacteria could be sequestering CO_2 by two mechanisms: 1) increasing pH while growing, which would enhance CO_2 dissolution into the growth medium and induce calcite precipitation as typically observed in the MICP process; 2) microorganisms could be sequestering CO_2 by unknown CO_2 metabolisms, not necessarily linked to MICP.

3.3.6 Relationship between pH, urease activity, MICP, and CO_2 sequestration

In this study, the relationship among pH, urease activity, MICP, and CO_2 sequestration was investigated using the Spearman's rank correlation analysis. The results showed that pH, urease activity, and MICP are strongly linked, because the isolates having higher urease activity caused higher final pH values of the media, and presented higher MICP rates. The analysis resulted with strong correlations between urease activity and MICP (ρ=0.9; p-value<0.001), urease activity and pH (ρ=0.9; p-value<0.001), and also MICP and pH (ρ=1; p-value<0.001) (**Table 3-6**).

TABLE 3-6- CORRELATION RESULTS.

	Spearman's rho (ρ)	**p-value**		**Spearman's rho (ρ)**	**p-value**
Urease Activity & MICP	0.900	0.0003	MICP & Abiotic CO_2 sequestration	0.533	0.01
Urease Activity & Total CO_2 sequestration	0.700	0.001	MICP & Biotic CO_2 sequestration	-0.100	0.01
Urease Activity & Abiotic CO_2 sequestration	-0.500	0.001	MICP & pH	1.000	0.0001
Urease Activity & Biotic CO_2 sequestration	0.746	0.003	pH & Total CO_2 sequestration	0.600	0.001
Urease Activity & pH	0.900	0.0003	pH & Abiotic CO_2 sequestration	0.533	0.001
MICP & Total CO_2 sequestration	0.600	0.002	pH & Biotic CO_2 sequestration	-0.100	0.01

In addition, the analysis results showed the relationship between urease activity and CO_2 sequestration; this correlation is stronger with abiotic CO_2 sequestration (ρ=0.746; p-value<0.01) than biotic CO_2 sequestration (ρ=-0.5; p-value<0.01) (**Table 3-6**). In case of pH and MICP, the correlation results were very strong (ρ=1; p-value<0.01). Among the results, biotic CO_2 sequestration was found to be not linked with pH and MICP.

3.3.7 Effects of growth medium components on CO_2 sequestration

The Plackett-Burman (PB) experimental design was employed in order to investigate the effects of each growth medium component on the CO_2 sequestration. In the PB design, a total of 11 variables, namely, tryptone, yeast extract, tricine, ammonium sulfate, glutamic acid, urea, meat extract, peptone, sodium chloride, nickel (II) chloride, and glucose were investigated.

TABLE 3-7- A 16-RUN PLACKETT-BURMAN EXPERIMENTAL DESIGN FOR THE TOP THREE PERFORMING ISOLATES. A TOTAL OF 11 PARAMETERS IN g/L WERE INVESTIGATED TO FIND THE MOST SIGNIFICANT FACTORS FOR CO_2 SEQUESTRATION.

Trial	Tryptone	Yeast extract	Tricine	Ammonium sulfate	Glutamic acid	Urea	Meat extract	Peptone	Sodium chloride	Nickel (II) chloride	Glucose
1	1	5	0.45	5	2	2	3	5	5	0.01	0.25
2	1	5	4.5	5	0.2	2	0.3	5	0.5	0.1	2.5
3	10	5	0.45	0.5	0.2	20	0.3	5	5	0.01	2.5
4	10	0.5	0.45	0.5	2	2	3	5	0.5	0.1	2.5
5	5.5	2.75	2.475	2.75	1.1	11	1.65	2.75	2.75	0.055	1.375
6	10	5	0.45	5	2	20	0.3	0.5	0.5	0.1	0.25
7	1	0.5	0.45	0.5	0.2	2	0.3	0.5	0.5	0.01	0.25
8	1	0.5	4.5	0.5	2	20	0.3	5	5	0.1	0.25
9	5.5	2.75	2.475	2.75	1.1	11	1.65	2.75	2.75	0.055	1.375
10	10	0.5	4.5	5	2	2	0.3	0.5	5	0.01	2.5
11	5.5	2.75	2.475	2.75	1.1	11	1.65	2.75	2.75	0.055	1.375
12	5.5	2.75	2.475	2.75	1.1	11	1.65	2.75	2.75	0.055	1.375
13	10	0.5	4.5	5	0.2	20	3	5	0.5	0.01	0.25
14	1	0.5	0.45	5	0.2	20	3	0.5	5	0.1	2.5
15	1	5	4.5	0.5	2	20	3	0.5	0.5	0.01	2.5
16	10	5	4.5	0.5	0.2	2	3	0.5	5	0.1	0.25

These 11 variables were selected since they are the main components of the isolation media, and media components are known to affect the growth and other cellular metabolisms [164]. The PB design allowed us to analyze several medium components simultaneously in the

growth medium instead of investigating one component at a time. The concentrations of each medium component used in each PB design medium are listed in **Table 3-7**.

After preparing the 16 different PB media, the isolates were grown in each of these media. Calcification and urease activity measurements followed by CO_2 sequestration determination were performed for each PB media. The outputs of the PB design, such as each variable's effects on the urease activity and CO_2 sequestration, *p* values, and the model coefficients, were obtained using the Design Expert software and represented in **Table 3-8**, **Table 3-9**, **Table 3-10**, and **Table 3-11**.

TABLE 3-8- THE % EFFECTS, COEFFICIENTS, AND P-VALUES OF THE PLACKETT-BURMAN DESIGN TO INDICATE THE IMPORTANT VARIABLES FOR THE UREASE ACTIVITY (U/ML) OF TR1, TR3, AND TR20. $p<0.05$ INDICATES THAT THE EFFECT IS SIGNIFICANT.

UREASE ACTIVITY	TR1			TR3			TR20		
	Effect (%)	Coefficient	p	Effect (%)	Coefficient	p	Effect (%)	Coefficient	p
Intercept	4.71			7.17			7.68		
Tryptone	7.82	-0.42	<0.0001	21.14	-0.80	<0.0001	3.65	0.89	<0.0001
Yeast extract	4.25	-0.31	0.0002	4.84	-0.38	<0.0001	4.16	0.95	<0.0001
Tricine	12.41	-0.52	<0.0001	11.68	-0.59	<0.0001	0.96	0.46	<0.0001
Ammonium sulfate	1.83	0.20	0.0005	0.10	-0.056	<0.0001	0.27	-0.24	<0.0001
Glutamic acid	5.84	-0.36	<0.0001	0.051	0.039	0.0002	2.89	0.79	<0.0001
Urea	54.79	1.10	<0.0001	9.70	0.54	<0.0001	59.81	3.60	<0.0001
Meat extract	6.69	0.38	<0.0001	6.66	-0.45	<0.0001	0.028	0.078	<0.0001
Peptone	2.95	-0.26	0.0003	0.68	0.14	<0.0001	0.81	0.42	<0.0001
Sodium chloride	0.10	-0.047	0.0335	6.65	-0.45	<0.0001	0.71	-0.39	<0.0001
Nickel (II) chloride	0.79	0.13	0.0019	0.21	0.080	<0.0001	4.80	-1.02	<0.0001
Glucose	2.30	0.23	0.0004	7.94	-0.049	<0.0001	5.20	-1.06	<0.0001

TABLE 3-9-THE % EFFECTS, COEFFICIENTS, AND P-VALUES OF THE PLACKETT-BURMAN DESIGN TO INDICATE THE IMPORTANT VARIABLES FOR THE UREASE ACTIVITY (U/ML) OF TR12 AND CV1. P<0.05 INDICATES THAT THE EFFECT IS SIGNIFICANT.

UREASE ACTIVITY	TR12			CV1		
	Effect (%)	Coefficient	p	Effect (%)	Coefficient	p
Intercept	2.38			2.46		
Tryptone	5.84	-0.059	<0.0001	5.47	-0.074	<0.0001
Yeast extract	5.25	0.053	<0.0001	3.90	-0.015	0.0004
Tricine	13.43	-0.033	<0.0001	1.50	-0.21	<0.0001
Ammonium sulfate	1.02	0.048	<0.0001	0.02	-0.053	<0.0001
Glutamic acid	5.84	0.0051	0.0151	3.00	-0.071	<0.0001
Urea	55.72	0.59	<0.0001	72.5	0.41	<0.0001
Meat extract	5.71	0.0095	0.0023	0.03	0.013	0.0007
Peptone	3.95	0.034	<0.0001	1.00	-0.058	<0.0001
Sodium chloride	0.20	-0.0051	0.0152	0.80	-0.068	<0.0001
Nickel (II) chloride	0.60	-0.067	<0.0001	3.00	-0.11	<0.0001
Glucose	2.20	-0.043	<0.0001	9.00	-0.055	<0.0001

TABLE 3-10-THE % EFFECTS, COEFFICIENTS, AND P-VALUES OF THE PLACKETT-BURMAN DESIGN TO INDICATE THE IMPORTANT VARIABLES FOR THE CO_2 SEQUESTRATION OF TR1, TR3, AND TR20. P<0.05 INDICATES THAT THE EFFECT IS SIGNIFICANT.

CO_2 SEQUESTRATION	**TR1**			**TR3**			**TR20**		
	Effect (%)	**Coefficient**	**p**	**Effect (%)**	**Coefficient**	**p**	**Effect (%)**	**Coefficient**	**p**
Intercept	2.61			2.53			2.59		
Tryptone	0.53	0.033	<0.0001	0.70	-0.044	<0.0001	2.02	-0.064	<0.0001
Yeast extract	1.36	0.053	<0.0001	0.036	9.9×10^{-3}	<0.0001	0.13	0.016	<0.0001
Tricine	0.42	0.029	<0.0001	0.39	-0.033	<0.0001	0.43	-0.029	<0.0001
Ammonium sulfate	1.64	0.058	<0.0001	0.42	0.034	<0.0001	1.30	0.051	<0.0001
Glutamic acid	2.23	0.067	<0.0001	0.053	0.012	<0.0001	0.15	0.018	<0.0001
Urea	88.27	0.42	<0.0001	91.25	0.50	<0.0001	93.31	0.43	<0.0001
Meat extract	1.61	0.057	<0.0001	0.021	-7.7×10^{-3}	<0.0001	0.18	-0.019	<0.0001
Peptone	1.56	0.056	<0.0001	0.54	-0.039	<0.0001	0.06	0.012	<0.0001
Sodium chloride	1.29	0.051	<0.0001	1.25	0.058	<0.0001	0.14	0.017	<0.0001
Nickel (II) chloride	0.48	0.032	<0.0001	3.27	-0.094	<0.0001	1.87	-0.062	<0.0001
Glucose	0.55	0.034	<0.0001	2.04	-0.074	<0.0001	0.38	-0.028	<0.0001

TABLE 3-11-THE % EFFECTS, COEFFICIENTS, AND P-VALUES OF THE PLACKETT-BURMAN DESIGN TO INDICATE THE IMPORTANT VARIABLES FOR THE CO_2 SEQUESTRATION OF TR12 AND CV1. p<0.05 INDICATES THAT THE EFFECT IS SIGNIFICANT.

CO_2 SEQUESTRATION	TR12			CV1		
	Effect (%)	Coefficient	p	Effect (%)	Coefficient	p
Intercept	2.38			2.46		
Tryptone	0.938	-0.059	<0.0001	2.178	-0.074	<0.0001
Yeast extract	0.760	0.053	<0.0001	0.088	-0.015	0.0002
Tricine	0.297	-0.033	<0.0001	18.09	-0.21	<0.0001
Ammonium sulfate	0.638	0.048	<0.0001	1.111	-0.053	<0.0001
Glutamic acid	0.007	0.0051	0.0158	2.010	-0.071	<0.0001
Urea	95.29	0.59	<0.0001	67.37	0.41	<0.0001
Meat extract	0.024	0.0095	0.0027	0.064	0.013	0.0003
Peptone	0.324	0.034	<0.0001	1.336	-0.058	<0.0001
Sodium chloride	0.007	-0.0051	0.0158	1.809	-0.068	<0.0001
Nickel (II) chloride	1.214	-0.067	<0.0001	4.725	-0.11	<0.0001
Glucose	0.493	-0.043	<0.0001	1.205	-0.055	<0.0001

According to the PB design results, all of the media contents were found highly significant (p<0.01) for both CO_2 sequestration and urease activity (**Table 3-8** to **Table 3-11**). Urea, however, was found to be the most important medium component for both ureolysis and CO_2 sequestration (**Fig. 3-8**). The only exception was TR3, which had tryptone as the most important factor for urease activity. In the case of CO_2 sequestration, urea was always the most important component for all isolates, since the hydrolysis of urea led to pH increase and, hence, enhanced the CO_2 dissolution in the growth medium (**Table 3-10** and **Table 3-11**).

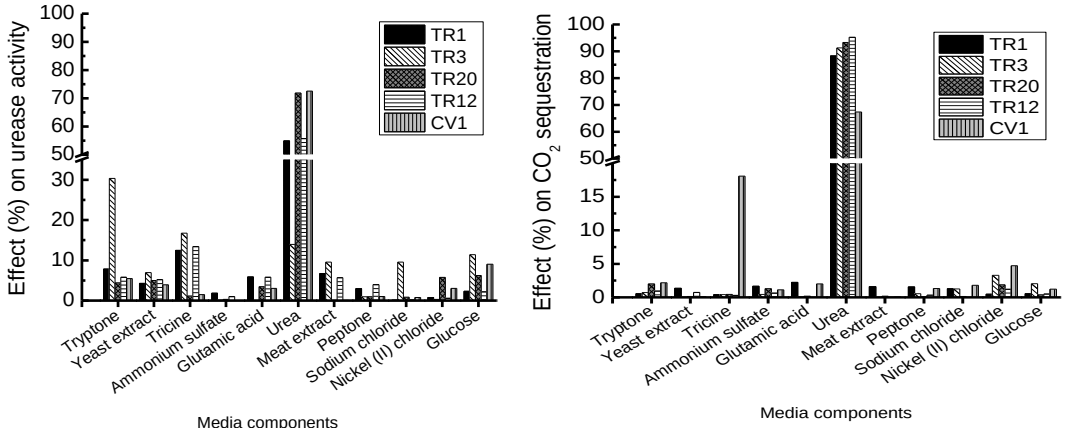

FIGURE 3-8- EFFECTS (%) OF MEDIA COMPONENTS ON THE UREASE ACTIVITY AND CO_2 SEQUESTRATION OF THE ISOLATES.

In addition to the determination of the important medium components for CO_2 sequestration, the Design Expert software was used to optimize the growth media components for each isolate in order to maximize their CO_2 sequestration rates. The predicted concentrations of each component in the media, determined by the software analysis, are listed in **Table 3-12**.

TABLE 3-12-THE NEW GROWTH MEDIA RECIPES PREDICTED BY DESIGN EXPERT SOFTWARE FOR MAXIMIZED CO_2 SEQUESTRATION.

Factors ($g\ L^{-1}$)	**Isolates**				
	TR1	**TR3**	**TR20**	**TR12**	**CV1**
Tryptone	4.58	1	1.22	1	7.22
Yeast extract	5	3.48	1.41	5	4.73
Tricine	2.65	1	0.45	1.2	0.45
Ammonium sulfate	4.68	3.42	5	5	0.5
Glutamic acid	2	1.04	1.13	0.95	0.57
Urea	20	20	20	20	20
Meat extract	3	1.27	1.17	1.81	2.21
Peptone	4.93	0.5	4.77	5	0.71
Sodium chloride	4.9	4.83	3.43	1.29	0.5
Nickel (II) chloride	0.08	0.01	0.01	0.01	0.01
Glucose	2.39	0.27	0.35	0.28	0.25
Medium Name	**M1**	**M3**	**M20**	**M12**	**MC1**

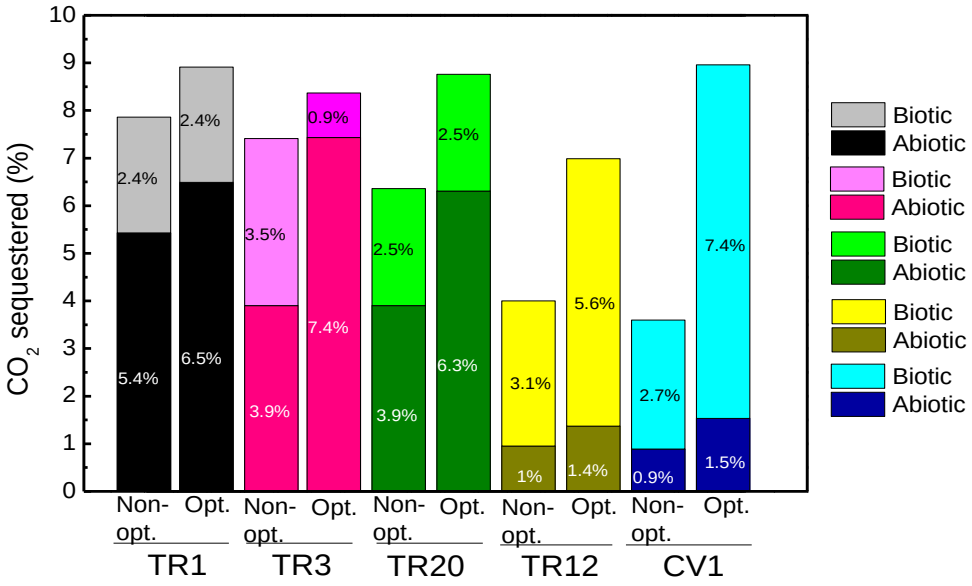

FIGURE 3-9-THE COMPARISON OF SEQUESTERED CO_2 (%) BY THE FIVE ISOLATES GROWN IN THEIR ISOLATION (NON-OPT.) AND OPTIMIZED (OPT.) MEDIA. THE DARKER AND LIGHTER COLORS IN EACH COLUMN STAND FOR ABIOTIC AND BIOTIC CO_2 SEQUESTRATION RESULTS, RESPECTIVELY.

The CO_2 sequestration rates were determined for the selected five isolates using their predicted medium compositions (**Table 3-12**). The results showed that the CO_2 sequestrations (abiotic + biotic) increased by 13.4%, 12.9%, and 37.7% for TR1, TR3, and TR20, respectively (**Figure 3-9**). The increase in CO_2 sequestrations were more pronounced with the worst ureolytic isolates (TR12 and CV1) with a CO_2 sequestration increase of 74.7% and 148.9%, respectively. The abiotic and biotic effects on the CO_2 sequestration in the optimized growth media were also determined. The results showed that the PB optimization did not affect the biotic CO_2 sequestration of TR1 and TR20 (**Figure 3-9**). However, the biotic sequestration of TR12 and CV1 increased by 84.3% and 174.2%, respectively. Only TR3 showed a decrease (73.2%) in its biotic sequestration (**Figure 3-9**). On the other hand, the abiotic CO_2 sequestrations increased in all optimized media. Therefore, the results indicate that the PB design was a powerful statistical tool to identify the significant factors for urease activity and CO_2 sequestration through MICP; and develop better growth medium conditions to significantly enhance CO_2 sequestration.

3.3.8 Discussion

Calcite formations in caves and travertines are believed to be formed mainly through the abiotic precipitation of calcium carbonate. Recently, biotic precipitation through MICP has been suggested as a potential mechanism for calcite formations in caves and travertines [4, 64]. In the MICP, ureolytic microbes have been shown to play an important role in geological formations and to participate in CO_2 sequestration [120, 121, 150]. However, there is very little understanding on how environmental bacteria affect the CO_2 sequestration through MICP. In the present study, ureolytic environmental isolates were obtained to better understand the relationship between urease activity, MICP, CO_2 sequestration, and growth conditions. Such understanding will be fundamental for the development of alternative solutions to sequester CO_2.

In this study, MICP isolates were obtained, for the first time, from the 'Cave Without A Name' and the Pamukkale travertines. The unknown physiology and microbial composition of these habitats led us to investigate 13 different growth medium to attempt to obtain diverse microorganisms involved in MICP. The isolation of diverse microorganisms is one of the major challenges for microbiologists, since it requires deep understanding on the physiology and metabolism of microorganisms to simulate conditions as close as possible to their original habitat [165-167]. In order to deal with this problem, different components including different electron donors, electron acceptors and carbon sources, and various concentrations in media formulations have been used, and researchers have started to isolate more diverse microorganisms [166, 167]. For example, in a previous study, growth medium containing various carbon sources and complex compounds allowed researchers to obtain more diverse isolates than the growth medium having only one carbon source [168]. However, Stott and collaborators revealed that no bacterial growth was achieved in defined complex media such as Nutrient, Tryptic Soy or Luria-Bertani broths, as their samples were geothermal soils [167]. In another study, relatively low concentrations of nutrients present in a diluted growth medium resulted in increasing number of different isolates from environmental samples [119]. Similarly, in our study, we were mostly successful in isolating microorganisms from the cave and travertine by using 10 x diluted nutrient broth. The preference of our isolates for non-rich growth media could be explained by the oligotrophic nature of caves and travertines, as well as the adaptation of these microorganisms to these habitats [146, 149]. Therefore, in both of these sites, oligotrophic growth media were more appropriate for the isolations of the microorganisms.

In isolation studies, it is common to obtain many isolates that are actually clonal isolates [169, 170]. Therefore, researchers use DNA fingerprinting techniques, such as ARDRA, to distinguish

these clonal isolates. Previous studies have shown that the sensitivity of ARDRA to identify clonal isolates is dependent on the type of enzyme used [171, 172]. Some enzymes, such as *Msp*I and *Hha*I, have been described to be more appropriate to distinguish clonal isolates [156, 173]. In the literature, it is, however, still a matter of debate which enzyme, *Msp*I or *Hha*I, can better distinguish clonal isolates [173]. Hence, we investigated both enzymes with our MICP isolates. In our study, *Msp*I enzyme was better than *Hha*I. In fact, the clustering of the phylotypes obtained with the *Msp*I enzyme was very similar to the results obtained through sequencing, which suggests that *Msp*I is more suitable for the selection of unique MICP clones.

The sequencing of the unique clones isolated in this study showed the presence of *Bacilli*, *Sphingobacteria, Flavobacteria* and α-, β-, and γ-*Proteobacteria* in these habitats. Similar observations were also made by previous researchers working with karstic samples [64, 120, 121]. Interestingly, the *Sporosarcina* genus, which was the predominant genus in our study, was not observed by these researchers in their karstic samples. However, other researchers were able to isolate several *Sporosarcina* species from soil samples using different isolation media containing urea [82, 174] or not [87, 175-177].

Based on our findings, it is possible that the addition of urea in all growth media used in this study led to the selection of species having higher urease activities. This finding is also consistent with the conclusions of Hammes and collaborators that observed that urea, when added to the medium for bacterial isolation, led to the selection of ureolytic microorganisms [82]. In fact, we observed that the isolates presenting higher urease activity belonged to the *Sporosarcina* genus; except for the cave isolate CV1. It is, however, not surprising to see that most of the *Sporosarcina* isolates presented higher urease activities, since this genus is well-known to be ureolytic [85].

Another interesting observation about these isolates with high urease activity was that they had a preference for alkaline pH. This preference for high pH values is typically observed in calcifying microorganisms [86]. This microbial adaptation of ureolytic microorganism to alkaline environments can be explained by the degradation of urea and production of ammonia as a by-product. The production of ammonia leads to pH increase in the surrounding environment. The results obtained are consistent with previous studies that showed that ureolytic bacteria tend to be alkaliphilic microorganisms, with optimum growth at pH values between 8 to 9 [7]. It is important to point out, however, that even though the pH of the original travertine and the cave water samples were 7 and 7.4, respectively, the presence of these microorganisms in sampling sites can be explained by the tolerance of these microbes to wide pH ranges as shown in **Table 3-3**. To relate these findings to the environmental samples, in the travertine water sample, we found higher ammonia concentrations than the cave (**Table 3-2**), which would explain the larger number of MICP isolates obtained from the travertine than the cave.

Further investigation of the urease and MICP activities by the isolates determined that microorganisms from the same genus, such as *Sporosarcina* sp. TR1 and *Sporosarcina* sp. CV1 or *Sphingobacterium* sp. CV2 and *Sphingobacterium* sp. CV4 had different urease and MICP activities. This finding contradicts a previous report that suggested that the urease activity or the rate of MICP were dependent on the genus of the microorganisms [82]. In the calcification and CO_2 uptake experiments during MICP, we observed that calcium carbonate precipitation and the CO_2 uptake by the isolates were completed within 5 to 10 h, which were mostly in the exponential phases of these microorganisms. The calcite precipitation in the exponential phase has also been previously observed in another study [4]. In fact, the calcification process has been

described to correlate well with the CO_2 uptake as the amount of calcite precipitated was previously described to be directly proportional to the CO_2 sequestrated [7].

The stoichiometric reaction of ureolysis in the calcium carbonate formation shows that 1 mol of urea hydrolyzed will sequester 1 mol of CO_2 to form 1 mol of calcium carbonate, which precipitates in the medium [7, 64], therefore the number of moles of CO_2 sequestered should be equal to the number of moles of calcium carbonate precipitated. This could potentially be true in soils, but is certainly not accurate in aquatic systems, since the CO_2 in the air tend to dissolve in the water or in the growth medium, and depending on the pH of the water, the CO_2 can be converted to carbonates [25, 178]. Additionally, it is important to point out that bacterial cells release CO_2 due to respiration and can change the pH of the growth medium, which would also affect the carbonate system [145]. These factors should be taken into consideration in order to clarify the true biotic role of the MICP process in the CO_2 sequestration of aquatic systems.

In order to better understand the biotic and abiotic CO_2 sequestration processes during MICP, we compared the CO_2 concentrations in the headspaces in the growth medium with different pH values (abiotic results), and in the growth medium at the end of the MICP assays (abiotic + biotic results) (**Table 3-4**). As suggested by Lee and collaborators, the pH played an important role in the abiotic uptake. For instance, in the abiotic assay (without bacterial cells), the ATCC 1832 medium was able to serve as a CO_2 sink and, hence, decreased the CO_2 content present in the headspace by 5.4%. In the presence of cells (biotic and abiotic process together), however, the CO_2 decreased by 7.8%. These results suggest that the biotic CO_2 uptake was 2.4%. In case of the NB3 medium, the CO_2 decreased by 3.9% and 3.5% in the abiotic and biotic processes, respectively. In the medium NB, the abiotic and biotic processes were able to sequester 3.9% and 2.5%, respectively. For the isolates TR12 and CV1, their growth media

showed almost no effect on the abiotic uptake of CO_2 and the cells were able to sequestered 2.7% and 3.1% of CO_2, respectively. Based on our findings, the five isolates investigated were able to sequester different amounts of CO_2. The results suggested that CO_2 sequestration through MICP is strain-specific and depends on the environmental factors, such as pH, which can be seen through correlation analysis results (**Table 3-6**).

When we take into consideration the amount of calcium carbonate formed by MICP and the CO_2 dissolved in each medium, we observed that stoichiometrically more CO_2 is being sequestered than we can account for. The conversion of CO_2 sequestered by TR1, TR3, TR20, CV1, and TR12 to moles shows that 0.054, 0.051, 0.043, 0.025, and 0.027 moles of CO_2 is being sequestered, respectively. In addition, when we calculate the number of moles of CO_2 in the $CaCO_3$ precipitate and carbonates in the growth medium for each isolate (**Table 3-13**), we get $6.4x10^{-4}$, $6.9x10^{-4}$, $6.9x10^{-4}$, $2.6x10^{-4}$, and $1.8x10^{-4}$ moles, respectively. Hence, when comparing these two sequestration results, it is clear that the MICP is not the only CO_2 sequestration mechanism.

TABLE 3-13- TITRATION RESULTS OF CARBONATES IN THE GROWTH MEDIA ENRICHED WITH 10% CO_2.

Isolate	Initial			After 24 h incubation (with Ca^{2+})			After 24 h incubation (no Ca^{2+})		
	pH	$[CO_3^{-2}]$ (M)	$[HCO_3^{-1}]$ (M)	pH	$[CO_3^{-2}]$ (M)	$[HCO_3^{-1}]$ (M)	pH	$[CO_3^{-2}]$ (M)	$[HCO_3^{-1}]$ (M)
TR1	7.6	0	0.0044	8.3	0	0.103	8.9	0.0212	0.0942
TR3	7.5	0	0.0030	9	0.0585	0.095	9.2	0.0842	0.0888
TR20	7.3	0	0.0074	9.3	0.1127	0.0727	9.3	0.1135	0.0762
CV1	7.3	0	0.0012	7.2	0	0.0025	7.3	0	0.0027
TR12	7.3	0	0.0008	7.5	0	0.0047	8.3	0.0002	0.0242

It is possible that besides the uptake mechanisms observed in this study, there might be other possible CO_2 fixing mechanisms being performed by these microorganisms, such as the Calvin-Benson reductive pentose phosphate cycle, the reductive citric acid (Arnon-Buchanan)

cycle, the hydroxypropionate (Fuchs-Holo) bi-cycle, the 3-hydroxypropionate/4-hydroxybutyrate and dicarboxylate/ 4-hydroxybutyrate cycles, as previously described [179]. In fact, Ortiz and collaborators, came across some of the genes involved in these CO_2 fixation pathways when investigating a cave ecosystem [146].

In this study, for the different isolates, we used different growth medium, which could explain the different urease activities, calcification rates and CO_2 sequestration capabilities of these isolates. In order to investigate the effects of the different medium components on the CO_2 sequestration through MICP, we used the Plackett-Burman (PB) experimental design. PB design is a well-established and widely used optimization technique that allows the identification of environmental factors playing significant roles on microbial metabolisms [2, 3, 75, 81-83, 141, 180, 181]. In this study, the PB design allowed us to identify the significance of each medium component for each isolate and also assisted on the selection of the appropriate concentrations of each component to enhance CO_2 sequestration by each isolate. The PB results showed that urea was the most important component in all isolates' growth media, which makes sense since urea is a key factor in ureolysis and all these isolates are ureolytic [25]. The PB results also allowed the enhancement of CO_2 sequestration, by the two worst ureolytic isolates, TR12 and CV1. These results suggested that CO_2 sequestration through MICP depends on the microbe itself and the microbial growth conditions. Further analyses of the biotic and abiotic effects on the CO_2 sequestration on these optimized media demonstrated that the optimization helped the microorganisms (TR12 and CV1) increase their CO_2 uptake metabolism to allow the enhancement of the biotic CO_2 uptake. Moreover, the change in the composition of the media led to higher abiotic CO_2 sequestrations in certain growth media. This higher abiotic sequestration, were observed with growth media with more nutrients (or higher

concentrations). This could be explained by the CO_2 diffusivity, which is dependent on the viscosity of the medium and temperature [142, 143]. Moreover, CO_2 solubility has been described to depend on environmental factors such as pH, temperature and pressure, and on intrinsic parameters such as salinity, sugar, fat, and protein contents [144]. Hence, it is likely that by changing the medium composition, the viscosity of the medium changed and led to higher CO_2 uptake.

3.4 CONCLUSIONS

This study suggests that caves and travertines contain microorganisms involved on calcification processes and CO_2 sequestration. These findings also suggest that caves and travertines could be potential natural carbon sinks. Furthermore, calcifying bacteria were found to induce CO_2 removal from the atmosphere through two possible mechanisms; a) biotic sequestration through MICP and b) abiotic sequestration by changing the environment pH. In both cases, cells play significant roles in the CO_2 sequestration: first, they can act as nucleation sites for calcite precipitation; second, they can potentially sequester CO_2 by their fixation metabolisms; and third, they can increase the surrounding environmental pH, which would allow increasing atmospheric CO_2 dissolution in aquatic systems and calcite precipitation, when calcium is present. In this study, when considering the biotic and abiotic CO_2 sequestration mechanisms by the MICP, the isolates, TR1, TR3, TR20, CV1 and TR12, were able to assist in the CO_2 sequestration by 78.6, 74.1, 63.6, 36, and 40% respectively, in their isolation media. Moreover, the Plackett-Burman design showed to be a powerful tool to determine the components and concentrations of each growth medium to significantly increase the abiotic CO_2 sequestrations for each isolate, and biotic CO_2 sequestrations for the isolates TR12 and CV1.

CHAPTER 4 SPOROSARCINA PASTEURII AND OPTIMIZED CARBONATE MICRO-PARTICLE PRODUCTION USING RESPONSE SURFACE METHODOLOGY

4.1 RATIONALE AND OBJECTIVES

Calcium carbonate is estimated to form 4% of the Earth and is used by several industries such as construction, paint, plastic, rubber, ceramic, glass, steel, oil refining and paper industries [2, 26-28, 30-32]. Calcium carbonate is also frequently employed in drinking and waste water treatment, desulphurization of flue gas, and reduction of soil acidity [34, 77, 182, 183]. Moreover, calcium carbonate has been used in the fabrication of biocompatible composite materials for drug delivery, biosensing, and protein encapsulation [33]. Therefore, the optimization of the conditions to produce calcium carbonate is essential.

Calcium carbonate precipitation is a chemical reaction commonly facilitated by microorganisms and is designated as "microbially-induced calcium carbonate precipitation" (MICP). Metabolic reactions such as photosynthesis, sulfate reduction, urea hydrolysis, and iron reduction have been associated with MICP [5, 6]. We used urea hydrolysis in this study. The stoichiometric reactions of urea hydrolysis are [6, 72, 75, 141]:

$$H_2NCONH_2 \text{ (urea)} + H_2O \rightarrow 2NH_3 + CO_2 , \quad (4\text{-}1)$$

$$2NH_3 + CO_2 + H_2O \leftrightarrow 2NH_4^+ + CO_3^- , \text{ and} \quad (4\text{-}2)$$

$$Ca^{2+} + CO_3^- \rightarrow CaCO_3 . \quad (4\text{-}3)$$

MICP is achieved by urea-hydrolyzing bacteria, and the reaction is affected by various factors, such as the presence of urea, calcium and nickel ions [75, 81-83, 85, 141, 181]. During the urea hydrolysis, urease, a nickel metalloenzyme produced by bacteria, produced ammonium and bicarbonate (in Eqs. 4-1 and 4-2), and this leads to an increase in pH, which accelerates the te

precipitation (in Eq. 4-3) [81, 86, 184]. The urease enzyme requires two nickel ions to be fully functional, which makes the concentration of nickel an essential parameter for studies of MICP [81, 185]. Calcium concentration is another important variable, since a certain amount of calcium ions are required to interact with the negatively charged bacterial cells that act as nucleation sites to initiate precipitation [75].

Traditional growth methods investigate one-factor at a time to determine the most important factors and the optimum conditions for MICP and other bacterial responses, which tends to be laborious and tedious. Furthermore, these traditional methods are able to predict the importance of individual factors, but very frequently dismiss their synergistic and antagonistic effects [186]. Response surface methodology (RSM) determines the individual role of each factor, as well as their antagonistic and synergistic effects among the factors. Additionally, it assists on the experimental design to minimize the number of experiments to be performed [187]. This methodology has been applied in various processes to optimize conditions, such as bacterial growth and enzymatic reactions [186, 188-190]. However, no study has been done with RSM to determine the optimum conditions for MICP. Therefore, in this study, the RSM was used to determine the optimum concentrations of urea, calcium and nickel for *Sporosacina pasteurii* to maximize precipitation. A second order transferred polynomial model (as an inverse model) was also obtained, which defines the precipitation rate as a function of urea, calcium and nickel concentration.

4.2 MATERIALS AND METHODS

4.2.1 Bacteria and cultivation procedure

The microorganism investigated in this study was *S. pasteurii* ATCC 11859. The standard medium used to grow this microorganism was a base growth medium (ATCC 1832 medium),

which contained 10 g L^{-1} tryptone, 5 g L^{-1} yeast extract, 4.5 g L^{-1} tricine, 5 g L^{-1} ammonium sulfate, 2 g L^{-1} glutamic acid supplemented with 10 g L^{-1} urea at pH 8.3 [184]. All the chemicals used in this study were obtained from Sigma-Aldrich unless stated otherwise. Prior to each experiment, a single isolated colony was transferred to 30 m: filter-sterilized (0.22 µm, Corning Inc., USA) base growth medium and grown overnight at 28°C for 18 h on a rotary shaker incubator at 200 rpm. After this period, the cells were harvested by centrifugation (10,000 rpm, 10 min), and then suspended in phosphate buffered saline (PBS) (Amresco Inc., USA) to an optical density of 0.4 at 600 nm. All experiments were performed with this initial optical density unless indicated otherwise. The bacterial inoculum (5 %, v/v), the working volume (300 mL in each Erlenmeyer flask), temperature (28°C), and shaking velocity (200 rpm) were kept constant for all experiments, except the experiments held in the microplate reader.

4.2.2 Experimental design

In order to enhance the calcium carbonate precipitation by *S. pasteurii*, optimum concentrations of the environmental variables were determined using the CCD within the 'Design Expert' software (version 7.0.0, Stat-Ease, Inc., Minneapolis, USA). For this design, different concentrations of urea (X_1), nickel (II) nitrate (X_2) and calcium chloride (X_3) were utilized. The CCD contained a total of 20 experiments with 14 experimental designs for non-center points (factorial and star points) and 6 for the center point. To detect the effect of major key variables responsible for calcium carbonate precipitation, each variable was considered at five different levels in the CCD: negative star, minimum, center, maximum and positive star points coded as -α, -1, 0, +1 and +α, respectively (**Figure 4-1**) [191].

The full experimental design with regard to their range of concentrations was presented in **Table 4-1** and **Table 4-2**. The rate of calcium carbonate precipitation was considered to be the

main experimental response. Ammonium production rate, growth rate and pH increase rate were measured as secondary responses.

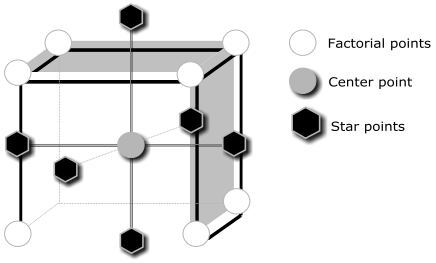

FIGURE 4-1- A MODIFIED FIGURE OF CENTRAL COMPOSITE DESIGN FOR THREE FACTORS.

TABLE 4-1- EXPERIMENTAL RANGE AND THE LEVELS OF INDEPENDENT VARIABLES.

Variables	**Units**	**Symbol coded**	**Range of chemical concentrations**				
Urea	g L^{-1}	X_1	7	25	0.86	31.14	16
Nickel (II) nitrate	g L^{-1}	X_3	0.0076	0.0291	0.0002	0.0364	0.0183
Calcium chloride	g L^{-1}	X_2	7	25	0.86	31.14	16
Levels			**-1**	**+1**	**-1.682**	**+1.682**	**0**

TABLE 4-2- THE DESIGN MATRIX OF CCD EXPERIMENTS USED IN THIS STUDY.

II.	**Factor 1**	**Factor 2**	**Factor 3**
	X_1: Urea	**X_2: Calcium chloride**	**X_3: Nickel (II) nitrate**
Factorial points			
1	-1	-1	-1
2	1	-1	-1
3	-1	1	-1
4	1	1	-1
5	-1	-1	1
6	1	-1	1
7	-1	1	1
8	1	1	1
Star points			
9	-1.682	0	0
10	1.682	0	0
11	0	-1.682	0
12	0	1.682	0
13	0	0	-1.682
14	0	0	1.682
Central points			
15	0	0	0
16	0	0	0
17	0	0	0
18	0	0	0
19	0	0	0
20	0	0	0

4.2.3 Sampling procedure

At 0, 1, 2, 3, 4, 5, 6, 7, 8, 9, 10, 12, 18, 20, 22, 24, 48, and 72 h time intervals, an aliquot of 10 mL of the cell culture was aseptically removed and the pH was measured. Then the samples were centrifuged at 10,000 rpm for 10 min and the supernatant was filtered through 0.22 µm filters. The filtrates were kept at -20^{o}C until analyses of urease activity, ammonium and calcium concentrations were performed.

4.2.4 Determination of ammonium concentration and urease activity

The concentration of ammonium was determined by using the Nessler assay [192]. Samples were mixed with sodium potassium tartrate solution and Nessler reagent, and incubated for 5 min at room temperature. After incubation, absorbances were read at 425 nm. Urease activity was also determined according to a previously described method [82]. One unit of urease activity was defined as the amount of enzyme that hydrolyzes 1 µmol of urea per min.

4.2.5 Determination of calcium carbonate precipitation

In order to determine the calcium concentration, atomic absorption spectroscopy (Perkin Elmer AAnalyst^{TM} 200) was used according to Tobler and collaborators [85]. Calcium chloride was used to make a standard curve for measuring the calcium ion concentrations.

4.2.6 Calculation of rates

The rates (h^{-1}) generated by the ureolysis reaction were assumed to be a first order kinetic [59, 193], and therefore, the following equation was used to calculate the rates:

$$r = -\frac{d[A]}{dt} = k[A], \qquad (4\text{-}4)$$

where *k* is the first order rate constant $(time)^{-1}$ and [A] is the reactant concentration (g L^{-1}). The integrated first-order rate law is:

$$\ln[A] = -kt + \ln [A]_0 . \quad (4\text{-}5)$$

A plot of *ln*[A] vs. time *t* giving a straight line with a slope of –k was used to determine the rate of reactant production. To determine the rates (h^{-1}) of ammonium production, pH increase, and calcium carbonate precipitation, Eq. 4-5 was used by plotting the *ln*[A] vs. time. In our study, [A] represents ammonium, pH, and calcium concentration for each rate calculation, respectively.

4.2.7 Determination of growth rates

A 96-well plate reader (Synergy MX Microplate reader, BioTek, USA) was used to obtain the microbial growth rates in the conditions described in **Table 4-2** by measuring the absorbance at 600 nm for 24 h in each well. In the 96-well plate, each condition was in triplicate. The auto-reader of the instrument was employed with the following conditions: 28°C and continuous slow shaking (1020 cycles min^{-1}). The growth rates (μ) were calculated (h^{-1}) based on the following equation:

$$OD = OD_0 e^{\mu t}, \quad (4\text{-}6)$$

where OD is the optical density at time *t* at the end of the exponential phase; and OD_0 is the optical density at the beginning of the bacterial exponential phase (t_0).

4.2.8 Data analysis

The 'Design Expert' software was used for the regression and graphical analyses. Since the inverse polynomial has been suggested in the literature for biological systems, it was used in this study. Compared to ordinary polynomials, it has greater flexibility and provides a more realistic fit [194]. The quadratic model for predicting the optimal point was expressed by combining Eq. 4-7 and Eq. 4-8.

$$Y_i = b_0 + \sum_{1}^{3} b_i X_i + \sum_{1}^{3} b_{ii} X_i^2 + \sum_{1}^{3} i \sum_{1}^{3} j\, b_{ij} X_i X_j \quad \text{and} \quad (4\text{-}7)$$

$$Y' = \frac{1}{Y_i + 0.05}, \quad (4\text{-}8)$$

where Y_i is the predicted response by the software; X_i and X_j are the input variables influencing the response; b_0 is the offset term; b_i is the i^{th} linear coefficient; b_{ii} is the quadratic coefficient and b_{ij} is the ij^{th} interaction coefficient [114, 195]. The statistical analysis of the model was performed using the analysis of variance (ANOVA). The quality of the inverse polynomial model equation was determined statistically by the coefficient of determination R^2, and the *F*-test.

4.2.9 Optimization

The optimized concentrations were obtained by graphical and statistical analysis using the Design Expert, and its settings were based on the criterion of desirability. Therefore, maximum rates of calcium carbonate precipitation, growth, ammonium production and pH increase were selected as the desired outcomes in the Design Expert software. In order to confirm the results of the optimum concentrations of urea, calcium, and nickel predicted by the Design Expert, experimental assays were performed, and the following controls were run: the "condition-10", which was the combination of urea, calcium and nickel with the highest calcium carbonate precipitation rate among all the CCD experiments tested; and the "control" medium, which is the medium used in all calcium carbonate precipitation studies with *S. pasteurii*,. The control medium is composed of 20 g L^{-1} urea, 2.8 g L^{-1} calcium chloride and no nickel [2, 59, 81, 141, 181, 193]. Growth, pH increase, ammonium production and calcium carbonate precipitation rates were analyzed again and compared with all these media.

4.2.10 Scanning electron microscopy and energy dispersive X-ray spectroscopy analyses

To confirm that the bacteria were able to produce calcium carbonate micro-particles, scanning electron microscopy (SEM) and energy dispersive X-ray spectroscopy (EDS) analyses were performed (JEOL JSM-6010LA). Glass slides were incubated in each flask of CCD conditions with bacteria in triplicate for 96 hours. After the incubation, the glass slides were removed with a sterile spatula and washed twice with sterile distilled water to remove any dissolved salts and loosely attached cells. The glass slides were dried at 40°C overnight. SEM images and EDS data were taken after fixation and staining procedures as previously described [196].

4.3 RESULTS AND DISCUSSION

In this study, a CCD was employed to determine the optimum conditions for calcium carbonate precipitation. The environmental factors investigated in the present study were urea, calcium chloride, and nickel (II) nitrate. These factors were defined as X_1, X_2 and X_3 (**Table 4-1**), respectively.

TABLE 4-3- THE OBSERVED AND THE PREDICTED RESULTS OF THE RESPONSES.

	Response 1		**Response 2**	
	Calcium carbonate precipitation rate (h^{-1})		**Growth rate (μ_{max}) (h^{-1})**	
	Observed	**Predicted**	**Observed**	**Predicted**
1	0.002	-0.003154	0.2379	0.19
2	0.026	0.037	0.7051	0.75
3	0.000070	-0.00229	0.4002	0.47
4	0.017	0.028	0.3279	0.45
5	0.004	0.00047	0.2878	0.25
6	0.035	0.045	0.9039	0.92
7	0.00006	-0.00317	0.3232	0.37
8	0.019	0.031	0.3419	0.47
9	0.000145	0.012	0.1519	0.18
10	0.097	0.075	0.8744	0.73
11	0.007	0.00366	0.3198	0.38
12	0.00028	-0.00671	0.4004	0.23
13	0.008	0.00328	0.7873	0.72
14	0.015	0.00938	0.8355	0.78
15	0.005	0.00829	0.8045	0.82
16	0.010	0.00829	0.8200	0.82
17	0.007	0.00829	0.8122	0.82
18	0.009	0.00829	0.8161	0.82
19	0.007	0.00829	0.8142	0.82
20	0.010	0.00829	0.8151	0.82

The rates of calcium carbonate precipitation (**Table 4-3**), bacterial growth (**Table 4-3**), pH increase (**Figure 4-2**), and ammonium production (**Figure 4-3**) were measured, and analyzed with the Design Expert software. The rates of calcium carbonate precipitation and growth were considered the responses (dependent variables) for the optimization.

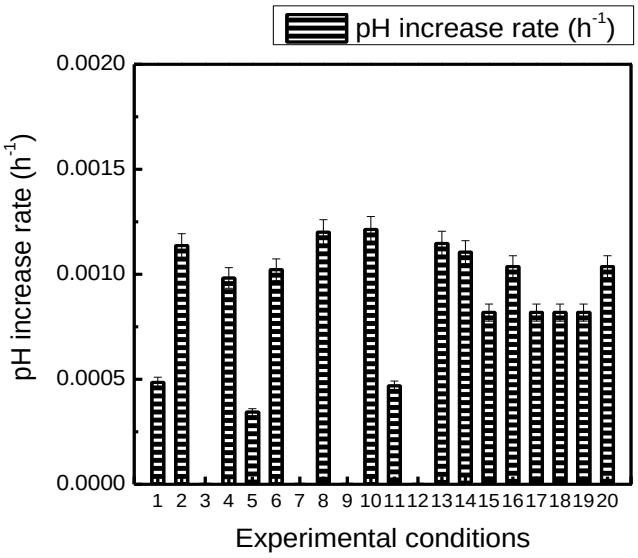

FIGURE 4-2- COMPARISON OF PH INCREASE RATES OF THE CCD EXPERIMENTAL CONDITIONS.

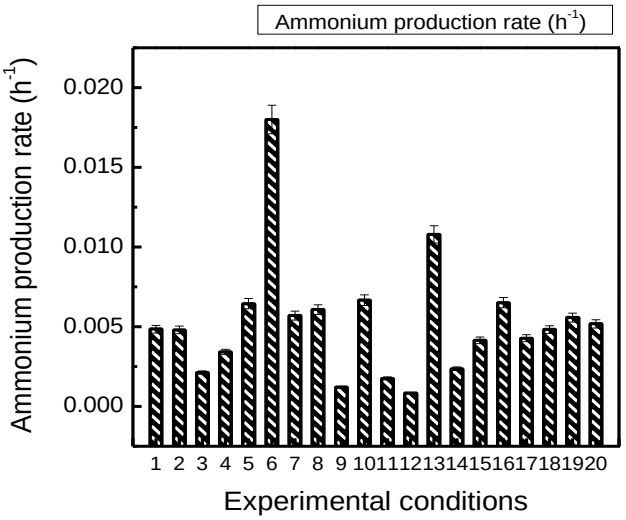

FIGURE 4-3- COMPARISON OF AMMONIUM PRODUCTION RATES DATA OF THE CCD EXPERIMENTAL DESIGN.

The RSM analyses showed that both urea and calcium chloride concentrations significantly affected the growth and calcium carbonate precipitation rates (**Table 4-4** and **Table 4-5**).

TABLE 4-4-ANOVA FOR THE MODEL, AND THE LEAST-SQUARES FIT AND PARAMETER ESTIMATE OF THE DESIGN ANALYSIS FOR THE TRANSFORMED CALCIUM CARBONATE PRECIPITATION RATE.

	Calcium carbonate precipitation rate analysis			
	Standard error	**F value**	**Significant level**	**Parameter estimate x 10^{-3}**
Model	-	36.68	<0.0001	-
Intercept	0.31		-	17.24
X_1	0.21	256.00	<0.0001	-3.33
X_2	0.21	14.02	0.0038	0.78
X_3	0.21	3.96	0.0745	-0.41
X_1^2	0.20	40.04	<0.0001	-1.28
X_2^2	0.20	9.01	0.0133	0.61
X_3^2	0.20	1.42	0.2602	-0.24
X_1X_2	0.27	1.12	0.3157	0.29
X_1X_3	0.27	0.26	0.6184	-0.14
X_2X_3	0.27	0.59	0.4584	0.21
Lack of fit	-	2.26	0.1956	-
R^2	0.9706			
Adjusted R^2	0.9441			
Predicted R^2	0.8322			
Adequate Precision	22.538			

TABLE 4-5- ANOVA FOR THE GROWTH RATE MODEL AND THE LEAST-SQUARES FIT AND PARAMETER ESTIMATES OF EXPERIMENTAL DESIGN ANALYSIS.

	Growth rate analysis			
	Standard error	**F-value**	**Significant level**	**Parameter estimate**
Model	-	13.02	0.0002	-
Intercept	0.042		-	0.820
X_1	0.028	34.86	0.0002	0.160
X_2	0.028	2.54	0.0967	-0.044
X_3	0.028	0.49	0.9103	0.020
X_1^2	0.027	22.47	0.0149	-0.180
X_2^2	0.027	45.38	0.0013	-0.023
X_3^2	0.034	0.72	0.8872	-0.005
X_1X_2	0.036	15.26	0.0149	-0.140
X_1X_3	0.036	0.68	0.8348	0.030
X_2X_3	0.036	1.15	0.6632	-0.039
R^2	0.9213			

In the experiments, the calcium carbonate precipitation rates were observed to be between 0.00006 h^{-1} and 0.0970 h^{-1}, while the growth rates varied from 0.1519 h^{-1} to 0.9039 h^{-1} (**Table 4-3**). It was found that high urea and low calcium chloride concentrations led to fast bacterial growth (**Table 4-3**, **Figure 4-4**, and **Figure 4-5**), while low urea concentrations resulted in reduced growth rates. These results are in agreement with Kenny and Cartwright [197]. On the other hand, higher "calcium concentration/urea concentration" ratios in the growth medium showed an inhibitory effect on the calcium carbonate precipitation rate (**Table 4-3**). It was also determined that although the metal ions, including calcium, are required for microbial growth, higher concentrations can slow down growth or even cause growth inhibition [83, 85, 198].

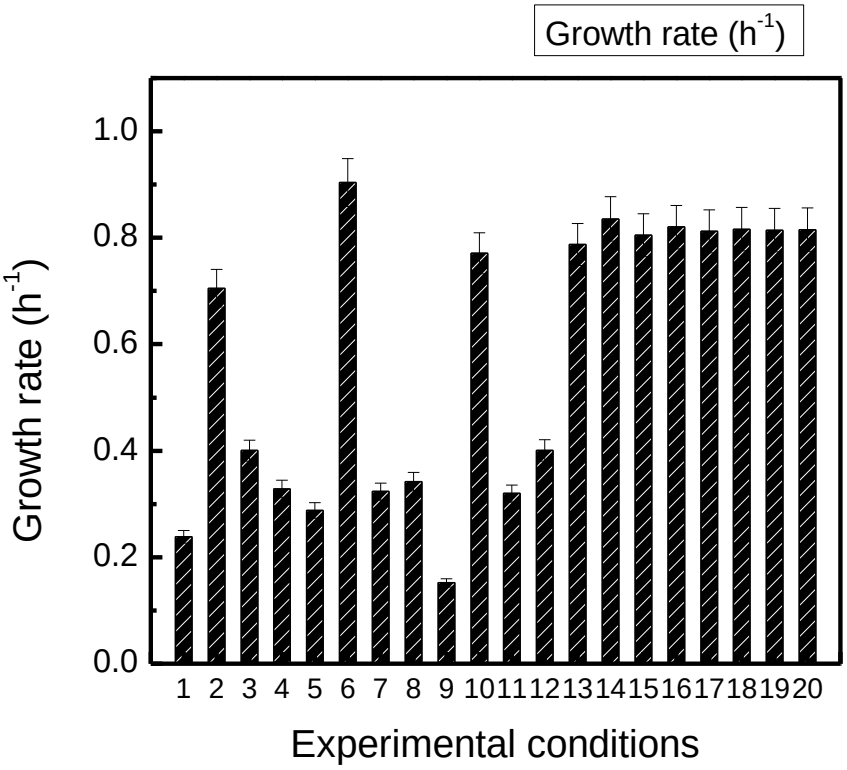

FIGURE 4-4- COMPARISON OF GROWTH RATES DATA OF THE CCD EXPERIMENTAL DESIGN.

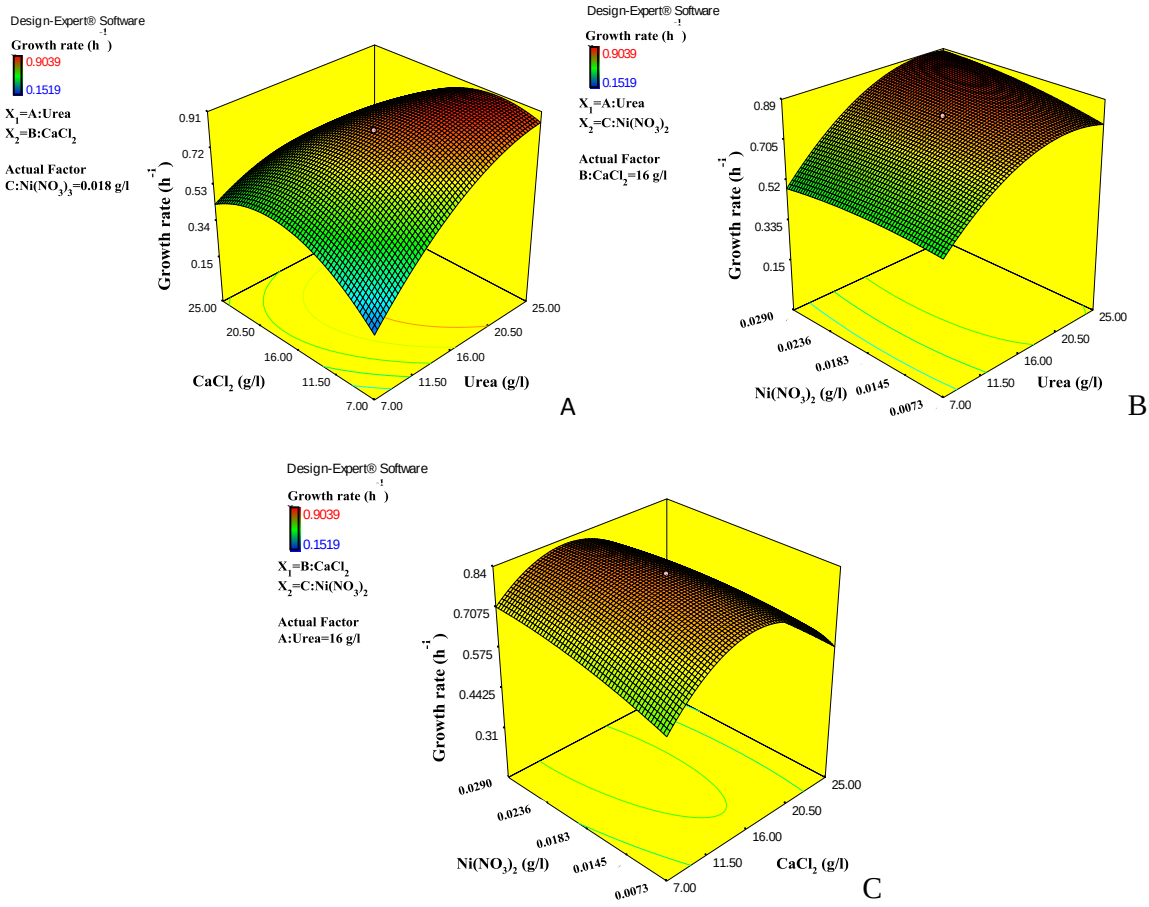

FIGURE 4-5- RESPONSE SURFACE PLOTS SHOWING (A) THE EFFECT OF UREA CONCENTRATION, $CACL_2$ CONCENTRATION AND THEIR MUTUAL EFFECTS; (B) THE EFFECT OF UREA CONCENTRATION, $NI(NO_3)_2$ CONCENTRATION AND THEIR MUTUAL EFFECTS; (C) THE EFFECT OF $NI(NO_3)_2$ CONCENTRATION, $CACL_2$ CONCENTRATION AND THEIR MUTUAL EFFECTS ON THE GROWTH RATE (h^{-1}).

In the case of pH, Cabrera and his colleagues demonstrated that increase in pH is linked to higher urease activity [199]. According to Mortensen and collaborators, the carbonate precipitation rate depends on pH, *i.e.,* higher calcium carbonate precipitation rates were observed under higher pH [86]. Bachmeier and collaborators went further by demonstrating that the increase in pH values, up to 9.4, is necessary to maximum calcium carbonate precipitation [81]. Sánchez-Román and his colleagues also observed a pH increase from 7.2 to 9 in their calcium carbonate precipitating media [83]. In our study, we also observed that pH is linked to urease

activity and calcium carbonate precipitation. In all the experimental conditions tested, both pH and calcium carbonate precipitation rates increased, except for conditions 3, 7, 9 and 12. These four conditions, besides having almost no calcium carbonate precipitation and no pH increase, presented low ammonium production. Masover and his friends determined that the urea hydrolysis and the amount of ammonia produced is a function of the initial urea concentration; due to the high urea concentration, urease activity would be high, and therefore leading to a pH increase [200]. It is worth to note that these four poor performing conditions in CCD had low concentrations of urea; however they contained high calcium concentrations. The ratios of "urea concentration/calcium concentration" were 0.28, 0.28, 0.053 and 0.51, respectively for these poorly performing conditions. Conversely, this ratio was 1 or greater in the rest of the conditions presenting pH increases. This suggests that the "urea concentration/calcium concentration" ratio has a direct effect on the pH change.

Besides the effects of urea and calcium on the calcium carbonate precipitation, nickel concentration was also investigated in this study. Bachmeier and collaborators reported that nickel ion concentration has a great effect on calcium carbonate precipitation [81], and Lv and his friends explained that there is a relationship between nickel concentration and urease activity [185]. Bergdale and his collaborators also studied different concentrations of nickel, and showed a positive effect of nickel on the urease activity [201]. In our study, the results show that the nickel concentration affected both the growth and the calcium carbonate precipitation rates.

The mutual effects of those three environmental factors, urea, nickel, and calcium, are represented in **Figure 4-6**. The results suggest that high calcium carbonate precipitation rates can be achieved if urea and nickel concentrations in the growth media increase, and calcium concentration decreases.

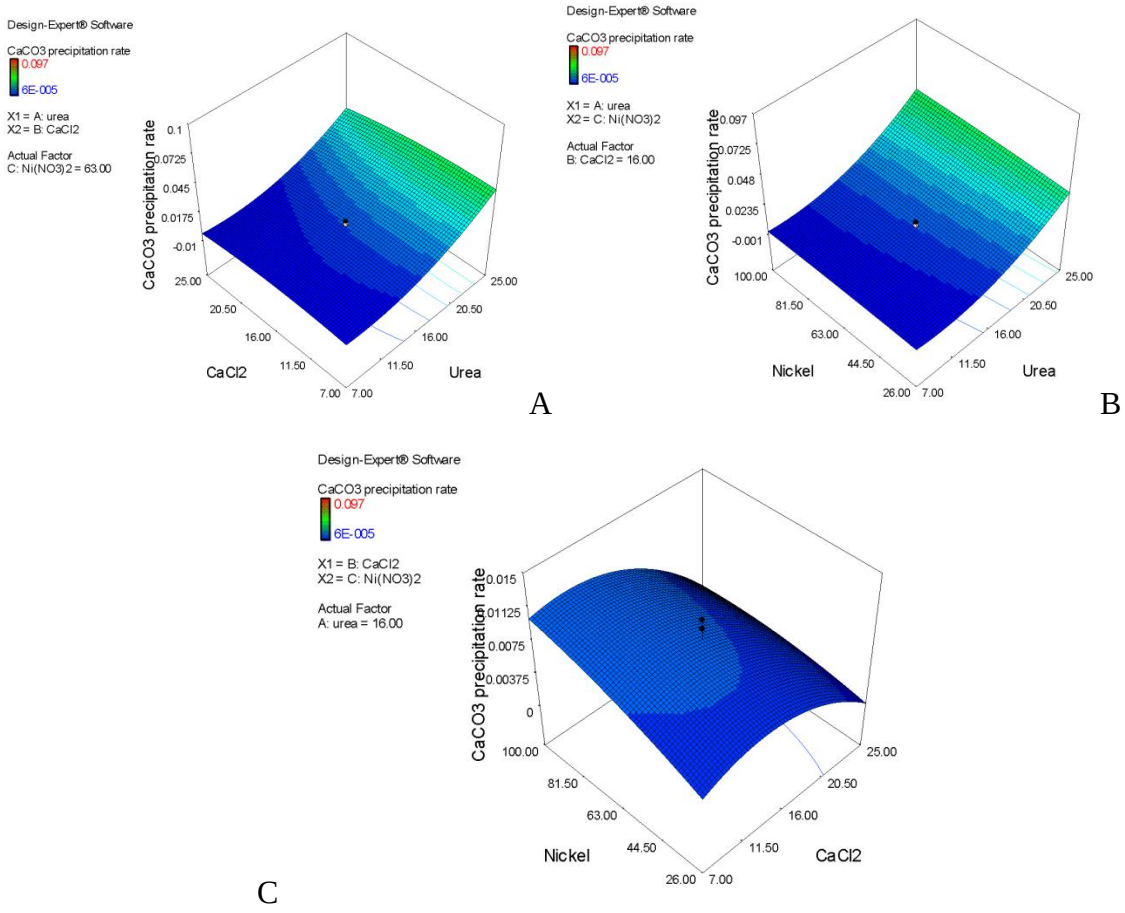

FIGURE 4-6- RESPONSE SURFACE PLOTS SHOWING (A) THE EFFECT OF UREA AND CALCIUM CONCENTRATIONS AND THEIR MUTUAL EFFECT; (B) THE EFFECT OF UREA AND NICKEL CONCENTRATIONS AND THEIR MUTUAL EFFECT; (C) THE EFFECT OF NICKEL AND CALCIUM CONCENTRATION AND THEIR MUTUAL EFFECT ON THE CALCIUM CARBONATE PRECIPITATION RATE (H^{-1}).

The results show that if urea concentration goes up and calcium concentration is kept at its minimum in (A), while nickel concentration is at the central level (63 µM), calcium carbonate precipitation rate will increase. In (B), while the calcium concentration is at the central level (16 g L^{-1}), calcium carbonate precipitation rate will increase when both urea and nickel concentrations are increased. In (C), the urea concentration at the central level (16 g L^{-1}), calcium carbonate precipitation rate increases when calcium decreases and nickel concentration increases (**Figure 4-6**).

In the RSM, R^2 values should be above 0.60 to be significant, and the larger the R^2 the more statistically significant is the model [195]. In our study, the R^2 value obtained was 0.97 (**Table 4-4**) indicating that our statistical model can explain 97% of the variability in the response. The adjusted R^2 value, which is a measure of the amount of variation around the mean that can be explained by the model, and is determined by the number of terms in the model, was obtained 0.94 (**Table 4-4**). This high value also confirms the high significance of our model [189, 190, 195]. According to Tatineni and colleagues, adjusted R^2 values might be slightly smaller than the R^2 values, if a model has many terms, which is the case of our study [189]. The predicted R^2 value, which is a measure of the amount of variation explained by the model, was 0.83 (**Table 4-4**) which is an acceptable value, since it is within 20% of the adjusted R^2 value. The coefficient of variation and adequate precision of the response data (**Table 4-4**) were determined through ANOVA in order to confirm that RSM and its results are acceptable and reproducible. The coefficient of variation of the design was found to be 4.63%, meaning that there is a very small acceptable experimental variability which is less than 5% of the upper limit for reproducibility [189, 190].

Additionally, multiple regression analyses were applied, and it was attained that the environmental factors not only have significant linear interactions with the response, but also have quadratic effects. Thus, an inverse polynomial equation was fitted to the results of the CCD. The regression equation predicted by the software was described below:

$$\frac{1}{Y_i + 0.05} = 20.772 + 0.106X_1 - 0.249X_2 + 26.387X_3 + 0.0035X_1X_2 - 1.441X_1X_3 + 2.162X_2X_3 - 0.016X_1^2 + 0.0075X_2^2 - 2083.6X_3^2 \quad , \quad (4\text{-}9)$$

in which Y_i is the response, and represents the calcium carbonate precipitation rate (h^{-1}). X_1, X_2, and X_3 are the concentrations (g L^{-1}) of urea, calcium chloride and nickel (II) nitrate, respectively.

The statistical significance of the second-order model equations were checked by F-test (ANOVA), and the results were given in **Table 4-4**. The ANOVA of the quadratic regression model demonstrated that the model was highly significant (p<0.0001). This implies that the linear effects of urea (p<0.0001) and calcium (p<0.0038), and the quadratic effects of urea, X_1^2 (p<0.0001); and calcium, X_2^2 (p<0.0133) are highly significant at the 5% significance level (**Table 4-4**). Since the concentrations of urea and calcium are significant at the quadratic level, a slight variation in these concentrations will greatly change the precipitation rates. Furthermore, values of p>0.10 generally indicate non-statistically significant factors, and values between 0.05<p<0.10 are accepted as marginally significant [114]. Since the p-value for X_3 was 0.0745, it was accepted as a significant factor.

As seen on **Table 4-4**, the lack of fit is not significant for the precipitation model (p=0.195). This means that there is only 19.5% chance that a lack of fit could occur due to noise. In the RSM design, insignificant values for the lack of fit factors combined with larger p-values usually exist to determine the significance of the model [195].

4.3.1 Optimization

Design Expert was used to determine the optimum concentrations of urea, calcium and nickel for *S. pasteurii* in order to obtain maximum growth and calcium carbonate precipitation rates. An optimum calcium carbonate precipitation rate, 0.187 h^{-1}, under 42.12 g L^{-1} urea, 6.93 g L^{-1} calcium chloride, and 0.071 g L^{-1} nickel (II) nitrate was predicted by the software, and this was represented by **Figure 4-7**.

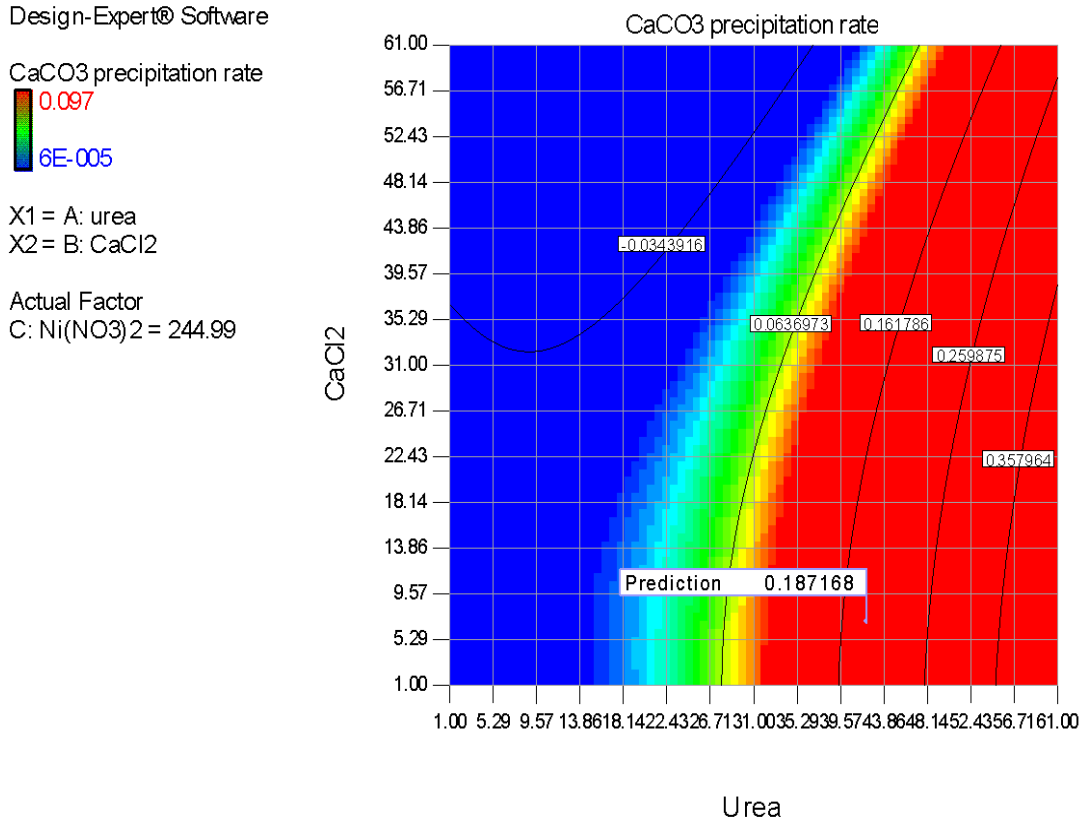

FIGURE 4-7- THE CONTOUR CURVE PLOT OF THE OPTIMUM CONDITIONS FOR THE HIGHEST CALCIUM CARBONATE PRECIPITATION RATE; A REVIEW OF THE OPTIMIZATION.

In order to determine whether the optimized condition really improved the calcium carbonate precipitation, experiments were run in triplicates together with two control media (**Table 4-6**). One of the control media was selected as the condition-10 of the CCD (**Table 4-2**), since it presented the highest calcium carbonate precipitation rate among the other CCD media investigated (**Table 4-3** and **Figure 4-8**). The second control was the standard medium composition described in the literature as the optimal medium for microbially-induced calcite precipitation [59, 82, 85, 141].

TABLE 4-6- COMPOSITIONS OF THE THREE MEDIA TESTED AFTER OPTIMIZATION: STANDARD MEDIUM, CONDITION-10, AND THE OPTIMIZED MEDIUM.

Concentrations (g/L)	Media		
	Standard	Condition-10 of the CCD	Optimized
Urea	20	31.14	42.12
Calcium	2.8	16	6.93
Nickel	-	0.018	0.071

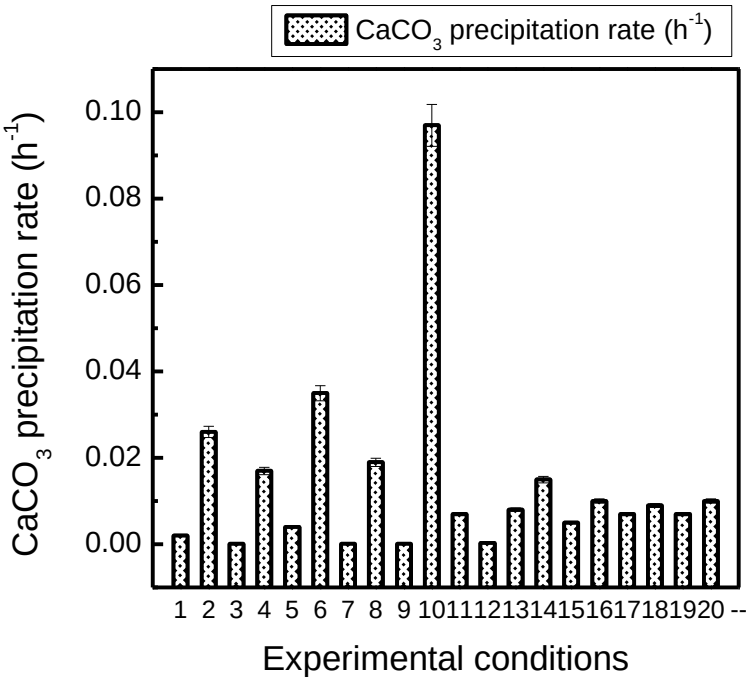

FIGURE 4-8- COMPARISON OF CALCIUM CARBONATE PRECIPITATION RATES OF THE CCD EXPERIMENTAL CONDITIONS.

The results showed that the optimized medium allowed higher growth rate (0.91 h^{-1}), calcium precipitation rate (0.145 h^{-1}), and urease activity (3.4 U mL^{-1}) than the standard medium described in the literature, which were 0.58, 0.11 and 1.35 h^{-1} (**Table 4-7**), respectively. It is noteworthy; however, that the growth and the calcium carbonate precipitation rates (**Table 4-3**) do not have a linear relationship since the optimized medium showed the best urease activity and calcium carbonate precipitation, but lower growth rates than condition-10 (**Table 4-7**). This finding disagrees with a previous study that infers growth and calcium carbonate precipitation

rates are directly related [82]. Similar result can be observed in **Figure 4-3**, which shows higher precipitation rates for some conditions, but lower growth rates, than the optimized condition.

TABLE 4-7- THE SUMMARY OF THE EXPERIMENTAL RESULTS OBTAINED FROM THREE TEST MEDIA.

	Media		
	Standard	**Condition-10 of the CCD**	**Optimized**
EDS data [% calcium (ave.)]	5.58	12.23	39.57
Urease activity (U mL^{-1})	1.35	0.71	3.40
Growth rate (h^{-1})	0.58	1.08	0.91
Precipitation rate (h^{-1})	0.117	0.139	0.145

In summary, higher calcium carbonate precipitation rates do not mean faster growth rates. On the other hand, the growth rates are statistically linked to urease activity. Bergdale and his collaborators also described that the higher the growth rate, the higher will be the urease activity [201].

4.3.2 Scanning electron microscopy and energy dispersive X-ray spectroscopy analyses

SEM was used to prove the formation of calcium carbonate particles by *S. pasteurii.* Calcium carbonate crystals were observed as a rhombohedral structure that aggregated into spherical and semi-spherical structures [201].

Similar shapes were observed in our results (**Figure 4-9**). The size of the calcium carbonate particles varied between 0.1 and 10 μm. Moreover, the EDS analyses confirmed that the particles observed in the SEM were calcium carbonate precipitates. The EDS also showed that the optimized medium had the highest calcium carbonate precipitation among the samples tested as depicted by the high calcium peak in the EDS analyses (**Figure 4-10**). The elemental mapping of the samples allowed visualization of the regions where calcium carbonate particles had formed (**Figures 4-11**, **4-12**, and **4-13**).

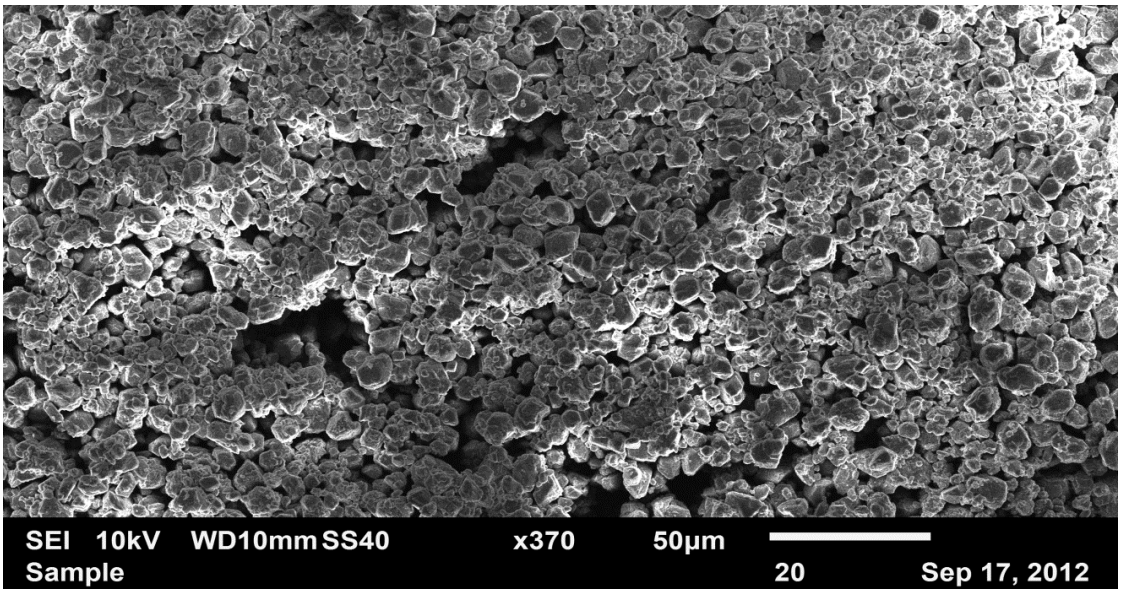

FIGURE 4-9- SEM IMAGE OF CALCIUM CARBONATE PRECIPITATED ON A GLASS SLIDE USING OPTIMIZED MEDIUM, WHICH SHOWED THE HIGHEST CALCIUM CARBONATE PRECIPITATION RATE. THE SCALE BAR IS 50µM.

4.4 CONCLUSIONS

The optimum concentrations of urea, calcium and nickel were investigated using the RSM to maximize calcium carbonate precipitation and growth rate of *S. pasteurii*. The results demonstrated that the calcium carbonate precipitation rate requires high urea and nickel concentrations, and low calcium concentrations. Furthermore, it was shown that the calcium carbonate precipitation rate is not directly related to growth rate as previously suggested. The RSM was shown to be a robust method for MICP studies to determine confluent effects of environmental variables and determine the optimum conditions not only for growth but also for the calcium carbonate production.

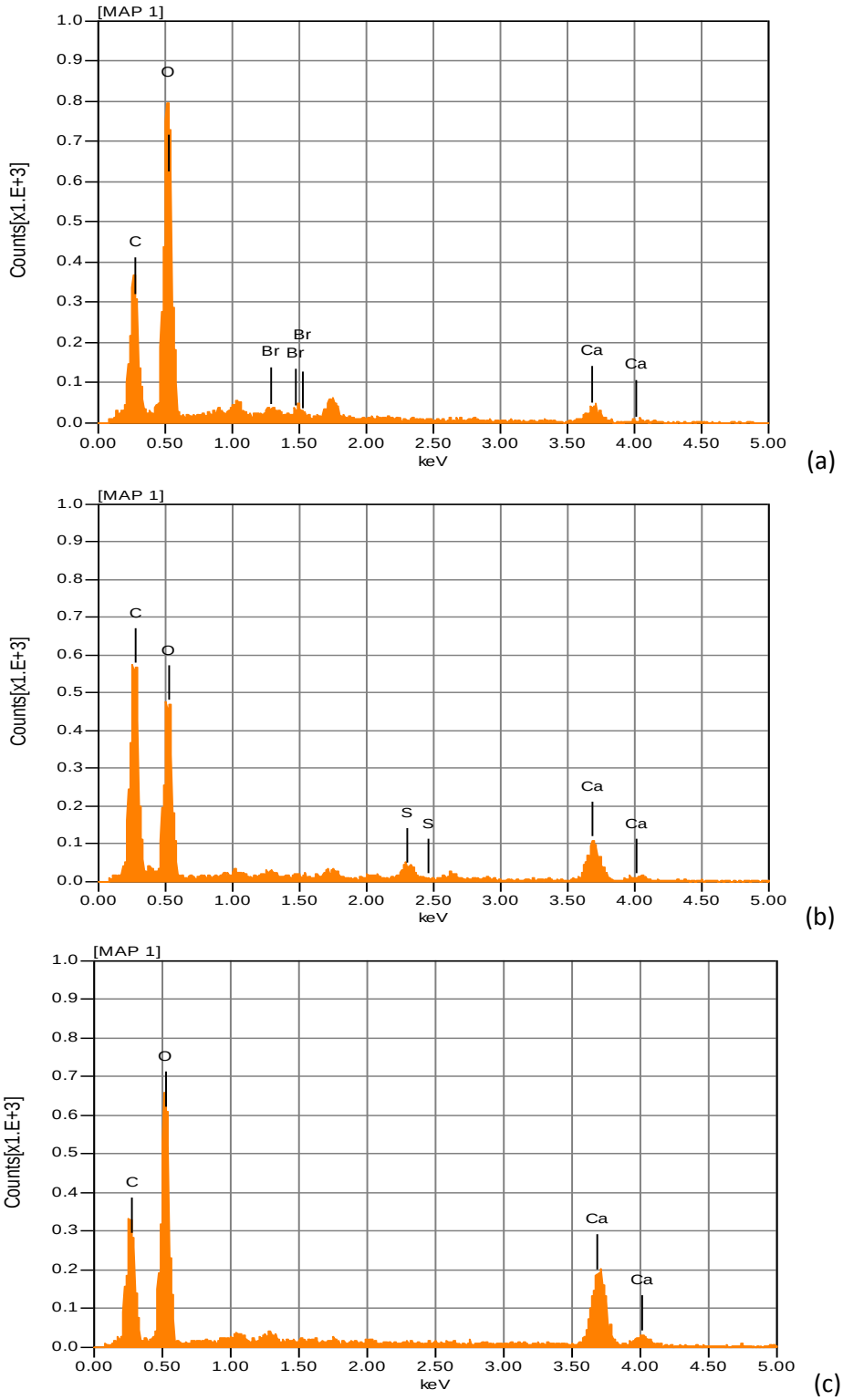

FIGURE 4-10- EDS RESULTS OF CALCIUM CARBONATE IN THE A) STANDARD MEDIUM, B)CONDITION-10, C) OPTIMIZED MEDIUM.

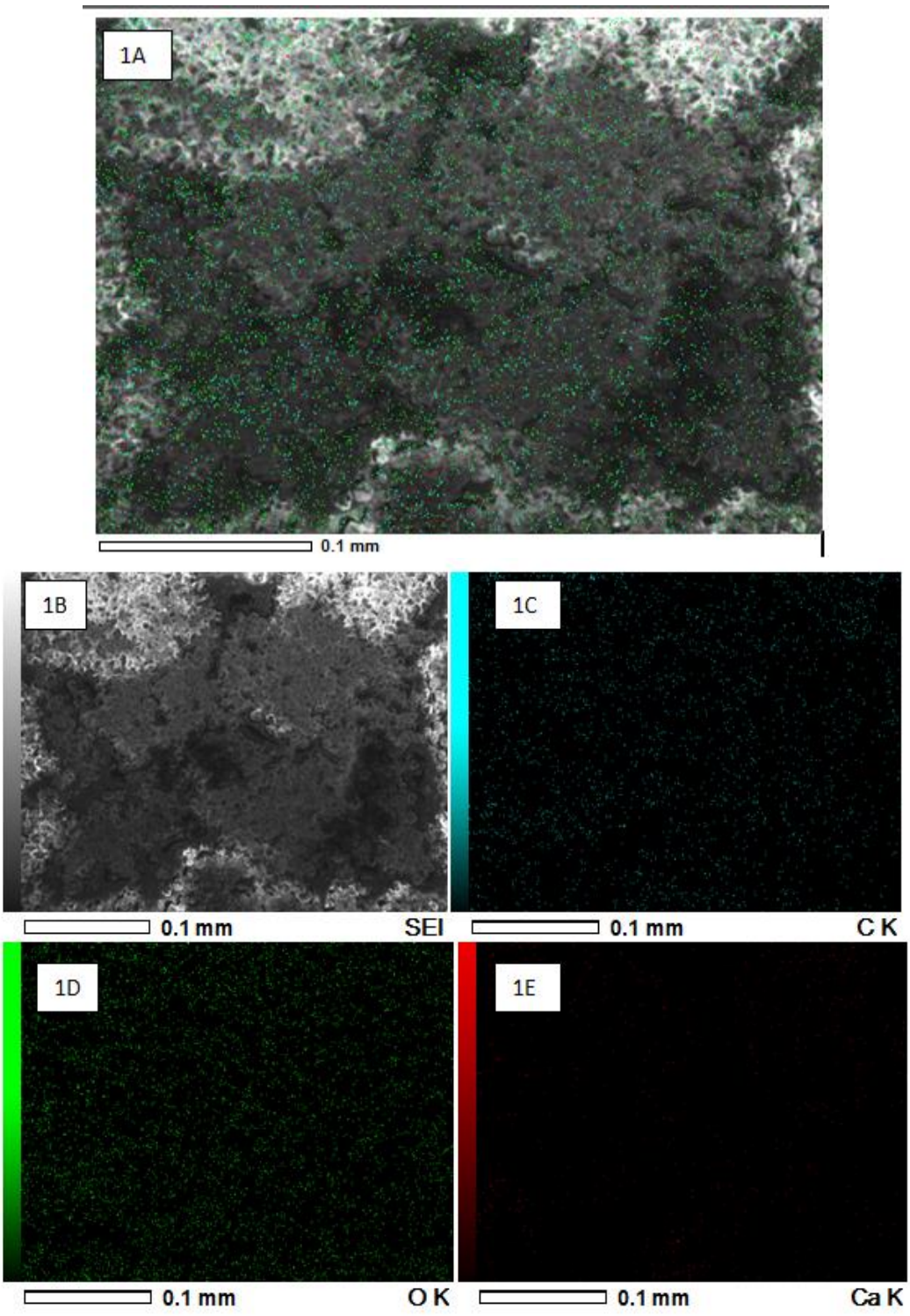

FIGURE 4-11- THE ELEMENTAL ANALYSIS MAPPING USING EDS FOR THE STANDARD MEDIUM (370X); 1A) MAPPING. 1B) SEM. 1C) CARBON. 1D) OXYGEN. 1E) CALCIUM.

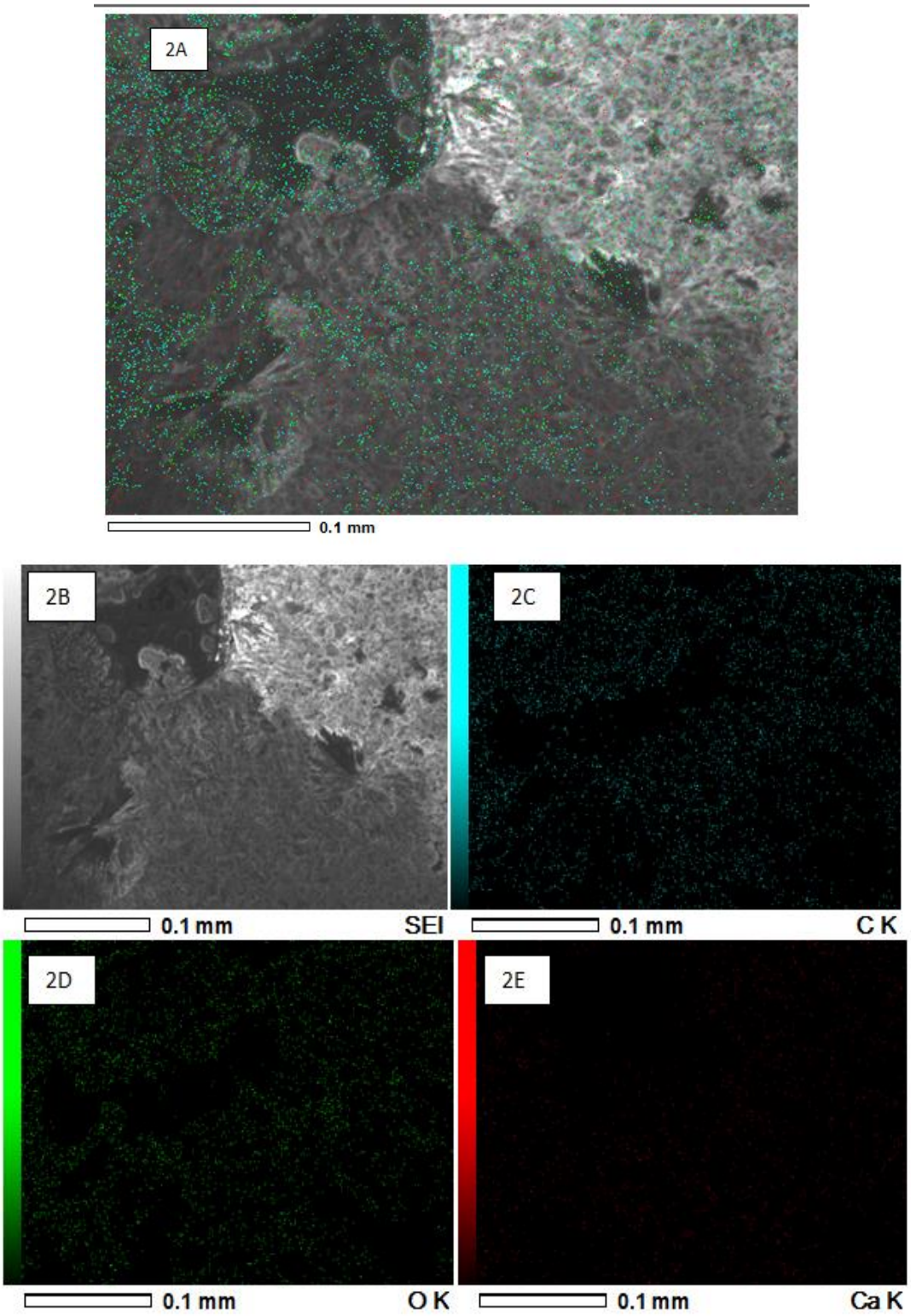

FIGURE 4-12- THE ELEMENTAL ANALYSIS MAPPING USING EDS FOR THE CONDITION-10 (370X); 2A) MAPPING. 2B) SEM. 2C) CARBON. 2D) OXYGEN. 2E) CALCIUM.

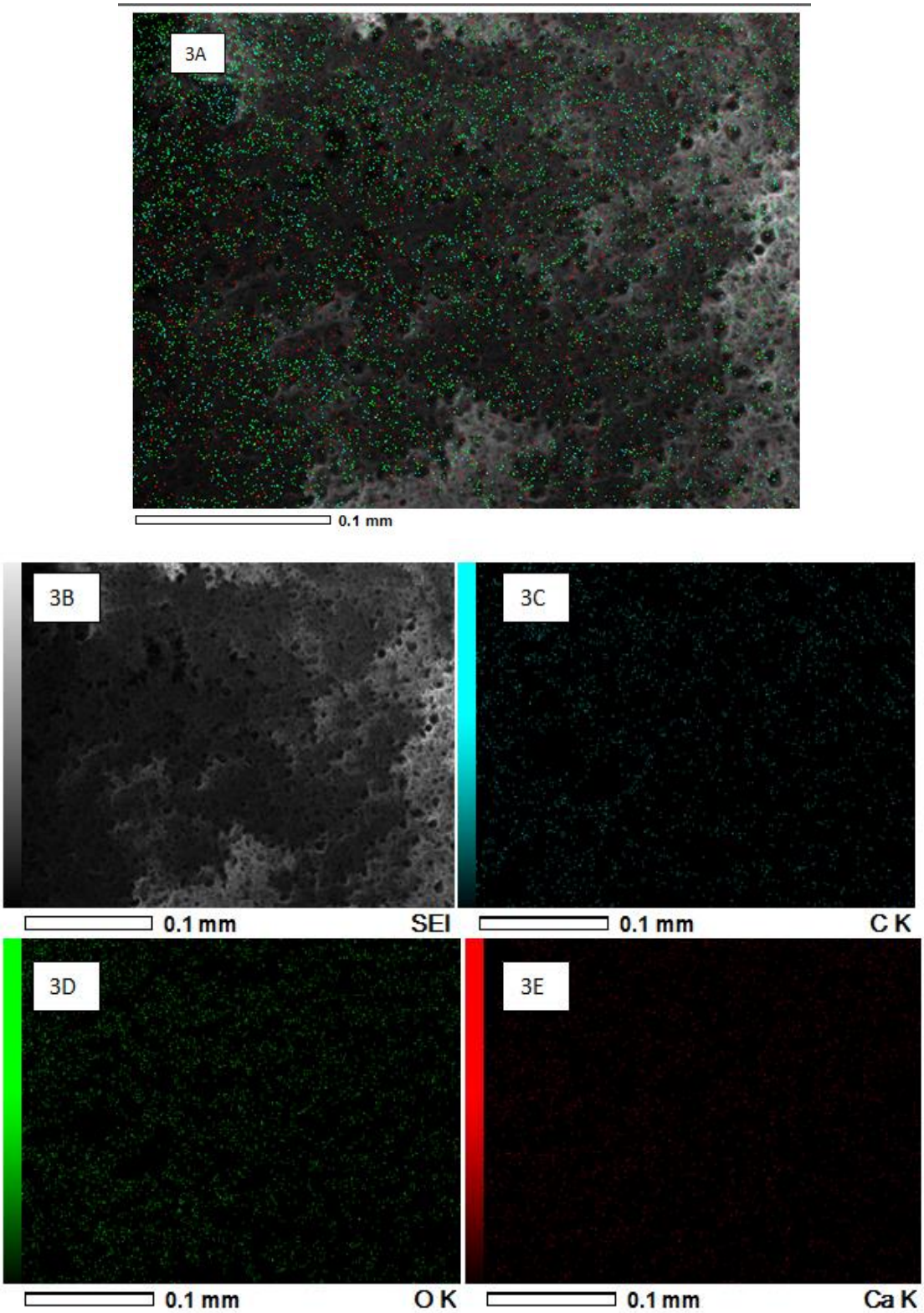

FIGURE 4-13- THE ELEMENTAL ANALYSIS MAPPING USING EDS FOR THE OPTIMIZED MEDIUM (370X); 3A) MAPPING. 3B) SEM. 3C) CARBON. 3D) OXYGEN. 3E) CALCIUM.

SUMMARY AND FUTURE DIRECTIONS

Previous studies have recently indicated that most microorganisms, including heterotrophs, may sequester some CO_2 as part of their normal metabolism to contribute to the production of cell biomass, these studies also showed that diverse microorganisms can be involved in CO_2 sequestration. These findings were obtained through labeled $^{13}CO_2$. In such study they reported that heterotrophs sequester CO_2 into their cell macromolecules, such as membrane lipids [23]. Another study showed that heterotrophic marine bacteria could assimilate dissolved inorganic carbon in the dark [202]. In general, these studies suggested that the rate or the amount of CO_2 sequestered depends largely on the bacterial species and also on the type of heterotrophic substrate used for growth. In our study, we also demonstrated that ureolytic heterotrophic microorganisms can sequester CO_2 through MICP. However, little is known about the actual mechanisms and pathways involved in heterotrophic CO_2 sequestration.

A solution to gain a better understanding of these CO_2 sequestration pathways is to use –OMIC tools. With the advent of OMICs, it has been possible to gain a better understanding of the genetic makeup of diverse microorganisms, as well as their functions. For instance, Genomics provide information about the genetic potential of an organism, while transcriptomics analyses provide details about transcribed genes. Proteomics, on the other hand, allows the determination of proteins produced during certain microbial conditions. Recently, metabolomics have been attracting researchers interest, as it allows the identification of specific metabolites, which gives a more integrated approach, since changes in metabolites are directly connected to the organism's phenotype [203]. In other words, metabolomics is a concept that monitors the metabolites in biological systems providing a qualitative and quantitative measure of molecules involved in metabolism and required for the maintenance, growth and function of organism [204].

As future directions for this study, investigations of karstic communities using the –OMICs approaches will shed a light on the mechanisms, pathways, and ability of different environmental microorganisms that could be potentially sequestering CO_2. Therefore, future studies with ureolytic microbial communities and isolates should be done. In these future studies, we could investigate the isolates CV1, TR12, and TR3, which presented higher biotic CO_2 sequestration yields.

Within the future experiments, two hypotheses can be investigated; (i) CO_2 is sequestered through microorganism's metabolism, and therefore the atmospheric CO_2 goes to the cellular biomass, (ii) CO_2 is sequestered through the MICP process, and hence the atmospheric CO_2 goes to the precipitate of calcium carbonate. In order to investigate these hypotheses, the metabolite profile of the best CO_2 sequestrating isolates can be examined. Similar approach can be done with the environmental microbial community, to gain a better understanding on the role of these ureolytic microorganisms in the community as a whole. Through these investigations, the following questions will be answered: "Where does CO_2 go with MICP?" and "Is the CO_2 going into the biomass or to the $CaCO_3$ precipitate or both?" This approach would also allow us to determine metabolisms involved in CO_2 sequestration other than MICP by the environmental isolates and microbial communities [204]. It would also be extremely valuable to use –OMICs to compare the ureolytic consortia obtained in this study with the total microbial community present in the original sites. This investigation would determine the percentage of the karstic microbial community that is ureolytic and is potentially involved in the MICP process in these environments.

REFERENCES

1. Hammes, F.; Verstraete*, W., Key Roles Of Ph And Calcium Metabolism In Microbial Carbonate Precipitation. *Reviews In Environmental Science And Biotechnology* **2002,** *1*, (1), 3-7.

2. Whiffin, V. S. Microbial $Caco_3$ Precipitation For The Production Of Biocement. Murdoch University, 2004.

3. Okyay, T. O.; Rodrigues, D. F., Optimized Carbonate Micro-Particle Production By Sporosarcina Pasteurii Using Response Surface Methodology. *Ecological Engineering* **2014,** *62*, (0), 168-174.

4. Castanier, S.; Le Métayer-Levrel, G.; Perthuisot, J.-P., Ca-Carbonates Precipitation And Limestone Genesis — The Microbiogeologist Point Of View. *Sedimentary Geology* **1999,** *126*, (1–4), 9-23.

5. Douglas, S.; Beveridge, T. J., Mineral Formation By Bacteria In Natural Microbial Communities. *FEMS Microbiology Ecology* **1998,** *26*, (2), 79-88.

6. Parks, S. L. Kinetics Of Calcite Precipitation By Ureolytic Bacteria Under Aerobic And Anaerobic Conditions. Montana State University, 2009.

7. Okwadha, G. D. O.; Li, J., Optimum Conditions For Microbial Carbonate Precipitation. *Chemosphere* **2010,** *81*, (9), 1143-1148.

8. Gray, C. J.; Engel, A. S., Microbial Diversity And Impact On Carbonate Geochemistry Across A Changing Geochemical Gradient In A Karst Aquifer. *ISME J* **2013,** *7*, (2), 325-337.

9. Bustos-Serrano, H. The Carbonate System In Natural Waters. University Of Miami, 2010.

10. Salek, S. S.; Kleerebezem, R.; Jonkers, H. M.; Witkamp, G.-J.; Van Loosdrecht, M. C. M., Mineral CO2 Sequestration By Environmental Biotechnological Processes. *Trends In Biotechnology* **2013,** *31*, (3), 139-146.

11. Zhu, X.; Logan, B. E., Microbial Electrolysis Desalination And Chemical-Production Cell For CO2 Sequestration. *Bioresource Technology* **2014,** *159*, (0), 24-29.

12. Lal, R., Carbon Sequestration. *Philosophical Transactions: Biological Sciences* **2008,** *363*, (1492), 815-830.

13. Berg, I. A., Ecological Aspects Of The Distribution Of Different Autotrophic CO2 Fixation Pathways. *Applied And Environmental Microbiology* **2011,** *77*, (6), 1925-1936.

14. Li, W.; Chen, W.-S.; Zhou, P.-P.; Yu, L.-J., Influence Of Enzyme Concentration On Bio-Sequestration Of CO2 In Carbonate Form Using Bacterial Carbonic Anhydrase. *Chemical Engineering Journal* **2013,** *232*, (0), 149-156.

15. Hart, K. M.; Oppenheimer, S. F.; Moran, B. W.; Allen, C. C. R.; Kouloumbos, V.; Simpson, A. J.; Kulakov, L. A.; Barron, L.; Kelleher, B. P., CO2 Uptake By A Soil Microcosm. *Soil Biology And Biochemistry* **2013,** *57*, (0), 615-624.

16. Bharti, R. K.; Srivastava, S.; Thakur, I. S., Production And Characterization Of Biodiesel From Carbon Dioxide Concentrating Chemolithotrophic Bacteria, Serratia Sp. ISTD04. *Bioresource Technology* **2014,** *153*, (0), 189-197.

17. Tu, C.; Foster, L.; Alvarado, A.; Mckenna, R.; Silverman, D. N.; Frost, S. C., Role Of Zinc In Catalytic Activity Of Carbonic Anhydrase IX. *Archives Of Biochemistry And Biophysics* **2012,** *521*, (1–2), 90-94.

18. Smith, K. S.; Ferry, J. G., Prokaryotic Carbonic Anhydrases. *FEMS Microbiology Reviews* **2000,** *24*, (4), 335-366.

19. Jo, B. H.; Kim, I. G.; Seo, J. H.; Kang, D. G.; Cha, H. J., Engineered Escherichia Coli With Periplasmic Carbonic Anhydrase As A Biocatalyst For CO2 Sequestration. *Applied And Environmental Microbiology* **2013,** *79*, (21), 6697-6705.

20. Ramanan, R.; Kannan, K.; Sivanesan, S.; Mudliar, S.; Kaur, S.; Tripathi, A.; Chakrabarti, T., Bio-Sequestration Of Carbon Dioxide Using Carbonic Anhydrase Enzyme Purified From Citrobacter Freundii. *World J Microbiol Biotechnol* **2009,** *25*, (6), 981-987.

21. Krulwich, T. A.; Padan, E.; Sachs, G., Molecular Aspects Of Bacterial Ph Sensing And Homeostasis. *Nature Reviews Microbiology* **2011,** *9*, (5), 330+.

22. Kresge, N.; Simoni, R. D.; Hill, R. L., The Discovery Of Heterotrophic Carbon Dioxide Fixation By Harland G. Wood. *Journal Of Biological Chemistry* **2005,** *280*, (18), E15.

23. Roslev, P.; Larsen, M. B.; Jørgensen, D.; Hesselsoe, M., Use Of Heterotrophic CO2 Assimilation As A Measure Of Metabolic Activity In Planktonic And Sessile Bacteria. *Journal Of Microbiological Methods* **2004,** *59*, (3), 381-393.

24. Hesselsoe, M.; Nielsen, J. L.; Roslev, P.; Nielsen, P. H., Isotope Labeling And Microautoradiography Of Active Heterotrophic Bacteria On The Basis Of Assimilation Of 14CO2. *Applied And Environmental Microbiology* **2005,** *71*, (2), 646-655.

25. Lee, J.; Kim, C.; Mahanty, B., Mineralization Of Gaseous CO2 By Bacillus Megaterium In Close Environment System. *Water Air Soil Pollut* **2014,** *225*, (1), 1-8.

26. Gol'dberg, M. A.; Smirnov, V. V.; Kutsev, S. V.; Shibaeva, T. V.; Shvorneva, L. I.; Sergeeva, N. S.; Sviridova, I. K.; Barinov, S. M., Hydroxyapatite-Calcium Carbonate Ceramic Composite Materials. *Inorg Mater* **2010,** *46*, (11), 1269-1273.

27. Kumins, C. A., Surface-Treated Calcium Carbonates In A High-Solid Paint System. *Industrial & Engineering Chemistry* **1952,** *44*, (8), 1844-1849.

28. Velts, O.; Uibu, M.; Kallas, J.; Kuusik, R., Waste Oil Shale Ash As A Novel Source Of Calcium For Precipitated Calcium Carbonate: Carbonation Mechanism, Modeling, And Product Characterization. *Journal Of Hazardous Materials* **2011,** *195*, (0), 139-146.

29. Whiffin, V. S.; Van Paassen, L. A.; Harkes, M. P., Microbial Carbonate Precipitation As A Soil Improvement Technique. *Geomicrobiology Journal* **2007,** *24*, (5), 417-423.

30. Yashina, A.; Meldrum, F.; Demello, A., Calcium Carbonate Polymorph Control Using Droplet-Based Microfluidics. *Biomicrofluidics* **2012,** *6*, (2), 022001-022010.

31. Yun, Y.-H.; Kim, S.-B.; Kang, B.-A.; Lee, Y.-W.; Oh, J.-S.; Hwang, K.-S., B-Wollastonite Reinforced Glass-Ceramics Prepared From Waste Fluorescent Glass And Calcium Carbonate. *Journal Of Materials Processing Technology* **2006,** *178*, (1–3), 61-66.

32. Yur'ev, A. B.; Godik, L. A.; Devyatkin, Y. D.; Kozyrev, N. A.; Tokarev, A. V., Reduction Of Rail Steel By Calcium Carbonate. *Steel Transl.* **2008,** *38*, (4), 312-314.

33. Gong, J.; Liu, T.; Song, D.; Zhang, X.; Zhang, L., One-Step Fabrication Of Three-Dimensional Porous Calcium Carbonate–Chitosan Composite Film As The Immobilization Matrix Of Acetylcholinesterase And Its Biosensing On Pesticide. *Electrochemistry Communications* **2009,** *11*, (10), 1873-1876.

34. Dejong, J. T.; Mortensen, B. M.; Martinez, B. C.; Nelson, D. C., Bio-Mediated Soil Improvement. *Ecological Engineering* **2010,** *36*, (2), 197-210.

35. Lin, Y.; Chan, C. M., 3 - Calcium Carbonate Nanocomposites. In *Advances In Polymer Nanocomposites*, Gao, F., Ed. Woodhead Publishing: 2012; Pp 55-90.

36. Decho, A. W., Overview Of Biopolymer-Induced Mineralization: What Goes On In Biofilms? *Ecological Engineering* **2010,** *36*, (2), 137-144.

37. Burne, R. V.; Moore, L. S., Microbialites; Organosedimentary Deposits Of Benthic Microbial Communities. *PALAIOS* **1987,** *2*, (3), 241-254.

38. Riding, R., Classification Of Microbial Carbonates. In *Calcareous Algae And Stromatolites*, Riding, R., Ed. Springer Berlin Heidelberg: 1991; Pp 21-51.

39. Reid, R. P.; Visscher, P. T.; Decho, A. W.; Stolz, J. F.; Bebout, B. M.; Dupraz, C.; Macintyre, I. G.; Paerl, H. W.; Pinckney, J. L.; Prufert-Bebout, L.; Steppe, T. F.; Desmarais, D. J., The Role Of Microbes In Accretion, Lamination And Early Lithification Of Modern Marine Stromatolites. *Nature* **2000,** *406*, (6799), 989-992.

40. Wright, D. T.; Oren, A., Nonphotosynthetic Bacteria And The Formation Of Carbonates And Evaporites Through Time. *Geomicrobiology Journal* **2005,** *22*, (1-2), 27-53.

41. Larson, E.; Mylroie, J., A Review Of Whiting Formation In The Bahamas And New Models. *Carbonates Evaporites* **2014,** *29*, (4), 337-347.

42. Lian, B.; Hu, Q.; Chen, J.; Ji, J.; Teng, H. H., Carbonate Biomineralization Induced By Soil Bacterium Bacillus Megaterium. *Geochimica Et Cosmochimica Acta* **2006,** *70*, (22), 5522-5535.

43. Ludwig, R.; Al-Horani, F. A.; Beer, D. D.; Jonkers, H. M., Photosynthesis-Controlled Calcification In A Hypersaline Microbial Mat. *Limnology And Oceanography* **2005,** *50*, (6), 1836-1843.

44. Durand, N.; Monger, H. C.; Canti, M. G., 9 - Calcium Carbonate Features. In *Interpretation Of Micromorphological Features Of Soils And Regoliths*, Stoops, G.; Marcelino, V.; Mees, F., Eds. Elsevier: Amsterdam, 2010; Pp 149-194.

45. Deocampo, D. M., Chapter 1 The Geochemistry Of Continental Carbonates. In *Developments In Sedimentology*, Alonso-Zarza, A. M.; Tanner, L. H., Eds. Elsevier: 2010; Vol. Volume 62, Pp 1-59.

46. Homa, E. S.; Chapra, S. C., Modeling The Impacts Of Calcite Precipitation On The Epilimnion Of An Ultraoligotrophic, Hard-Water Lake. *Ecological Modelling* **2011,** *222*, (1), 76-90.

47. Shirsath, S. R.; Sonawane, S. H.; Saini, D. R.; Pandit, A. B., Continuous Precipitation Of Calcium Carbonate Using Sonochemical Reactor. *Ultrasonics Sonochemistry* **2015,** *24*, (0), 132-139.

48. Sanderman, J., Can Management Induced Changes In The Carbonate System Drive Soil Carbon Sequestration? A Review With Particular Focus On Australia. *Agriculture, Ecosystems & Environment* **2012,** *155*, (0), 70-77.

49. Armenteros, I., Chapter 2 Diagenesis Of Carbonates In Continental Settings. In *Developments In Sedimentology*, Alonso-Zarza, A. M.; Tanner, L. H., Eds. Elsevier: 2010; Vol. Volume 62, Pp 61-151.

50. Okyay, T. O.; Rodrigues, D. F., Biotic And Abiotic Effects On CO2 Sequestration During Microbially-Induced Calcium Carbonate Precipitation. *FEMS Microbiology Ecology* **2015**.

51. Goffredo, S.; Vergni, P.; Reggi, M.; Caroselli, E.; Sparla, F.; Levy, O.; Dubinsky, Z.; Falini, G., The Skeletal Organic Matrix From Mediterranean Coral Balanophyllia Europaea Influences Calcium Carbonate Precipitation. *Plos ONE* **2011,** *6*, (7), E22338.

52. Knoll, A. H., Biomineralization And Evolutionary History. *Reviews In Mineralogy And Geochemistry* **2003,** *54*, (1), 329-356.

53. Hamdan, N. Carbonate Mineral Precipitation For Soil Improvement Through Microbial Denitrification. Arizona State University, 2011.

54. Pomar, L.; Hallock, P., Carbonate Factories: A Conundrum In Sedimentary Geology. *Earth-Science Reviews* **2008,** *87*, (3–4), 134-169.

55. Cailleau, G.; Mota, M.; Bindschedler, S.; Junier, P.; Verrecchia, E. P., Detection Of Active Oxalate–Carbonate Pathway Ecosystems In The Amazon Basin: Global Implications Of A Natural Potential C Sink. *CATENA* **2014,** *116*, (0), 132-141.

56. Verrecchia, E. P.; Dumont, J. L.; Rolko, K. E., Do Fungi Building Limestones Exist In Semi-Arid Regions? *Naturwissenschaften* **1990,** *77*, (12), 584-586.

57. Martin, G.; Guggiari, M.; Bravo, D.; Zopfi, J.; Cailleau, G.; Aragno, M.; Job, D.; Verrecchia, E.; Junier, P., Fungi, Bacteria And Soil Ph: The Oxalate-Carbonate Pathway As A Model For Metabolic Interaction. *Environmental Microbiology* **2012,** *14*, (11), 2960-2970.

58. Ferris FG; Stehmeier LG; Kantzas A; FM., M., Bacteriogenic Mineral Plugging. *J Of Can Pet Tech* **1996,** *35*, (8), 56-61.

59. Ferris, F. G.; Phoenix, V.; Fujita, Y.; Smith, R. W., Kinetics Of Calcite Precipitation Induced By Ureolytic Bacteria At 10 To 20°C In Artificial Groundwater. *Geochimica Et Cosmochimica Acta* **2003,** *68*, (8), 1701-10.

60. Beveridge, T. J., Ultrastructure, Chemistry And Function Of The Bacterial Cell Wall. *International Review Of Cytology* **1981,** *72*, 229-317.

61. Pentecost, A., *Growth And Calcification Of The Freshwater Cyanobacterium Rivularia Haematites*. 1987; Vol. 232, P 125-136.

62. Braissant, O.; Decho, A. W.; Dupraz, C.; Glunk, C.; Przekop, K. M.; Visscher, P. T., Exopolymeric Substances Of Sulfate-Reducing Bacteria: Interactions With Calcium At Alkaline Ph And Implication For Formation Of Carbonate Minerals. *Geobiology* **2007,** *5*, (4), 401-411.

63. Mcconnaughey, T. A.; Whelan, J. F., Calcification Generates Protons For Nutrient And Bicarbonate Uptake. *Earth-Science Reviews* **1997,** *42*, (1–2), 95-117.

64. Banks, E. D.; Taylor, N. M.; Gulley, J.; Lubbers, B. R.; Giarrizzo, J. G.; Bullen, H. A.; Hoehler, T. M.; Barton, H. A., Bacterial Calcium Carbonate Precipitation In Cave Environments: A Function Of Calcium Homeostasis. *Geomicrobiology Journal* **2010,** *27*, (5), 444-454.

65. Dupraz, C.; Reid, R. P.; Braissant, O.; Decho, A. W.; Norman, R. S.; Visscher, P. T., Processes Of Carbonate Precipitation In Modern Microbial Mats. *Earth-Science Reviews* **2009,** *96*, (3), 141-162.

66. Kawaguchi, T.; Decho, A. W., A Laboratory Investigation Of Cyanobacterial Extracellular Polymeric Secretions (EPS) In Influencing Caco3 Polymorphism. *Journal Of Crystal Growth* **2002,** *240*, (1–2), 230-235.

67. Fujita, Y.; Ferris, F. G.; Lawson, R. D.; Colwell, F. S.; Smith, R. W., Subscribed Content Calcium Carbonate Precipitation By Ureolytic Subsurface Bacteria. *Geomicrobiol. J.* **2000,** *17*, (4), 305-18.

68. Reddy, M. S., Application Of Calcifying Bacteria For Remediation Of Stones And Cultural Heritages. *Frontiers In Microbiology* **2014,** *5*.

69. Le Métayer-Levrel, G.; Castanier, S.; Orial, G.; Loubière, J. F.; Perthuisot, J. P., Applications Of Bacterial Carbonatogenesis To The Protection And Regeneration Of Limestones In Buildings And Historic Patrimony. *Sedimentary Geology* **1999,** *126*, (1–4), 25-34.

70. Tiano, P.; Biagiotti, L.; Mastromei, G., Bacterial Bio-Mediated Calcite Precipitation For Monumental Stones Conservation: Methods Of Evaluation. *Journal Of Microbiological Methods* **1999,** *36*, (1–2), 139-145.

71. Rodriguez-Navarro, C.; Rodriguez-Gallego, M.; Ben Chekroun, K.; Gonzalez-Muñoz, M. T., Conservation Of Ornamental Stone By Myxococcus Xanthus-Induced Carbonate Biomineralization. *Applied And Environmental Microbiology* **2003,** *69*, (4), 2182-2193.

72. Dick, J.; De Windt, W.; De Graef, B.; Saveyn, H.; Van Der Meeren, P.; De Belie, N.; Verstraete, W., Biodeposition Of A Calcium Carbonate Layer On Degraded Limestone By *Bacillus* Species. *Biodegradation* **2006,** *17*, (4), 357-367.

73. Anne, S.; Rozenbaum, O.; Andreazza, P.; Rouet, J.-L., Evidence Of A Bacterial Carbonate Coating On Plaster Samples Subjected To The Calcite Bioconcept Biomineralization Technique. *Construction And Building Materials* **2010,** *24*, (6), 1036-1042.

74. Tiano, P.; Cantisani, E.; Sutherland, I.; Paget, J. M., Biomediated Reinforcement Of Weathered Calcareous Stones. *Journal Of Cultural Heritage* **2006,** *7*, (1), 49-55.

75. De Muynck, W.; De Belie, N.; Verstraete, W., Microbial Carbonate Precipitation In Construction Materials: A Review. *Ecological Engineering* **2010,** *36*, (2), 118-36.

76. Fujita, Y.; Taylor, J. L.; Gresham, T. L. T.; Delwiche, M. E.; Colwell, F. S.; Mcling, T. L.; Petzke, L. M.; Smith, R. W., Stimulation Of Microbial Urea Hydrolysis In Groundwater To Enhance Calcite Precipitation. *Environmental Science & Technology* **2008,** *42*, (8), 3025-3032.

77. Zhang, T.; Klapper, I., Mathematical Model Of Biofilm Induced Calcite Precipitation. *Water Science & Technology* **2010,** *61*, (11), 2957-2964.

78. Mitchell, A. C.; Dideriksen, K.; Spangler, L. H.; Cunningham, A. B.; Gerlach, R., Microbially Enhanced Carbon Capture And Storage By Mineral-Trapping And Solubility-Trapping. *Environmental Science & Technology* **2010,** *44*, (13), 5270-5276.

79. Chu, J.; Stabnikov, V.; Ivanov, V., Microbially Induced Calcium Carbonate Precipitation On Surface Or In The Bulk Of Soil. *Geomicrobiology Journal* **2012,** *29*, (6), 544-549.

80. Bang, S.; Min, S.; Bang, S. S.; Meyer, F. D.; Stetler, L. D., Microbiologically-Induced Soil Stabilization: Application Of *Sporosarcina Pasteurii* For Fugitive Dust Control. In *Geo-Frontiers*

2011: Advances In Geotechnical Engineering, Han, J.; Alzamora, D. E., Eds. American Society Of Civil Engineers: Dallas, Texas, USA, 2011; Pp 4002-4011.

81. Bachmeier, K. L.; Williams, A. E.; Warmington, J. R.; Bang, S. S., Urease Activity In Microbiologically-Induced Calcite Precipitation. *Journal Of Biotechnology* **2002,** *93*, (2), 171-181.

82. Hammes, F.; Boon, N.; De Villiers, J.; Verstraete, W.; Siciliano, S. D., Strain-Specific Ureolytic Microbial Calcium Carbonate Precipitation. *Applied And Environmental Microbiology* **2003,** *69*, (8), 4901-4909.

83. Sánchez-Román, M.; Rivadeneyra, M. A.; Vasconcelos, C.; Mckenzie, J. A., Biomineralization Of Carbonate And Phosphate By Moderately Halophilic Bacteria. *FEMS Microbiology Ecology* **2007,** *61*, (2), 273-284.

84. Stocks-Fischer, S.; Galinat, J. K.; Bang, S. S., Microbiological Precipitation Of Caco3. *Soil Biology And Biochemistry* **1999,** *31*, (11), 1563-1571.

85. Tobler, D. J.; Cuthbert, M. O.; Greswell, R. B.; Riley, M. S.; Renshaw, J. C.; Handley-Sidhu, S.; Phoenix, V. R., Comparison Of Rates Of Ureolysis Between *Sporosarcina Pasteurii* And An Indigenous Groundwater Community Under Conditions Required To Precipitate Large Volumes Of Calcite. *Geochimica Et Cosmochimica Acta* **2011,** *75*, (11), 3290-3301.

86. Mortensen, B. M.; Haber, M. J.; Dejong, J. T.; Caslake, L. F.; Nelson, D. C., Effects Of Environmental Factors On Microbial Induced Calcium Carbonate Precipitation. *Journal Of Applied Microbiology* **2011,** *111*, (2), 338-49.

87. Reddy, G. S. N.; Matsumoto, G. I.; Shivaji, S., Sporosarcina Macmurdoensis Sp. Nov., From A Cyanobacterial Mat Sample From A Pond In The Mcmurdo Dry Valleys, Antarctica. *International Journal Of Systematic And Evolutionary Microbiology* **2003,** *53*, (5), 1363-1367.

88. Zamarreño, D. V.; Inkpen, R.; May, E., Carbonate Crystals Precipitated By Freshwater Bacteria And Their Use As A Limestone Consolidant. *Applied And Environmental Microbiology* **2009,** *75*, (18), 5981-5990.

89. Boquet, E.; Boronate, A.; Ramos-Cormenzana, A., Production Of Calcite (Calcium Carbonate) Crystals By Soil Bacteria Is A General Phenomenon. *Nature* **1973,** *246*, 527-529.

90. Stuart, C. A.; Stratum, E. V.; Rustigian, R., Further Studies On Urease Production By Proteus And Related Organisms. *J. Of Bacteriol.* **1945,** *49*, (5), 437-44.

91. Christensen, W. B., Urea Decomposition As A Means Of Differentiating Proteus And Paracolon Cultures From Each Other And From Salmonella And Shigella Types. *Journal Of Bacteriology* **1946,** *52*, (4), 461-466.

92. Mobley, H. L.; Hausinger, R. P., Microbial Ureases: Significance, Regulation, And Molecular Characterization. *Microbiological Reviews* **1989,** *53*, (1), 85-108.

93. Achal, V.; Mukherjee, A.; Basu, P. C.; Reddy, M. S., Lactose Mother Liquor As An Alternative Nutrient Source For Microbial Concrete Production By *Sporosarcina Pasteurii*. *J. Of Ind. Microbiol. And Biotech.* **2009,** *36*, (3), 433-38.

94. Hu, L. T.; Mobley, H. L., Expression Of Catalytically Active Recombinant Helicobacter Pylori Urease At Wild-Type Levels In Escherichia Coli. *Infection And Immunity* **1993,** *61*, (6), 2563-2569.

95. Mclean, R. J. C.; Nickel, J. C.; Cheng, K.-J.; Costerton, J. W.; Banwell, J. G., The Ecology And Pathogenicity Of Urease-Producing Bacteria In The Urinary Tract. *Critical Reviews In Microbiology* **1988,** *16*, (1), 37-79.

96. Kandeler, E.; Gerber, H., Short-Term Assay Of Soil Urease Activity Using Colorimetric Determination Of Ammonium. *Biol. And Fertil. Of Soils* **1988,** *6*, (1), 68-72.

97. Koneman, E.; Winn, J. W.; Allen, S.; Laskin, I.; Bennett, J. W.; Janda, W.; Procop, G.; Schreckenberger, P.; Woods, G., *Koneman's Color Atlas And Textbook Of Diagnostic Microbiology*. 6th Ed.; Lippincott Williams & Wilkins Co., Philadelphia, New York.: 2006.

98. Holt, J. G., *Bergey's Manual Of Determinative Bacteriology*. 9th Ed.; Williams & Wilkins Co., Philadelphia, New York.: 2000.

99. Deng, S.; Popova, I. E.; Dick, L.; Dick, R., Bench Scale And Microplate Format Assay Of Soil Enzyme Activities Using Spectroscopic And Fluorometric Approaches. *Appl. Soil Ecol.* **2013,** *64*, (0), 84-90.

100. Takeuchi, Y.; Salcher, M. M.; Ushio, M.; Shimizu-Inatsugi, R.; Kobayashi, M. J.; Diway, B.; Mering, C.; Pernthaler, J.; Shimizu, K. K., In Situ Enzyme Activity In The Dissolved And Particulate Fraction Of The Fluid From Four Pitcher Plant Species Of The Genus Nepenthes. *Plos ONE* **2011,** *6*, (9), 25144.

101. Okyay, T. O.; Rodrigues, D. F., Biotic And Abiotic Effects On CO2 Sequestration During Microbially-Induced Calcium Carbonate Precipitation. *FEMS Microbiol Ecol* **2015**.

102. Jimenez-Lopez, C.; Jroundi, F.; Pascolini, C.; Rodriguez-Navarro, C.; Piñar-Larrubia, G.; Rodriguez-Gallego, M.; González-Muñoz, M. T., Consolidation Of Quarry Calcarenite By Calcium Carbonate Precipitation Induced By Bacteria Activated Among The Microbiota Inhabiting The Stone. *International Biodeterioration & Biodegradation* **2008,** *62*, (4), 352-363.

103. Burbank, M.; Weaver, T.; Lewis, R.; Williams, T.; Williams, B.; Crawford, R., Geotechnical Tests Of Sands Following Bioinduced Calcite Precipitation Catalyzed By Indigenous Bacteria. *Journal Of Geotechnical And Geoenvironmental Engineering* **2013,** *139*, (6), 928-936.

104. Kumaresan, D.; Wischer, D.; Stephenson, J.; Hillebrand-Voiculescu, A.; Murrell, J. C., Microbiology Of Movile Cave—A Chemolithoautotrophic Ecosystem. *Geomicrobiology Journal* **2014,** *31*, (3), 186-193.

105. Johnston, M.; Muench, B.; Banks, E.; Barton, H., Human Urine In Lechuguilla Cave: The Microbiological Impact And Potential For Bioremediation. *Journal Of Cave And Karst Studies* **2012,** *74*, (3), 278-291.

106. Ortiz, M.; Neilson, J.; Nelson, W.; Legatzki, A.; Byrne, A.; Yu, Y.; Wing, R.; Soderlund, C.; Pryor, B.; Pierson, L., III; Maier, R., Profiling Bacterial Diversity And Taxonomic Composition On Speleothem Surfaces In Kartchner Caverns, AZ. *Microb Ecol* **2013,** *65*, (2), 371-383.

107. Baker, A.; Fairchild, I. J., Drip Water Hydrology And Speleothems. *Nature Education Knowledge* **2012,** *3*, (10), 16.

108. Jameson, R. A.; Alexander, E. C. *The Waters Of Mystery Cave - Interpretive Report*; Department Of Geology And Geophysics, University Of Minnesota: 1994.

109. Pentecost, A.; Bayari, S.; Yesertener, C., Phototrophic Microorganisms Of The Pamukkale Travertine, Turkey: Their Distribution And Influence On Travertine Deposition. *Geomicrobiology Journal* **1997,** *14*, (4), 269-283.

110. Simsek, S.; Günay, G.; Elhatip, H.; Ekmekçi, M., Environmental Protection Of Geothermal Waters And Travertines At Pamukkale, Turkey. *Geothermics* **2000,** *29*, (4–5), 557-572.

111. Klindworth, A.; Pruesse, E.; Schweer, T.; Peplies, J.; Quast, C.; Horn, M.; Glöckner, F. O., Evaluation Of General 16S Ribosomal RNA Gene PCR Primers For Classical And Next-Generation Sequencing-Based Diversity Studies. *Nucleic Acids Research* **2013,** *41*, (1), 1-11.

112. Colwell, R. K. *Estimates: Statistical Estimation Of Species Richness And Shared Species From Samples.*, Version 9; 2013.

113. Okyay, T. O.; Rodrigues, D. F., High Throughput Colorimetric Assay For Rapid Urease Activity Quantification. *Journal Of Microbiological Methods* **2013,** *95*, (3), 324-326.

114. Lee, C. T., *Introductory Biostatistics*. John Wiley & Sons, Inc., New Jersey: 2003.

115. Gill, S. R.; Pop, M.; Deboy, R. T.; Eckburg, P. B.; Turnbaugh, P. J.; Samuel, B. S.; Gordon, J. I.; Relman, D. A.; Fraser-Liggett, C. M.; Nelson, K. E., Metagenomic Analysis Of The Human Distal Gut Microbiome. *Science* **2006,** *312*, (5778), 1355-1359.

116. Maughan, H.; Wang, P. W.; Diaz Caballero, J.; Fung, P.; Gong, Y.; Donaldson, S. L.; Yuan, L.; Keshavjee, S.; Zhang, Y.; Yau, Y. C. W.; Waters, V. J.; Tullis, D. E.; Hwang, D. M.; Guttman, D. S., Analysis Of The Cystic Fibrosis Lung Microbiota Via Serial Illumina Sequencing Of Bacterial 16S Rrna Hypervariable Regions. *Plos ONE* **2012,** *7*, (10), E45791.

117. Blackwood, C. B.; Hudleston, D.; Zak, D. R.; Buyer, J. S., Interpreting Ecological Diversity Indices Applied To Terminal Restriction Fragment Length Polymorphism Data: Insights From Simulated Microbial Communities. *Applied And Environmental Microbiology* **2007,** *73*, (16), 5276-5283.

118. Marsh, A. J.; O'Sullivan, O.; Hill, C.; Ross, R. P.; Cotter, P. D., Sequencing-Based Analysis Of The Bacterial And Fungal Composition Of Kefir Grains And Milks From Multiple Sources. *Plos ONE* **2013,** *8*, (7), E69371.

119. Button, D. K.; Schut, F.; Quang, P.; Martin, R.; Robertson, B. R., Viability And Isolation Of Marine Bacteria By Dilution Culture: Theory, Procedures, And Initial Results. *Applied And Environmental Microbiology* **1993,** *59*, (3), 881-891.

120. Fouke, B. W.; Bonheyo, G. T.; Sanzenbacher, B.; Frias-Lopez, J., Partitioning Of Bacterial Communities Between Travertine Depositional Facies At Mammoth Hot Springs, Yellowstone National Park, U.S.A. *Canadian Journal Of Earth Sciences* **2003,** *40*, (11), 1531-1548.

121. Fouke, B. W., Hot-Spring Systems Geobiology: Abiotic And Biotic Influences On Travertine Formation At Mammoth Hot Springs, Yellowstone National Park, USA. *Sedimentology* **2011,** *58*, (1), 170-219.

122. Deepa, R.; Venkatesh, K.; Parveen, J.; Banu, S.; Jayalakshmi, G. *Myroides Odoratus And Chryseobacterium Indologenes:Two Rare Isolates In The Immunocompromised*; July 1, 2014, 2014; Pp 327-330.

123. Vaneechoutte, M., Dijkshoorn, L., Nemec, A., Kämpfer, P., Wauters, G. , Acinetobacter, Chryseobacterium, Moraxella, And Other Nonfermentative Gram-Negative Rods. In *Manual Of Clinical Microbiology*, 10 Ed.; Versalovic, J., Ed. ASM Press: Washington, DC, 2011; Pp 714-738.

124. Blättel, V.; Larisika, M.; Pfeiffer, P.; Nowak, C.; Eich, A.; Eckelt, J.; König, H., B-1,3-Glucanase From Delftia Tsuruhatensis Strain MV01 And Its Potential Application In Vinification. *Applied And Environmental Microbiology* **2011,** *77*, (3), 983-990.

125. Yu, X.-Y.; Li, Y.-F.; Zheng, J.-W.; Li, Y.; Li, L.; He, J.; Li, S.-P., Comamonas Zonglianii Sp. Nov., Isolated From Phenol-Contaminated Soil. *International Journal Of Systematic And Evolutionary Microbiology* **2011,** *61*, (2), 255-258.

126. Geng, Y.; Wang, K. Y.; Chen, D. F.; Huang, X. L., Isolation, Identification And Phylogenetic Analysis Of A Pathogenic Bacterium In Channel Catfish. *Wei Sheng Wu Xue Bao* **2006,** *46*, (4), 649-652.

127. Guentzel, M. N., Escherichia, Klebsiella, Enterobacter, Serratia, Citrobacter, And Proteus. In *Medical Microbiology*, 4th Edition Ed.; S., B., Ed. Galveston (TX): University Of Texas Medical Branch At Galveston, 1996.

128. Becker, K.; Schumann, P.; Wüllenweber, J.; Schulte, M.; Weil, H.-P.; Stackebrandt, E.; Peters, G.; Von Eiff, C., Kytococcus Schroeteri Sp. Nov., A Novel Gram-Positive Actinobacterium

Isolated From A Human Clinical Source. *International Journal Of Systematic And Evolutionary Microbiology* **2002,** *52*, (5), 1609-14.

129. Willoughby, J. J.; Russell, W. C.; Thirkell, D.; Burdon, M. G., Isolation And Detection Of Urease Genes In Ureaplasma Urealyticum. *Infection And Immunity* **1991,** *59*, (7), 2463-2469.

130. Zhang, W.; Zhang, G.; Liu, G.; Dong, Z.; Chen, T.; Zhang, M.; Dyson, P. J.; An, L., Bacterial Diversity And Distribution In The Southeast Edge Of The Tengger Desert And Their Correlation With Soil Enzyme Activities. *Journal Of Environmental Sciences* **2012,** *24*, (11), 2004-2011.

131. Gupta, R. S.; Bhandari, V.; Naushad, H. S., Molecular Signatures For The PVC Clade (Planctomycetes, Verrucomicrobia, Chlamydiae, And Lentisphaerae) Of Bacteria Provide Insights Into Their Evolutionary Relationships. *Frontiers In Microbiology* **2012,** *3*, 327.

132. Harke, M. J.; Gobler, C. J., Global Transcriptional Responses Of The Toxic Cyanobacterium, Microcystis Aeruginosa, To Nitrogen Stress, Phosphorus Stress, And Growth On Organic Matter. *Plos ONE* **2013,** *8*, (7), E69834.

133. Kadis, S.; Pugh, W. L., Urea Utilization By Leptospira. *Infection And Immunity* **1974,** *10*, (4), 793-801.

134. Botero, L.; Brown, K.; Brumefield, S.; Burr, M.; Castenholz, R.; Young, M.; Mcdermott, T., Thermobaculum Terrenum Gen. Nov., Sp. Nov.: A Non-Phototrophic Gram-Positive Thermophile Representing An Environmental Clone Group Related To The Chloroflexi (Green Non-Sulfur Bacteria) And Thermomicrobia. *Arch. Microbiol.* **2004,** *181*, (4), 269-277.

135. Kulichevskaya, I. S.; Ivanova, A. O.; Baulina, O. I.; Bodelier, P. L. E.; Damsté, J. S. S.; Dedysh, S. N., Singulisphaera Acidiphila Gen. Nov., Sp. Nov., A Non-Filamentous, Isosphaera-Like Planctomycete From Acidic Northern Wetlands. *International Journal Of Systematic And Evolutionary Microbiology* **2008,** *58*, (5), 1186-1193.

136. Omelchenko, M. V.; Wolf, Y. I.; Gaidamakova, E. K.; Matrosova, V. Y.; Vasilenko, A.; Zhai, M.; Daly, M. J.; Koonin, E. V.; Makarova, K. S., Comparative Genomics Of Thermus Thermophilus And Deinococcus Radiodurans: Divergent Routes Of Adaptation To Thermophily And Radiation Resistance. *BMC Evolutionary Biology* **2005,** *5*, 57-57.

137. Koops, H.-P.; Pommerening-Röser, A., Distribution And Ecophysiology Of The Nitrifying Bacteria Emphasizing Cultured Species. *FEMS Microbiology Ecology* **2001,** *37*, (1), 1-9.

138. Suzuki, K.; Benno, Y.; Mitsuoka, T.; Takebe, S.; Kobashi, K.; Hase, J., Urease-Producing Species Of Intestinal Anaerobes And Their Activities. *Applied And Environmental Microbiology* **1979,** *37*, (3), 379-382.

139. Sujith, P. P.; Mourya, B. S.; Krishnamurthi, S.; Meena, R. M.; Loka Bharathi, P. A., Mobilization Of Manganese By Basalt Associated Mn(II)-Oxidizing Bacteria From The Indian Ridge System. *Chemosphere* **2014,** *95*, (0), 486-495.

140. Achal, V.; Pan, X., Influence Of Calcium Sources On Microbially Induced Calcium Carbonate Precipitation By Bacillus Sp. CR2. *Applied Biochemistry And Biotechnology* **2014,** *173*, (1), 307-317.

141. Stocks-Fischer, S.; Galinat, J. K.; Bang, S. S., Microbiological Precipitation Of $Caco_3$. *Soil Biology And Biochemistry* **1999,** *31*, (11), 1563-71.

142. Wilke, C. R.; Chang, P., Correlation Of Diffusion Coefficients In Dilute Solutions. *Aiche Journal* **1955,** *1*, (2), 264-270.

143. Mccabe, M.; Maguire, D.; Lintell, N., The Anomalous Einstein-Stokes Behaviour Of Oxygen And Other Low Molecular Weight Diffusants. In *Oxygen Transport To Tissue XXVI*, Okunieff, P.; Williams, J.; Chen, Y., Eds. Springer US: 2005; Vol. 566, Pp 143-149.

144. Chaix, E.; Guillaume, C.; Guillard, V., Oxygen And Carbon Dioxide Solubility And Diffusivity In Solid Food Matrices: A Review Of Past And Current Knowledge. *Comprehensive Reviews In Food Science And Food Safety* **2014,** *13*, (3), 261-286.

145. Millero, F. J., Thermodynamics Of The Carbon Dioxide System In The Oceans. *Geochimica Et Cosmochimica Acta* **1995,** *59*, (4), 661-677.

146. Ortiz, M.; Legatzki, A.; Neilson, J. W.; Fryslie, B.; Nelson, W. M.; Wing, R. A.; Soderlund, C. A.; Pryor, B. M.; Maier, R. M., Making A Living While Starving In The Dark: Metagenomic Insights Into The Energy Dynamics Of A Carbonate Cave. *ISME J* **2014,** *8*, (2), 478-491.

147. Wakai, S.; Masanari, M.; Ikeda, T.; Yamaguchi, N.; Ueshima, S.; Watanabe, K.; Nishihara, H.; Sambongi, Y., Oxidative Phosphorylation In A Thermophilic, Facultative Chemoautotroph, Hydrogenophilus Thermoluteolus, Living Prevalently In Geothermal Niches. *Environmental Microbiology Reports* **2013,** *5*, (2), 235-242.

148. Könneke, M.; Schubert, D. M.; Brown, P. C.; Hügler, M.; Standfest, S.; Schwander, T.; Schada Von Borzyskowski, L.; Erb, T. J.; Stahl, D. A.; Berg, I. A., Ammonia-Oxidizing Archaea Use The Most Energy-Efficient Aerobic Pathway For CO(2) Fixation. *Proceedings Of The National Academy Of Sciences Of The United States Of America* **2014,** *111*, (22), 8239-8244.

149. Liu, Q.; Wang, H.; Zhao, R.; Qiu, X.; Gong, L., Bacteria Isolated From Dripping Water In The Oligotrophic Heshang Cave In Central China. *J. Earth Sci.* **2010,** *21*, (1), 325-328.

150. Amundson, R.; Kelly, E., The Chemistry And Mineralogy Of A CO2-Rich Travertine Depositing Spring In The California Coast Range. *Geochimica Et Cosmochimica Acta* **1987,** *51*, (11), 2883-2890.

151. Kacaroglu, F., Review Of Groundwater Pollution And Protection In Karst Areas. *An International Journal Of Environmental Pollution* **1999,** *113*, (1), 337-356.

152. APHA, *Standart Methods For The Examination Of Water And Wastewater*. 21st Ed.; American Public Health Association: Washington, D.C., 2005.

153. Qiagen Dneasy® Blood & Tissue Handbook. Http://Www.Qiagen.Com/Knowledge-And-Support/Resource-Center/Resource-Download.Aspx?Id=6b09dfb8-6319-464d-996c-79e8c7045a50&Lang=En (01.15.2014),

154. Rodrigues, D. F.; Sakata, S. K.; Comasseto, J. V.; Bícego, M. C.; Pellizari, V. H., Diversity Of Hydrocarbon-Degrading Klebsiella Strains Isolated From Hydrocarbon-Contaminated Estuaries. *Journal Of Applied Microbiology* **2009,** *106*, (4), 1304-1314.

155. Qiagen Qiaquick® Spin Handbook. Http://Www.Qiagen.Com/Knowledge-And-Support/Resource-Center/Resource-Download.Aspx?Id=05356d52-Ff29-4ac2-Be49-48cba2381cfa&Lang=En (01.16.2014),

156. Pourshafie, M.; Vahdani, P.; Popoff, M., Genotyping Clostridium Botulinum Toxinotype A Isolates From Patients Using Amplified Rdna Restriction Analysis. *Journal Of Medical Microbiology* **2005,** *54*, (10), 933-936.

157. Pavel, A. B.; Vasile, C. I., Pyelph - A Software Tool For Gel Images Analysis And Phylogenetics. *BMC Bioinformatics* **2012,** *13*, (1), 9.

158. Altschul, S. F.; Gish, W.; Miller, W.; Myers, E. W.; Lipman, D. J., Basic Local Alignment Search Tool. *J Mol Biol* **1990,** *215*, (3), 403-10.

159. Tamura, K.; Peterson, D.; Peterson, N.; Stecher, G.; Nei, M.; Kumar, S., MEGA5: Molecular Evolutionary Genetics Analysis Using Maximum Likelihood, Evolutionary Distance, And Maximum Parsimony Methods. *Molecular Biology And Evolution* **2011,** *28*, (10), 2731-2739.

160. Saitou, N.; Nei, M., The Neighbor-Joining Method: A New Method For Reconstructing Phylogenetic Trees. *Molecular Biology And Evolution* **1987,** *4*, (4), 406-425.

161. Khambhaty, Y.; Mody, K.; Jha, B.; Gohel, V., Statistical Optimization Of Medium Components For K-Carrageenase Production By Pseudomonas Elongata. *Enzyme And Microbial Technology* **2007,** *40*, (4), 813-822.

162. Cave Without A Name's Annual Temperature. Http://Www.Cavewithoutaname.Com/ Tours.Htm (01.21.2014),

163. Pamukkale Pamukkale Travertines' Annual Temperature. Http://Www.Pamukkale. Gov.Tr/EN/Content.Asp?Id=564 (01.21.2014),

164. Tempest, D. W.; Meers, J. L.; Brown, C. M., Influence Of Environment On The Content And Composition Of Microbial Free Amino Acid Pools. *Journal Of General Microbiology* **1970,** *64*, (2), 171-185.

165. Davis, K. E. R.; Joseph, S. J.; Janssen, P. H., Effects Of Growth Medium, Inoculum Size, And Incubation Time On Culturability And Isolation Of Soil Bacteria. *Applied And Environmental Microbiology* **2005,** *71*, (2), 826-834.

166. Pham, V. H. T.; Kim, J., Cultivation Of Unculturable Soil Bacteria. *Trends In Biotechnology* **2012,** *30*, (9), 475-484.

167. Stott, M. B.; Crowe, M. A.; Mountain, B. W.; Smirnova, A. V.; Hou, S.; Alam, M.; Dunfield, P. F., Isolation Of Novel Bacteria, Including A Candidate Division, From Geothermal Soils In New Zealand. *Environmental Microbiology* **2008,** *10*, (8), 2030-2041.

168. Alain, K.; Querellou, J., Cultivating The Uncultured: Limits, Advances And Future Challenges. *Extremophiles* **2009,** *13*, (4), 583-594.

169. Urdaneta, L.; Lal, A.; Barnabé, C.; Oury, B.; Goldman, I.; Ayala, F. J.; Tibayrenc, M., Evidence For Clonal Propagation In Natural Isolates Of Plasmodium Falciparum From Venezuela. *Proceedings Of The National Academy Of Sciences* **2001,** *98*, (12), 6725-6729.

170. Lagacé, L.; Pitre, M.; Jacques, M.; Roy, D., Identification Of The Bacterial Community Of Maple Sap By Using Amplified Ribosomal DNA (Rdna) Restriction Analysis And Rdna Sequencing. *Applied And Environmental Microbiology* **2004,** *70*, (4), 2052-2060.

171. Wu, X.-Y.; Walker, M. J.; Hornitzky, M.; Chin, J., Development Of A Group-Specific PCR Combined With ARDRA For The Identification Of Bacillus Species Of Environmental Significance. *Journal Of Microbiological Methods* **2006,** *64*, (1), 107-119.

172. Rodas, A. M.; Ferrer, S.; Pardo, I., 16S-ARDRA, A Tool For Identification Of Lactic Acid Bacteria Isolated From Grape Must And Wine. *Systematic And Applied Microbiology* **2003,** *26*, (3), 412-422.

173. Pereira, M. G.; Latchford, J. W.; Mudge, S. M., The Use Of Terminal Restriction Fragment Length Polymorphism (T-RFLP) For The Characterisation Of Microbial Communities In Marine Sediments. *Geomicrobiology Journal* **2006,** *23*, (5), 247-251.

174. Yoon, J. H.; Lee, K. C.; Weiss, N.; Kho, Y. H.; Kang, K. H.; Park, Y. H., Sporosarcina Aquimarina Sp. Nov., A Bacterium Isolated From Seawater In Korea, And Transfer Of Bacillus Globisporus (Larkin And Stokes 1967), Bacillus Psychrophilus (Nakamura 1984) And Bacillus Pasteurii (Chester 1898) To The Genus Sporosarcina As Sporosarcina Globispora Comb. Nov., Sporosarcina Psychrophila Comb. Nov. And Sporosarcina Pasteurii Comb. Nov., And Emended Description Of Th. *International Journal Of Systematic And Evolutionary Microbiology* **2001,** *51*, (3), 1079-86.

175. Zhang, Z.; Srichuwong, S.; Kobayashi, T.; Arakane, M.; Park, J.-Y.; Tokuyasu, K., Bioconversion Of L-Arabinose And Other Carbohydrates From Plant Cell Walls To A-Glucan By A Soil Bacterium, Sporosarcina Sp. N52. *Bioresource Technology* **2010,** *101*, (24), 9734-9741.

176. Claus, D.; Fahmy, F.; Rolf, H. J.; Tosunoglu, N., Sporosarcina Halophila Sp. Nov., An Obligate, Slightly Halophilic Bacterium From Salt Marsh Soils. *Systematic And Applied Microbiology* **1983,** *4*, (4), 496-506.

177. Bafana, A., Mercury Resistance In Sporosarcina Sp. G3. *Biometals* **2011,** *24*, (2), 301-309.

178. Weiss, R. F., Carbon Dioxide In Water And Seawater: The Solubility Of A Non-Ideal Gas. *Marine Chemistry* **1974,** *2*, (3), 203-215.

179. Ketjinda, W.; Sinchaipanid, N.; Limsuwan, P.; Leuenberger, H.; Mitrevej, A., Development Of Push-Pull Osmotic Tablets Using Chitosan-Poly(Acrylic Acid) Interpolymer Complex As An Osmopolymer. *AAPS Pharmscitech* **2011,** *12*, (1), 132-40.

180. Zambelli, B.; Musiani, F.; Benini, S.; Ciurli, S., Chemistry Of Ni2+ In Urease: Sensing, Trafficking, And Catalysis. *Accounts Of Chemical Research* **2011,** *44*, (7), 520-530.

181. Chou, C.; Seagren, E.; Aydilek, A.; Lai, M., Biocalcification Of Sand Through Ureolysis. *Journal Of Geotechnical And Geoenvironmental Engineering* **2011,** *137*, (12), 1179-1189.

182. Hammes, F.; Seka, A.; De Knijf, S.; Verstraete, W.; De Knijf, S.; Verstraete, W., A Novel Approach To Calcium Removal From Calcium-Rich Industrial Wastewater. *Water Research* **2003,** *37*, (3), 699-704.

183. Dragan, S.; Ozunu, A., Characterization Of Calcium Carbonates Used In Wet Flue Gas Desulphurization Processes. *Cent.Eur.J.Chem.* **2012,** *10*, (5), 1556-1564.

184. Bang, S. S.; Galinat, J. K.; Ramakrishnan, V., Calcite Precipitation Induced By Polyurethane-Immobilized *Bacillus Pasteurii*. *Enzyme And Microbial Technology* **2001,** *28*, (4–5), 404-409.

185. Lv, J.; Jiang, Y.; Yu, Q.; Lu, S., Structural And Functional Role Of Nickel Ions In Urease By Molecular Dynamics Simulation. *Journal Of Biological Inorganic Chemistry* **2011,** *16*, (1), 125-135.

186. Tang, X. J.; He, G. Q.; Chen, Q. H.; Zhang, X. Y.; Ali, M. A. M., Medium Optimization For The Production Of Thermal Stable B-Glucanase By *Bacillus Subtilis* ZJF-1A5 Using Response Surface Methodology. *Bioresource Technology* **2004,** *93*, (2), 175-181.

187. Steinberg, D. M.; Bursztyn, D., Response Surface Methodology In Biotechnology. *Quality Engineering* **2010,** *22*, (2), 78-87.

188. Boyacı, İ. H., A New Approach For Determination Of Enzyme Kinetic Constants Using Response Surface Methodology. *Biochemical Engineering Journal* **2005,** *25*, (1), 55-62.

189. Tatineni, R. D., K.; Potumarthi, R.; Mangamoori, L., Optimization Of Keratinase Production And Enzyme Activity Using Response Surface Methodology With *Streptomyces Sp.* 7. *Applied Biochemistry And Biotechnology* **2007,** *141*, (2), 187-201.

190. Wang, Q. H., Y.; Xu, Z.; Miao, J.; Li, G., Optimization Of Cold-Active Protease Production By The Psychrophilic Bacterium *Colwellia Sp.* NJ341 With Response Surface Methodology. *Bioresource Technology* **2008,** *99*, (6), 1926-1931.

191. Faes, A.; Fuerbringer, J.-M.; Mohamedi, D.; Hessler-Wyser, A.; Caboche, G.; Van Herle, J., Design Of Experiment Approach Applied To Reducing And Oxidizing Tolerance Of Anode Supported Solid Oxide Fuel Cell. Part I: Microstructure Optimization. *Journal Of Power Sources* **2011,** *196*, (17), 7058-7069.

192. Nollet, L. M. L., *Handbook Of Water Analysis*. Marcel Dekker, Inc., New York: 2000.

193. Dupraz S; Parmentier M; Ménez B; F., G., Experimental And Numerical Modeling Of Bacterially Induced Ph Increase And Calcite Precipitation In Saline Aquifers. *Chemical Geology* **2009,** *265*, (1–2), 44-53.

194. Mead, R.; Pike, D. J., A Biometrics Invited Paper: A Review Of Response Surface Methodology From A Biometric Viewpoint. *Biometrics* **1975,** *31*, (4), 803-851.

195. Montgomery, D. C. R., C. G.; Hubele, N. F., *Engineering Statistics, Fifth Ed.* John Wiley & Sons, Inc., New Jersey: 2011.

196. Mejias Carpio, I. E.; Santos, C. M.; Wei, X.; Rodrigues, D. F., Toxicity Of A Polymer-Graphene Oxide Composite Against Bacterial Planktonic Cells, Biofilms, And Mammalian Cells. *Nanoscale* **2012,** *4*, (15), 4746-4756.

197. Kenny, G. E.; Cartwright, F. D., Effect Of Urea Concentration On Growth Of *Ureaplasma Urealyticum* (T-Strain Mycoplasma). *Journal Of Bacteriology* **1977,** *132*, (1), 144-150.

198. Chen, Y.; Cheng, J. J.; Creamer, K. S., Inhibition Of Anaerobic Digestion Process: A Review. *Bioresource Technology* **2008,** *99*, (10), 4044-4064.

199. Cabrera, M. L.; Kissel, D. E.; Bock, B. R., Urea Hydrolysis In Soil: Effects Of Urea Concentration And Soil Ph. *Soil Biology And Biochemistry* **1991,** *23*, (12), 1121-1124.

200. Masover, G. K.; Catlin, H.; Hayflick, L., The Effect Of Growth And Urea Concentration On Ammonia Production By A Urea-Hydrolyzing Mycoplasma (*Ureaplasma Urealyticum*). *Journal Of General Microbiology* **1977,** *98*, (2), 587-593.

201. Bergdale, T. E.; Pinkelman, R. J.; Hughes, S. R.; Zambelli, B.; Ciurli, S.; Bang, S. S., Engineered Biosealant Strains Producing Inorganic And Organic Biopolymers. *Journal Of Biotechnology* **2012,** *161*, (3), 181-189.

202. Delorenzo, S.; Bräuer, S. L.; Edgmont, C. A.; Herfort, L.; Tebo, B. M.; Zuber, P., Ubiquitous Dissolved Inorganic Carbon Assimilation By Marine Bacteria In The Pacific Northwest Coastal Ocean As Determined By Stable Isotope Probing. *Plos ONE* **2012,** *7*, (10), E46695.

203. Barsch, A.; Patschkowski, T.; Niehaus, K., Comprehensive Metabolite Profiling Of Sinorhizobium Meliloti Using Gas Chromatography-Mass Spectrometry. *Funct Integr Genomics* **2004,** *4*, (4), 219-230.

204. Vanwonterghem, I.; Jensen, P. D.; Ho, D. P.; Batstone, D. J.; Tyson, G. W., Linking Microbial Community Structure, Interactions And Function In Anaerobic Digesters Using New Molecular Techniques. *Current Opinion In Biotechnology* **2014,** *27*, (0), 55-64.